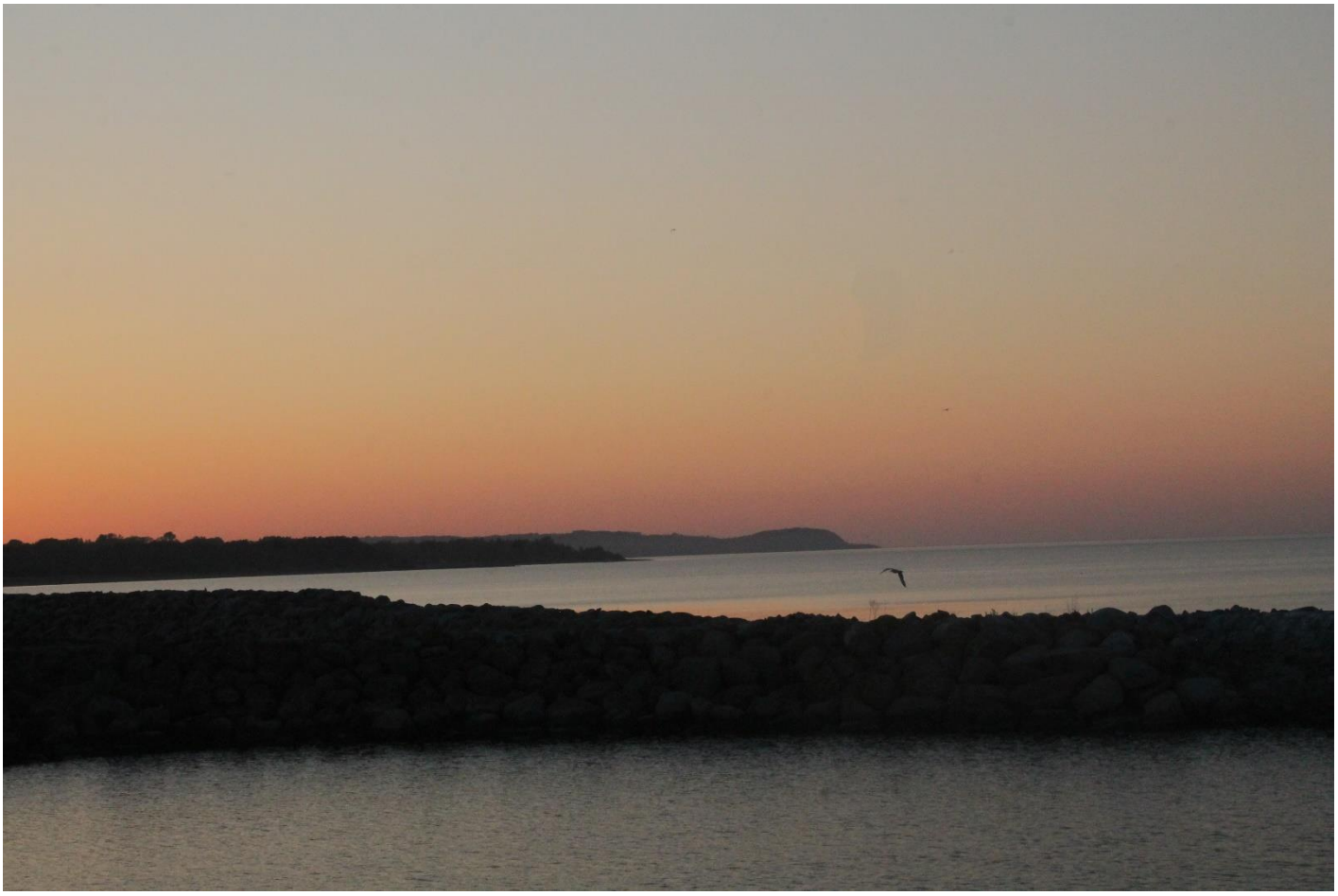
Stockholm University

# Master Thesis

Degree Project in
Geochemistry 60 hp

# The effect of benthic trawling on sediment carbon mineralization

Celine Golda



Stockholm 2024

Department of Geological Sciences
Stockholm University
SE-106 91 Stockholm

# Acknowledgements

First, and foremost I would like to thank and show my dear appreciation to my supervisors, Volker Brüchert and Clare Bradshaw for the opportunity to take part in this fascinating, interdisciplinary project. Volker, your enthusiasm for biogeochemistry and your ability to link so many different disciplines together have inspired me to learn and understand about the vast, complex processes that occur on Earth. Clare, thank you for giving me a glimpse into your world of biology and helping me to expand my fascination in biology, I will always keep the memories on Electra, deep in my heart. Thank you both for opening my eyes in the field of marine sciences and your encouragement and guidance throughout this project.

Secondly, thank you to Haoyi Yao for helping and guiding me with sample preparations and analyses; and Julia Steinbach for always being there to answer my questions in the lab and for finding quick solutions when the machines were not cooperating. Many thanks to the Electra crew and your hands-on assistance on board and Benedetta Esposito, for your cheerfulness; you made the cruise an unforgettable experience and I am so grateful for our friendship that has grown since. Thank you to all my friends in the Geoklubben, you have been my home, away from home. The biggest thank you to my family for your infinite support and for opening the world to me, you have taught me to never stop asking questions and have given my brothers and me opportunities that you never had, thank you. Last but not least, my dear Adrien, thank you for standing by my side, wherever I choose to go and for your encouraging words, when I need them most.

# Abstract

Physical disturbances caused by trawling has led to widespread concern within the scientific community, as it may cause long-lasting impacts to benthic ecosystems, sediment compositions, carbon storage and biogeochemical cycling. Most of the catch obtained by trawling is harvested from productive continental shelves, which play an important role in carbon sequestration and burial. Parts of the Baltic Sea are trawled between one to ten times annually and thus provides a prime locality to study trawling related effects on benthic ecosystems and on the geochemical system. Numerous studies have focused on the detrimental effects on the community structures of benthic ecosystems and trawling-induced changes to carbon storages and biogeochemical processes through complex models and trawling experiments. However, on-site studies on porewater geochemistry and fluxes of sites that have been heavily trawled in the past are often lacking in the literature and often do not account for the interaction of multiple environmental factors, and may underrepresent trawling-related effects. This study investigates the effects of trawling on carbon mineralization within the Bornholm basin of the Baltic Sea, which has been consistently trawled until 2019, with the aid of porewater geochemistry, solid-phase sediment profiles, benthic fluxes and macrofaunal abundances. The study in particular emphasizes the need to understand trawling-induced variabilities within the context of environmental variabilities.

Comparisons between various study localities in this study revealed greater differences in measured physical and chemical properties than those between high- and low-trawled locality pairs, suggesting that environmental variability significantly influences carbon mineralization. To accurately identify the spatial effects of trawling, it is essential to compare high/low- trawling intensity localities with similar sediment compositions, depths, and hydrographic conditions, minimizing the impact of overall concentration differences between sites. Trawling in the study area likely altered sediment porosities, composition, and water content, resulting in significant changes to benthic community structures and bioturbation and bioirrigation potentials, which may have long-term effects on the biogeochemical system. Changes in the biological activities within trawled regions substantially affect nutrient and carbon cycling, degradation rates, and fluxes. High-trawled areas within the current study exhibited greater retention and higher concentrations of TOC (total organic carbon), DIC (dissolved inorganic carbon) and nutrients in their porewaters due to reduced advective transports and macrofaunal consumption, as a consequence of lower bioturbation and bioirrigation potentials, whereby the transport of mineralization end-products ($NH_4^+$, $PO_4^{3-}$ and DIC) show a higher dependence on slow diffusive transport processes in comparison to low-trawled localities. Short-term biogeochemical effects are likely predominantly driven by physical disturbances from trawling, whereas long-term impacts are influenced by changes in benthic community structures due to trawling-induced variabilities in benthic habitats. Surface chlorophyll concentrations indicate recently settled organic material from spring phytoplankton blooms, with higher levels at high-trawled localities likely due to decreased grazing activity by macrofauna and microorganisms consistent with lower biomasses. The study concludes that while immediate biogeochemical impacts of trawling may have recovered, ongoing differences in macrofaunal abundance, dominance of specific organisms and bioturbation potential continue to influence carbon retention and fluxes in sediments within the study area.

**Table of Contents**


*1. Introduction* ..... *5*

**1.1 Rationale, aim and hypotheses** ..... **8**

*2. Materials and Methods* ..... *9*

**2.1 Site Description** ..... **9**
2.1.1 Study Locations ..... 11

**2.2 Field methods** ..... **13**
2.2.1 CTD + Rosette sampler ..... 13
2.2.2 Gemini coring ..... 14
2.2.2.1 Sediment properties ..... 14
2.2.2.2 Porewater analyses ..... 14
2.2.2.3 Benthic flux incubations ..... 15
2.2.3 Macrofauna ..... 16
2.2.3.1 Van Veen grabs ..... 16

**2.3 Laboratory methods** ..... **16**
2.3.1 Porewater and benthic flux samples ..... 17
2.3.1.1 DIC for porewaters and benthic fluxes ..... 17
2.3.1.2 $\delta^{13}C$ of DIC ..... 17
2.3.1.3 Nutrients ..... 18
2.3.2 Sediments ..... 21
2.3.2.1 Sediment grain sizes and sedimentation rates ..... 21
2.3.2.2 Particulate: TOC, $\delta^{13}C_{TOC}$, TC, TN, $\delta^{15}N_{totalN}$ and $\delta^{13}C_{totalC}$ ..... 21
2.3.2.3 Chlorophyll ..... 22

**2.4 Data processing and calculations** ..... **23**
2.4.1 Calculation of diffusive fluxes ..... 23

**2.5 Statistical analyses** ..... **24**

*3. Results* ..... *25*

**3.1 Physio-chemical characteristics of the bottom water** ..... **25**

**3.2 Physical properties of sediments** ..... **25**

**3.3 Biogeochemical properties of sediments and porewaters** ..... **28**
3.3.1 Sediment solid-phase concentration profiles ..... 28
3.3.1.1 Variability by localities ..... 28
3.3.1.2 Variability by trawling intensity between high- and low-trawled pairs ..... 33
3.3.2 Porewater concentration profiles ..... 34
3.3.2.1 Variability by localities ..... 34
3.3.2.2 Variability by trawling intensity between high- and low-trawled pairs ..... 37
3.3.3 Fluxes ..... 38
3.3.3.1 Fluxes calculated from benthic incubation experiments ..... 38
3.3.3.2 Fluxes calculated from porewater gradients through Fick's law ..... 39
3.3.4 Macrofauna ..... 40

*4. Discussion and Interpretation* ..... *42*

**4.1 Variabilities across study sites and considerations for upscaling the effects of trawling** ..... **42**

**4.2 Trawling and its effect on the seafloor and sediment properties** ..... **42**

**4.3 Trawling and its effect on solid-phase sediment concentration profiles** ..... **43**

**4.4 Statistical significance of high- and low-trawled pairs of porewater profiles** ..... **46**

**4.5 Trawling and its effect on carbon mineralization products in porewaters:** ..... **47**

**4.6 Trawling and its effect on fluxes:** ..... **48**

*5. Conclusion* ..... *50*

*6. References* ..... *52*

*7. Appendices* ..... *57*

**7.1 Appendix A: Tables with calculations** ..... **57**

**7.2 Appendix B: All chemical measurements** ..... **64**

## Definitions and Abbreviations

Carbon mineralization: “Carbon mineralization is defined as the conversion of organic to inorganic carbon and occurs mainly as a result of organic matter decomposition” (Ouyang et al., 2022).

Carbon sequestration: “The process by which carbon is stored in a carbon pool. The rate at which carbon is stored is referred to as the carbon sequestration rate” (Hendriks et al., 2020).

Redfield ratio: A stoichiometric ratio describing the average elemental composition in phytoplankton biomass (Tyrrell, 2001). It is defined by the molar ratios of Carbon (C), Nitrogen (N) and Phosphorus (P) and defines the stoichiometry of photosynthesis and remineralization reactions (Tyrrell, 2001). The most commonly used values for the redfield ratio are: C:N:P = 106:16:1

BSL – Below sea level
FID - Flame ionisation detector
SD - Standard deviation
BPc – Bioturbation potential
IPc – Bioirrigation potential

Chemical species:
POC – Particulate organic carbon
DIC – Dissolved inorganic carbon
TOC – Total organic carbon
TN – Total Nitrogen
TC – Total Carbon
$NaHCO_3$ – Sodium Bicarbonate
$H_3PO_4$ – Phosphoric acid
$NH_4^+$ – Ammonium
$PO_4^{-3}$ – Phosphate
$NO_3^-$ –Nitrate

# 1. Introduction

The ocean plays an invaluable role in accommodating diverse ecosystems, providing major food resources, and hosting the earths largest carbon reservoir. Bottom trawling constitutes 23% of globally sold fish, and contributes nearly one-third of the total wild marine catch (Amoroso et al., 2018; De Borger et al., 2021). Physical and chemical alterations as a result of sediment disturbances, pose long lasting impacts on marine ecosystems, biogeochemical cycles, sediment composition and marine carbon reservoirs (Durrieu De Madron et al., 2005; Van Denderen et al., 2020). In the North Sea, approximately 90% of the seabed is trawled between once and six times annually (Olsgard et al., 2008), mostly targeting productive continental shelves, while parts of the Kattegat and the Bornholm basin in the Baltic Sea are trawled one to ten times annually (Amoroso et al., 2018; Eigaard et al., 2017).

In contrast to fishing methods targeting midwater species, such as pelagic trawling, mobile demersal fishing equipment; including trawls, dredges and gillnets, have a significantly greater environmental impact and magnitude of disturbances (Durrieu De Madron et al., 2005). Previous studies conducted in the North Atlantic have shown that sediment disturbances for bottom trawling surpasses that of all other offshore anthropogenic activities combined (such as mining and waste disposal) (Benn et al., 2010; Oberle et al., 2016) and have been compared to the impacts of deforestation (Olsgard et al., 2008). Trawling equipment are specifically designed to capture species residing or grazing in benthic habitats near the seabed and employ this equipment by dredging weighted fishing gear on the seabed (figure 1). This dredging action and associated hydraulic drag leads to displacement and resuspension of sediments resulting in increased turbidity; with deeper sediments mixed until a certain depth (De Borger et al., 2021; Oberle et al., 2016), leaving between 10-35cm deep track scars in the sediments (Oberle et al., 2016). The magnitude of disturbance and the persistence of trawl track marks on the seabed are variable and are largely influenced by the sediment type, fishing equipment, topography of the seabed, current strengths, hydrodynamic conditions and trawling intensities (Bradshaw et al., 2021; Bruns et al., 2020; Oberle et al., 2016; Sciberras et al., 2016).

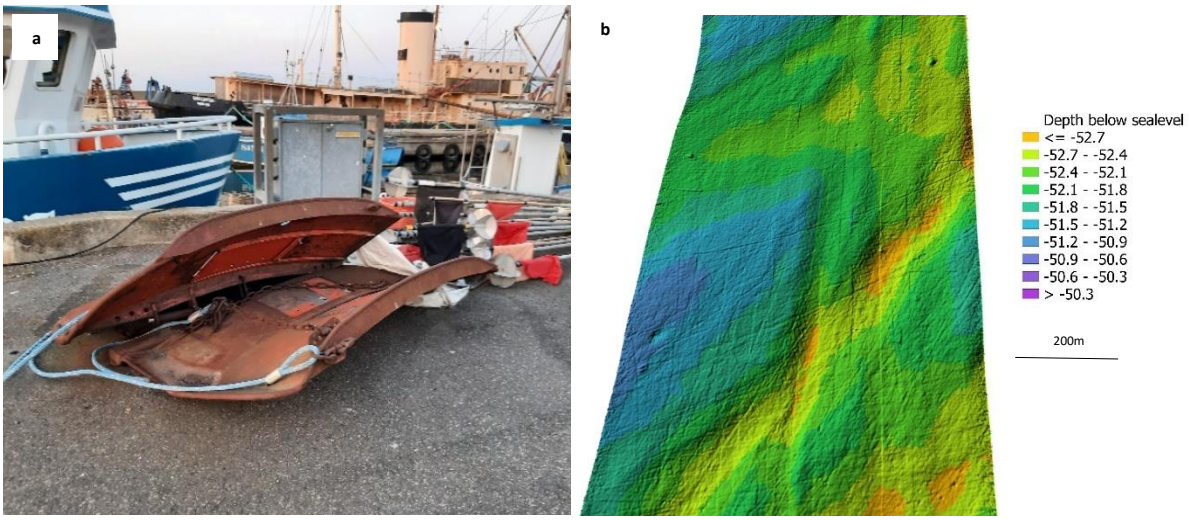



*Figure 1: a.) Otter trawl doors are attached to each side of the net to keep it open and are dragged across the seabed. b.) Bathymetry of seabed at Locality B, obtained through sidescan sonar and multibeam analysis by Prof. Martin Jakobsson during Electra cruise EL23IGV2 with visible criss-crossing trawl track marks. Deeper ridges in red and yellow are part of the natural bathymetry of the seabed.*

Fine-grained sediments such as silts and clays are particularly susceptible to suspension and may be winnowed and transported by currents to adjacent areas by trawling-induced disturbances (Bradshaw et al., 2021; Bruns et al., 2023). Sediments in the subtidal zones in continental shelves, contain a high percentage of mud with the largest carbon storage capacity and are sensitive to anthropogenic disturbances and mixing by trawling, dredging and the installation of offshore structures (Hendriks et al., 2020). Up to 80% of the marine organic carbon burial occurs in continental shelves and contributes to transporting up to 50% of the organic carbon to deeper parts of the ocean, thus playing a vital role in the global carbon cycling (Legge et al., 2020). Since most of the catch obtained by trawling are obtained from productive continental shelves (Amoroso et al., 2018), it is important to understand the overall impact of trawling on carbon reservoirs and carbon mineralization.
During carbon mineralization, organic carbon which is retained in living organisms, decomposing material, water and in sediments (Hendriks et al., 2020); is converted into inorganic carbon usually as a result of the degradation of organic matter (Ouyang et al., 2022). Since nitrogen and carbon are the fundamental constituents in all living matter, the cycling and interaction between these elements are important in understanding the effect that the availability of these has on primary production and mineralization of organic matter (Herbert, 1999).

There has been widespread concern over the adverse effects that trawling poses on benthic communities and changes in biogeochemical processes that regulate nutrient and carbon cycles.
Direct physical trawling disturbances lead to damage or mortality of benthic organisms by displacement and reworking of the sediments and indirectly modifies benthic habitats and sediment structure, and may furthermore affect species-specific trophic interactions in the food web (Bradshaw et al., 2024; Hiddink et al., 2017). Habitats on the seabed that have regularly been trawled have shown a decline in the marine plant biomass and long-lived benthic organisms and bottom-dwelling animals, whereas more short-lived opportunistic species including clams and sea stars dominate (Morys et al., 2021; Van Denderen et al., 2020; Watson et al., 2006). Furthermore, fishing gear that is dragged across the bottom of the ocean results in the largest bycatch rates, whereby less than one fifth of the catch are retained (Watson et al., 2006).

Short-term, small-scale effects related to trawling disturbances result from resuspension and redeposition of sediments, which leads to changes in the sediment composition, porosity, water content and turbidities of the overlying waters, causing modifications in the benthic community structure and their associated bioturbation and bioirrigation potentials, as well as leading to the mortality or damage of benthic organisms (Duplisea et al., 2001; Hiddink et al., 2017; Morys et al., 2021). The trawling-related disturbances have immediate effects on the biogeochemical system in the sediments as well as the overlying water table, as nutrients, organic matter and pollutants are suspended and redeposited. Long-term changes in the benthic community structure, due to transformed benthic habitats as a result of trawling, leads to long-term changes in the nutrient fluxes and biogeochemical processes within the sediments, since trawling related disturbances do not contribute to community metabolism, whereby nutrient fluxes are strongly governed by microbial metabolic pathways and are modified by carbon mixing of the sediments (Duplisea et al., 2001).

Compared to existing knowledge about the adverse effects of trawling on benthic habitats and ecosystems, our understanding of the effects on the overall cycling of carbon and biogeochemical processes in reworked sediments are limited and subject to contradictory results. Trawling has been associated to both an increase in sediment grain size through winnowing as well as a decrease in grain size as a result of particle fragmentation (Bradshaw et al., 2021; Bruns et al., 2023). It has also been attributed to an increase in the organic carbon contents directly after trawling (Pusceddu et al., 2005) as well as a decrease in organic carbon contents in heavily trawled areas (Pusceddu et al., 2014) and an alteration in the biogeochemical composition of organic matter (Bradshaw et al., 2021; Martín et al., 2014; Pusceddu et al., 2005). Furthermore, Olsgard et al. (2008) and Zacharia et al. (2006) found

only small changes in nutrient fluxes from mesocosm experiments, whereas Durrieu De Madron et al. (2005) found short-term effects on the release of nutrients from resuspension experiments. Moreover, carbon mineralization rates show a short-term increase which may have considerable effects on the carbon cycle in continental shelves (Van De Velde et al., 2018). Trawling can have considerable impacts on the regional and global carbon storage capacities and there is a great need in obtaining better estimates in carbon storages on a global scale (Legge et al., 2020).

Numerous studies have obtained short-term recovery rates for benthic species and biogeochemical processes and changes in seabed topography and sediment suspension by conducting trawling experiments in previously untrawled areas by comparing environmental conditions before and after the trawling events (Bradshaw et al., 2021; Morys et al., 2021; Palanques et al., 2001). These experiments, however, greatly underestimate the recovery rates, especially for mobile fauna, since they often study related changes after only one trawling event (Hiddink et al., 2017). More representative recovery rates may be obtained by conducting comparative studies between frequently trawled areas and untrawled areas with the use of high-resolution trawling intensity maps (Hiddink et al., 2017).

To summarize, within the marine environment, there are complex interactions and variabilities between biological processes, natural processes, trawling- induced disturbances and biogeochemical processes, which all effect the system and cycling of geochemical components differently (Bradshaw et al., 2024). There are limited studies that have focused on the combined effects of all processes and may therefore underrepresent trawling related effects. The aim of this study is to compare biogeochemical variations between 3 sites classified into high- and low-trawled localities, based on high resolution SAR (swept-area ratio) and fishing intensity maps interpolated from detailed information from fishing log books and fishing vessels equipped with VMS (vessel monitoring systems) (Bradshaw et al., 2024), in the Bornholm basin which has been trawled at low, medium and high intensities until 2019. The objective of this study is to understand environmental variabilities in the context of trawling-induced variabilities and whether trawling poses a persistent effect on marine biogeochemical processes and eventual carbon sequestration by identifying trawling related effects on a) surface sediment properties, b) solid-phase sediment profiles, c) porewater profiles, d) whole-core benthic incubation experiments and e) macrofaunal abundances. To accomplish this, on-site samples of sediments, sediment porewaters, overlying waters from whole-core benthic incubation experiments, macrofauna and CTD scans were obtained and analysed for chemical components and properties.

## 1.1 Rationale, aim and hypotheses

The aim of this study is to assess the effect of benthic trawling on biogeochemical seafloor disturbance and recovery in the Bornholm basin within the southern Baltic Sea, by means of on-site sampling, porewater and sediment chemical analyses, benthic flux incubation experiments and macrofaunal abundances. The sampling campaign was conducted from 05/06/2023 – 15/06/2023 during Electra cruise EL23IGV-2. More specifically, the study aims to identify the main drivers of carbon cycling/burial and to what extent carbon mineralization processes change due to seafloor disturbances, provide insight into whether benthic trawling poses a persistent effect on marine biogeochemical processes and eventual carbon sequestration, and whether and to what extent these changes are reversible.

The study assesses the following hypotheses:

- Variability between study sites lead to differences in concentration ranges in porewater and sediment concentrations. To identify the spatial effects of trawling on carbon mineralization and porewater geochemistry, it is crucial to compare locality pairs categorized into high- and low-trawling intensities at locations with similar conditions.
- Trawling causes analytically identifiable differences in biogeochemical components.
- Fluxes of dissolved inorganic carbon remain elevated in chronically disturbed areas.

The study assesses the following questions:

- Do sediments and porewater profiles reflect variabilities between study sites and if so, how are variabilities reflected in localities classified into pairs of high- and low-trawling intensity?
- How do porewater profiles compare to trends of early diagenesis and how can these comparisons be applied to discriminate between advective processes (bioturbation/bioirrigation) and/or diffusive processes?
- Can the study constrain evidence for trawling as the main driver of changes in biogeochemical and carbon mineralization processes within sediments and porewaters?
- Which chemical/biological processes have the largest effects on particle and solute mixing and flux rates, and are there ways to discriminate mixing effects to bioirrigation, bioturbation and/or trawling?
- Can the study establish a timeline for re-equilibration in the biogeochemical system after trawling?

# 2. Materials and Methods

## 2.1 Site Description

The study area is located in the Bornholm basin of the Baltic Sea on the south-eastern coast of Sweden approximately 17 kilometers off the coast of the Simrishamn habour (figure 2). This area has been trawled at low, medium and high intensities since the end of the 19$^{th}$ century until 2019 mainly with the use of otter trawls targeting cod and flatfish (Eero et al., 2007). The European commission has emplaced a prohibit on commercial fishing of the Eastern Baltic cod in 2019 specifically targeting demersal trawling fisheries (European Commission, 2019). The Bornholm basin spans an area of approximately 38,990km$^2$ reaching a maximum water depth of 100m at its the centre and is connected to the Bornholm Gate and Arkona basin through a large submarine channel (Christoffersen et al., 2007; Snoeijs-Leijonmalm et al., 2017). It is characterized by a strong thermohaline stratification as a result of freshwater input from the Baltic drainage basin and dense saltwater input from the North Sea through the Arkona basin influencing the redox conditions of bottom waters (Binczewska et al., 2018; Corell et al., 2023). A combination of a reduction in bottom water ventilation, low retention times, along with eutrophication from high nutrient inputs leads to water oxygen deficiencies and anoxia within the bottom waters (Binczewska et al., 2018; Corell et al., 2023). The depth of the halocline in the Bornholm Sea is at 50-60 metres, surface water salinity reaches 4-8 metres and deep-water salinity is at 13-17 metres (Snoeijs-Leijonmalm et al., 2017). The sediments in the Bornholm basin are mainly composed of fine-grained silts and clays with a small proportion of fine-grained sands that are high in organic matter, fining towards the north east of the basin and are mainly transported through submarine channels from the shallower Bornholm Gate and the Arkona basin and seasonally from the Oder River towards the south and accumulate mainly as a result of wave induced erosion of the coast (Christoffersen et al., 2007) . Phytoplankton blooms in the Baltic Sea are prominent from early spring to autumn (April – October) (HELCOM, 2002; Winogradow & Pempkowiak, 2014). Inflow of land derived biogenic substances lead to high primary production in the Baltic Sea (HELCOM, 2002).

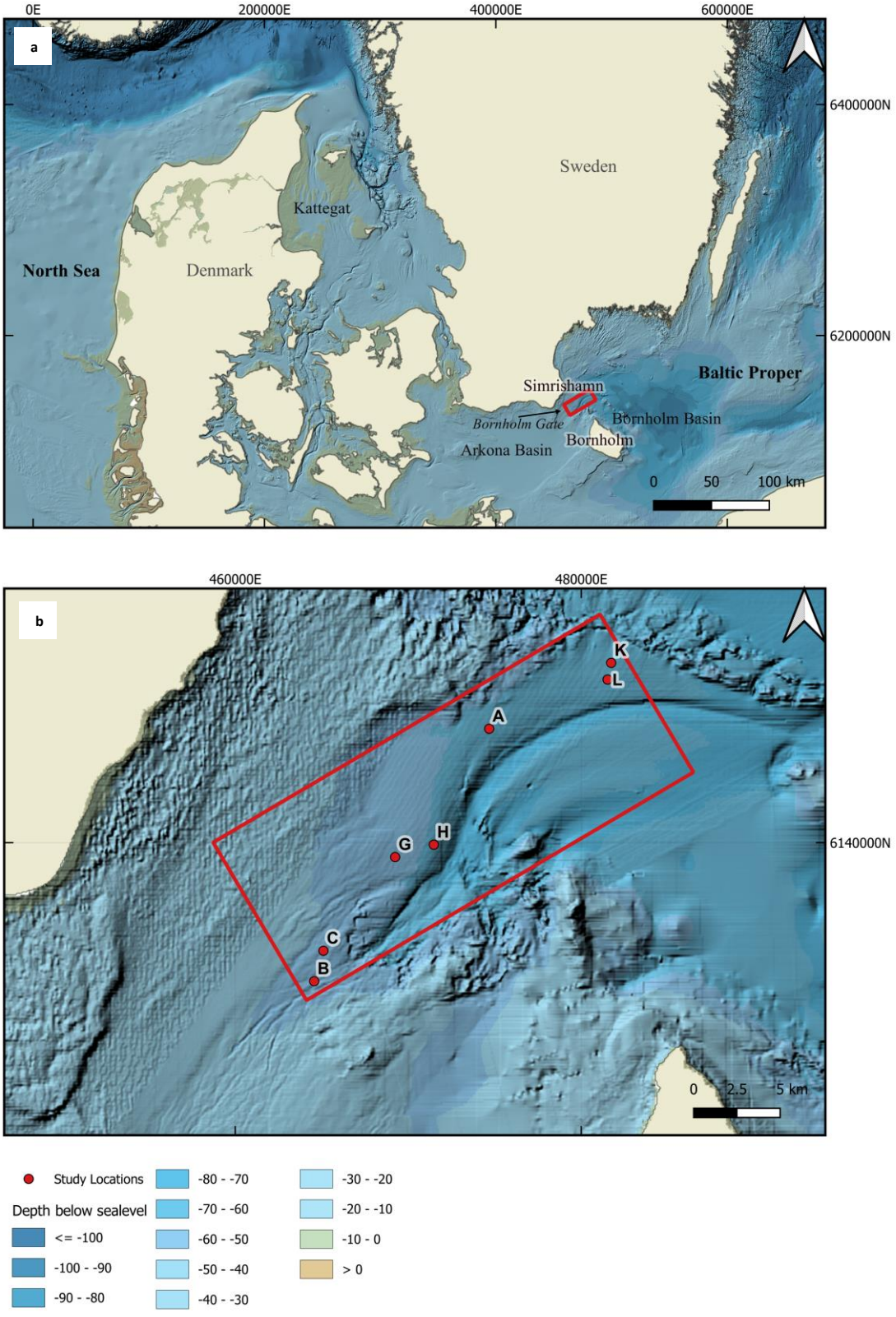



*Figure 2: a.) Overview map of study area, located southeast off the coast of Simrishamn, in the Bornholm basin. b.) Study sites and localities. Study sites were divided into pairs of high and low trawling: 1. A (High), 2. B(Low)/C(High), 3. G (Low)/H (High), 4. L(Low)/K(High).DTM files for bathymetry were downloaded from EMODnet: https://emodnet.ec.europa.eu/geoviewer/*

### *2.1.1 Study Locations*

The study area was divided into 4 sites across a 27-kilometer trajectory (table 1). 3 of the sites were classified into pairs of high- and low-trawling localities: 1. A (High), 2. B (Low)/C (High), 3. G (Low)/H (High), 4. L (Low)/K (High) (figure 3 and 4). The site pairs were chosen to have similar depths (50 – 65m), are relatively close to each other, are similar in their sedimentary composition, show comparable hydrographic conditions and display areas of high- and low-trawling intensities based on fishing route data from 2012-2016. Pairs K and L were selected, since L is located near a shipwreck and could therefore potentially show lower trawling intensities than the fishing statistics reveal. However, multibeam and side-scan sonar surveys revealed trawling tracks throughout most of locality L and is thus likely representative of a highly trawled area.
Identical localities were chosen for Electra research cruises EL19-IGV03 and EL20-IGV03 in 2019 and 2020 whereby the spatial distributions of the trawling intensities were obtained as follows described by Bradshaw et al. (2024). The trawling intensities were interpolated and calculated from logbooks and Swedish fishing vessels that are 12 meters or longer and are equipped with vessel monitoring systems (VMS), providing information on vessel speed, course, size and gear type. By interpolating VMS data to 1-minute intervals and integrating it with modeled bottom trawl gear widths, the swept area ratio (SAR) was calculated. The SAR was used to identify areas of High and Low fishing intensity for the years 2012 – 2016, reflecting long-term fishing patterns (after 2016 there was a decline in fish stocks). The SAR was then compared to fishing data from the ICES and confirmed with swept areas calculated for the years of 2016-2019 within a 250m radius of the sampling sites. High trawling localities (A, C, H, K, L) were chosen from SAR with >6$y^{-1}$ and low trawling localities (B, G) were chosen from SAR with <1$y^{-1}$ (Bradshaw et al., 2024). Localities were chosen on soft sediment seabeds with comparable water depths (50-65m) and hydrographic conditions (Bradshaw et al., 2024).
The sites and localities within the study area are as follows (table 1):

| Site | Locality | Trawling Intensity | Sampling Date | Coordinates Latitude N Longitude E | Depth: Sample BSL (m) |
|---|---|---|---|---|---|
| 1 | A | High | 11/06/2023 | 55.46N 14.60E | 62 |
| 2 | B | Low | 08/06/2023 | 55.33 N 14.44 E | 52 |
| | C | High | 07/06/2023 | 55.35 N 14.45 E | 51 |
| 3 | G | Low | 06/06/2023 | 55.40 N 14.51 E | 58 |
| | H | High | 05/06/2023 | 55.40 N 14.55 E | 63 |
| 4 | K | High | 13/06/2023 14/06/2023 | 55.50 N 14.71 E | 65 |
| | L | Low | 13/06/2023 15/06/2023 | 55.49 N 14.71 E | 65 |

*Table 1: Spatiotemporal attributes of Electra cruise EL23-IGV-2*

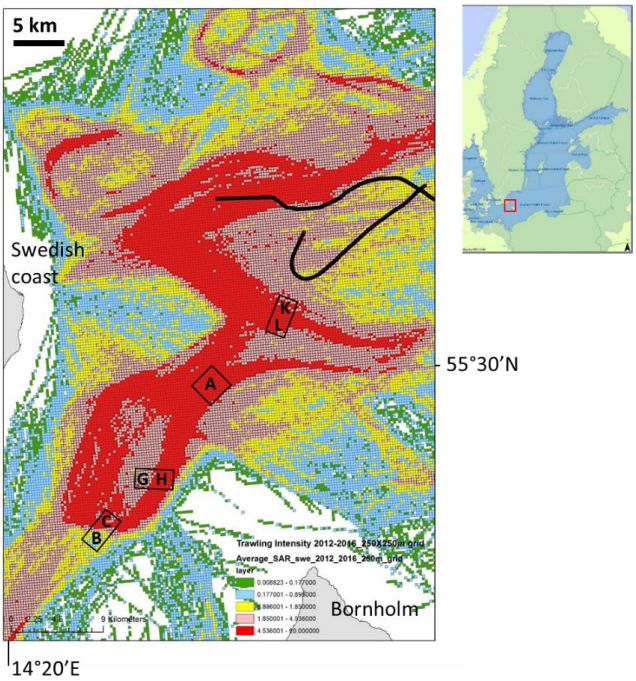



*Figure 3: Site classification and trawling intensities in study area. Displays 3 sites with paired High/Low trawling localities and 1 site with High trawling intensity. Colour scale represents average bottom trawling intensity between 2012 and 2016. Red indicates areas that are disturbed 1-5 x /year (SAR =1-5 $y^{-1}$). Blue indicates areas that are disturbed between 0.04-0.2 x /year (SAR=0.04-0.02$y^{-1}$). Bold tracks indicate trawl tracks from a contaminant investigation from 2019.Modified after (Bradshaw et al., 2024)*

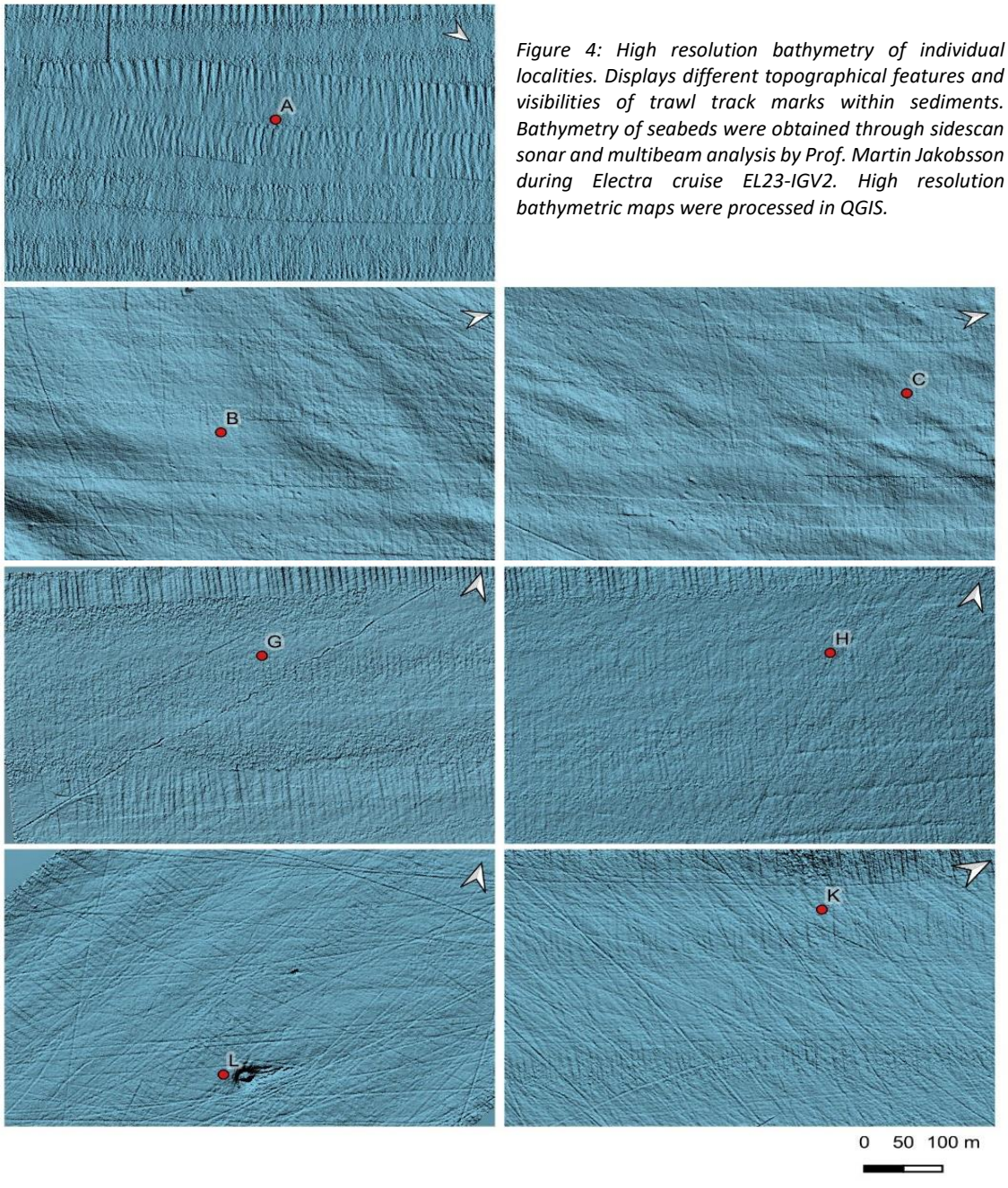



*Figure 4: High resolution bathymetry of individual localities. Displays different topographical features and visibilities of trawl track marks within sediments. Bathymetry of seabeds were obtained through sidescan sonar and multibeam analysis by Prof. Martin Jakobsson during Electra cruise EL23-IGV2. High resolution bathymetric maps were processed in QGIS.*

## 2.2 Field methods

At each locality a total of 19 Gemini cores, 3 van Veen grabs and bottom waters/water column profiles were collected via a CTD (Conductivity, Temperature, Depth) and Rosette sampler. For the scope of this study the main research focus is on the biogeochemical sediment and porewater data obtained from the Gemini cores and the benthic flux incubation experiments. Of the Gemini cores, 3 replicates were collected for sediment and porewater analyses and 4 replicates were collected for flux incubation experiments to determine the rate of exchange of carbon mineralization products between sediment and overlying seawater, an indicator of the total carbon mineralization activity in the sediment. Porewater and flux samples were analysed for DIC, $\delta^{13}C$ and nutrient concentrations ($PO_4^{3-}$, $NH_4^+$, and $NO_3^-$). Sediment samples were analysed for porosity, chlorophyll, TOC, $\delta^{13}C_{TOC}$, TC, TN, $\delta^{15}N$ and $\delta^{13}C_{totalC}$ contents. 6 cores and 3 van Veen grabs were collected for macrofauna analyses and 3 cores for DNA and C-quality analyses, these are beyond the scope of the study and will only be described briefly.

### *2.2.1 CTD + Rosette sampler*

A CTD (Conductivity, Temperature, Depth) was collected until a depth of 0.5m above the seabed (figure 5). The CTD measured the following parameters during descent every 25cm: $O_2$(mg/L), temperature (°C), salinity (PSU), conductivity (mS/cm), turbidity and exact coordinates. The bottom waters collected by four Niskin bottles mounted on a Rosette sampler at 0.5m above the seabed were stored in four 5L reserve tanks which were immediately stored in a cold room at 7-8°C and required for benthic flux incubation experiments.



*Figure 5: CTD (Conductivity, Temperature, Depth) mounted to the bottom of the instrument (not visible in the picture) and Rosette sampler with 12 x 5L Niskin bottles. The CTD measured various variables at different depths. Water samples were collected at approximately 0.5m above the seabed and were filled into reserve tanks required for the preparation of benthic flux incubations.*

### *2.2.2 Gemini coring*

At each locality a total of 19 cores were collected using a 2-core multicorer (figure 6). Difficulties in coring occurred in particularly sandy sediments which required multiple sampling trials. Coordinates were recorded for each core pair and cores for different parameters were chosen randomly throughout the day to account for possible local variabilities of the sediments. Generally, longer cores were chosen for samples collected for sediment properties and porewater analyses. The plastic tubes to retrieve the sediments were ~65cm in length and had a diameter of ~10cm. The cores were stored upright and gently closed off with rubber stoppers on both openings until sampling. The sediment depths ranged from ~6-30cm. The sediments were sampled on ship by placing the plastic tubes on a piston and gently pushing the material into a ring and slicing it with a spatula.

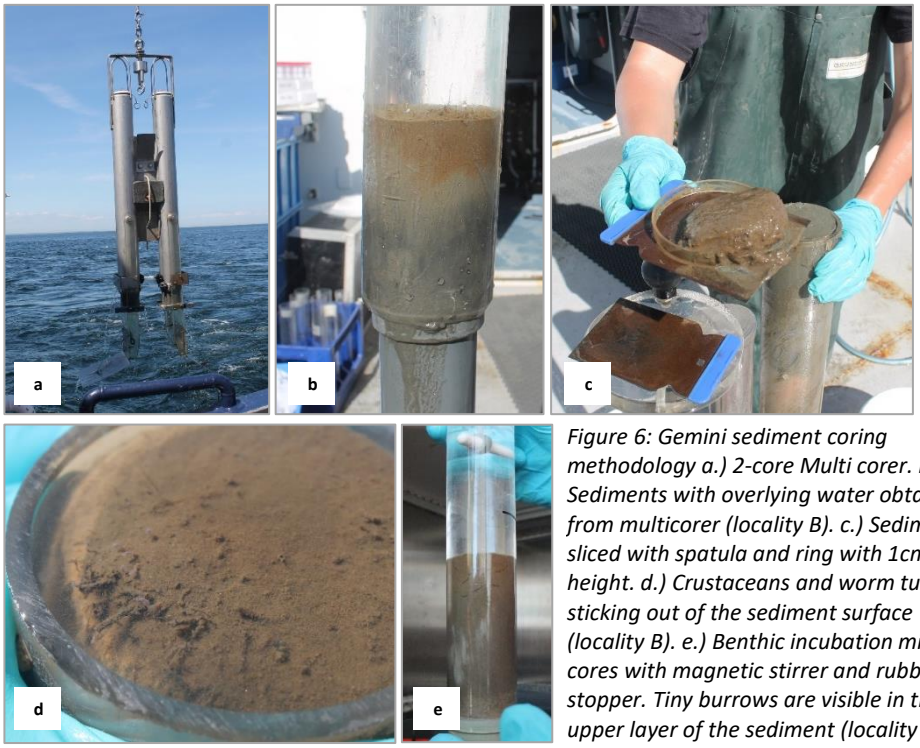



*Figure 6: Gemini sediment coring methodology a.) 2-core Multi corer. b.) Sediments with overlying water obtained from multicorer (locality B). c.) Sediment sliced with spatula and ring with 1cm height. d.) Crustaceans and worm tubes sticking out of the sediment surface (locality B). e.) Benthic incubation mini cores with magnetic stirrer and rubber stopper. Tiny burrows are visible in the upper layer of the sediment (locality C).*

#### *2.2.2.1 Sediment properties:*

At each locality, 3 of the Gemini cores were designated to sediment properties analyses (porosity, grainsize, chlorophyll, TOC, $\delta^{13}C_{TOC}$, TC, TN, $\delta^{15}N$ and $\delta^{13}C_{totalC}$ contents). Sediments were sampled on ship by gently pushing the piston through the plastic ring and slicing them with a spatula every centimetre to the bottom of the core. The samples were stored in plastic ziplock bags and frozen immediately after sampling for further analysis.

#### *2.2.2.2 Porewater analyses:*

At each locality, 3 of the Gemini cores were designated to porewater analyses (DIC, $\delta^{13}C$ and $PO_4^{3-}$, $NH_4^+$, and $NO_3^-$ concentrations). Sediments were sampled by gently pushing the piston through the plastic ring and slicing them with a spatula every 1cm until a 10cm sediment depth, every 2cm until 20 cm and every 5cm until the bottom of the core. The overlying water was collected with a syringe 1cm above the sediment surface and transferred to a 14mL Falcon tube. Sediments were collected into separate Falcon tubes, and sealed with parafilm, avoiding air bubbles.

The samples were stored in the fridge until porewater extractions. Porewaters were extracted using pre-soaked rhizon samplers (0.15µm pore size) and extracted through the vacuum of the 10mL syringe via a 3-way luer-type stop-cock (figure 7). 2mL of porewater was transferred into 2mL dark glass crimp vials and sealed without air for DIC and $\delta^{13}C$ analyses. The remaining porewater was transferred to 2mL Eppendorf containers for nutrient analyses and stored frozen.



*Figure 7: Methodology for porewater sampling. Rhizons were inserted into sediment filled Falcon tubes, attached to a syringe via a 3-way luer-type stock-cock. Porewater was drawn out through a vaccum created by the syringe.*

### *2.2.2.3 Benthic flux incubations:*

At each locality, 4 Gemini cores were designated for benthic flux incubation analyses ($O_2$, DIC, $\delta^{13}C$, $PO_4^{3-}$, $NH_4^+$, $NO_3^-$). Minicores (4.6 cm diameter, 30 cm length) were inserted into the larger cores with an approximate 50:50 ratio of sediment and overlying water (figure 8). Benthic incubation cores were capped and stored at 7-8°C. Bottom water was collected with a CTD Rosette sampler and measured for temperature, salinity, and $O_2$ with a WTW Multi3430 multimeter. The benthic incubation cores were refilled with the bottom water using a syringe and floating polystyrene disk, avoiding disturbances. A magnetic stirrer was placed 5-6 cm above the sediment to homogenize the overlying water. Cores were left uncapped in the incubator for 3-4 hours to stabilize before initial sampling ($t_0$). At $t_0$, 15 mL water samples were collected with a syringe and filtered to 0.45µm and the time $t_0$ was recorded. For DIC analysis, 2 mL was filtered into a dark glass crimp vial. For nutrient analysis, 12-13 mL was filtered into a Falcon tube and stored frozen. $O_2$ concentrations were measured with the multimeter and recorded for $t_0$. The water that was removed was replaced with tank bottom water. After 13-24 hours, the $t_1$, $O_2$ concentrations and times were recorded, and DIC and nutrient samples were collected as described above.




*Figure 8: Benthic flux incubations. a.) minicore with magnetic stirrer, capped with rubber stoppers on either side. Water:Sediment ratio was approximately 50:50. b.) Incubation container in 7-8°C cold room with bottom water reserve tank from Niskin bottles to the right and Multimeter measuring $O_2$ concentrations.*

### *2.2.3 Macrofauna*

#### *2.2.3.1 Van Veen grabs*

To obtain the macrofauna abundances in the overlying sediments, 3 van the Veen grabs were taken at each station (figure 9). The sediments were sieved on 0.5µm and 1mm sieves to extract the macrofauna and each fraction was preserved in labelled containers with an ethanol and glycerol mixture and stored in a ventilated room.

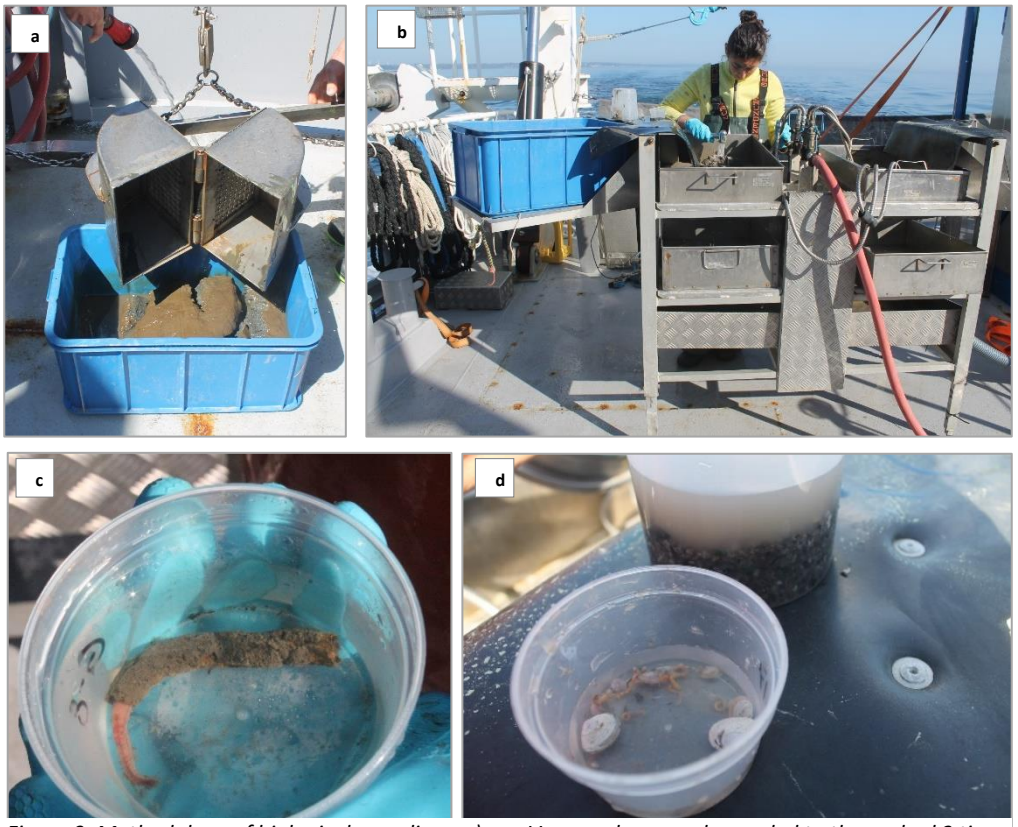



*Figure 9: Methodology of biological sampling. a.) van Veen grabs were descended to the seabed 3 times and emptied into blue crates. b.) Sediments were sieved for Macrofauna. (0.5µm and 1mm). c) Larger species were collected with tweezers (locality B). d.) Macrofauna were preserved within an ethanol and glycerol mixture (locality G).*

## 2.3 Laboratory methods

DIC of benthic fluxes and porewaters were measured on a SRI 8610 gas chromatograph containing a 1.5m Haysep D by FID on column injection. $\delta^{13}C$ of DIC was measured by stable isotope ratio mass spectrometry on the Thermo Scientific MAT 253 + Gas Bench 2. All nutrients were measured through spectrophotometric methods on the Thermo Scientific evolution 200 instrument with their specific wavelengths. Sediment samples were analysed for TOC, $\delta 13C_{TOC}$, TC, TN, $\delta 15N_{totalN}$ and $\delta 13C_{totalC}$ by isotope ratio mass spectrometry through combustion-GC-TCD (Thermal Conductivity Detector) detection on the Thermo Fisher Scientific EA IsoLink IRMS System containing a CNSOH analyser. Analyses and sample preparation done by myself include the DIC analyses of benthic fluxes and porewaters through gas chromatography and all nutrient and flux analyses through spectrophotometry. Sediment isotope mass spectrometry and weighing of sediments was done by myself with the help of Haoyi Yao from the Department of Geological Sciences (IGV) at Stockholm University. Haoyi Yao furthermore analysed all of the $\delta^{13}C$ of DIC by stable isotope ratio mass spectrometry. Freeze-drying, calculations of bulk densities, porosities and chlorophyll concentrations

of sediment samples were done by the Department of Ecology and Environment (DEEP) at Stockholm University. Abundances and wet weights of fauna were analysed and identified by Prof. Clare Bradshaw from DEEP. See detailed description of each analytical method below.

### *2.3.1 Porewater and Benthic fluxes*

#### *2.3.1.1 DIC for porewaters and benthic fluxes*

The porewater and flux samples of all cores yielded 292 samples in total and the DIC of all porewater and flux samples was measured on a SRI 8610 gas chromatograph containing a 1.5m Haysep D column and methanizer by FID (Flame Ionization Detector) on column injection with an $N_2$ carrier gas (Nitrogen 5.0 LAB Line) operated at 60mL/min. The oven temperature of the instrument was set to 80°C with an FID baseline at approximately 49.9-55.0 mV. DIC samples were prepared by transferring 0.5mL of sample into pretreated 12mL Labco Exetainers with a hypodermic needle (27G). The Labco Exetainers were prepared by adding 100µL of a 90% concentrated solution of $H_3PO_4$ and flushing them with Helium (Helium 5.0 LAB line) at a rate of approximately 100mL/min for ten minutes. A series of standards were prepared from a 20mM $NaHCO_3$ stock solution with a range of 0.125, 0.25, 0.5, 1.0, 2.0, 3.0, 4.0 and 20mM. 0.5mL of the $NaHCO_3$ standard solution and sample were transferred to the pretreated Labco exetainers and stored upright in a dry and dark box. To test the stability of the instrument, 50µL of 2 different gas standards were injected into the instrument prior to the sample analysis. Standard 1 had the following concentrations: $CO_2$ 1000ppm, $N_2O$ 1ppm, $CH_4$ 10ppm. Standard 2 had the following concentrations: $CO_2$ 10 000 ppm, $N_2O$ 5ppm and $CH_4$ 100ppm. Once the instrument was stable and had a constant baseline, 50µL of the $NaHCO_3$ standard and sample was injected into the instrument gradually while waiting for the baseline to stabilize after each injection. The final DIC concentrations were calculated from the calibration curve of the $NaHCO_3$ standards with known concentrations and the area obtained by the gas chromatograph for the standards and each sample. The $r^2$ for the regression line of the standards ranged between 0.9992-0.9999 (table 2).

| Dissolved Inorganic Carbon (DIC) analysis | | | |
|---|---|---|---|
| **Date** | **Samples** | **Regression line (y)** | **$r^2$** |
| 18/10/2023 | Porewater + fluxes: B | 532.81x | 0.9999 |
| 19/10/2023 | Porewater + fluxes: C | 612.49 | 0.9995 |
| 20/10/2023 | Porewater + fluxes: G | 538.22x | 0.9995 |
| 20/10/2023 | Porewater: H1+H2 | 538.22x | 0.9995 |
| 23/10/2023 | Porewater + fluxes: H3 | 572.99x | 0.9997 |
| 30/10/2023 | Porewater + fluxes: A | 544.95x | 0.9993 |
| 31/10/2023 | Porewater + fluxes: K1 | 543.72x | 0.9998 |
| 02/11/2023 | Porewater: K2 | 550.89x | 0.9996 |
| 03/11/2023 | Porewater: K3 and all fluxes | 542.2x | 0.9992 |
| 06/11/2023 | Fluxes: L | 553.36x | 0.9995 |
| 07/11/2023 | Porewater: L1+L2 | 545.83x | 0.9993 |

*Table 2: Date, descriptions and accuracy of regression lines of DIC analysis.*

#### *2.3.1.2 $\delta^{13}C$ of DIC*

For the analysis of $\delta^{13}C$ the same 292 porewater and flux samples prepared for the DIC analyses were analysed by stable isotope ratio mass spectrometry on the Thermo Scientific MAT 253 + Gas Bench 2. Standards were prepared by adding 200 ± 50 µg of the international standards NBS 18 and IAEA 603 and 200 ± 50 µg of in-house quality control of Carm 2 and Merck $CaCO_3$ into 12mL Labco Exetainers. After the addition of the standards and in-house quality control, 100µL of a 90% concentrated solution

of $H_3PO_4$ was added to the standards/in-house quality control exetainers and were flushed with Helium (Helium 5.0 LAB line) at a rate of 100mL/min for 10 minutes. Thereafter the $CO_2$ generated in the headspace of the exetainer as a result of $H_3PO_4$ addition was collected with a needle through the septum and injected into the machine and transported with a helium carrier gas. The GC column operated at approximately 70°C separating the molecular species. This yielded, 9 peaks with systematically decreasing areas on the screen. Since the first two peaks are often representative of oversaturation only the first 7 peaks were used to calculate the average area of the isotope ratios. The standard deviation for the 7 peaks was <0.08%. 3 corrections were made to obtain the final concentration of the samples. The first correction involved fitting a linear regression line of the sample peaks to the linear regression obtained from the in-house control standards. The second correction was a drift correction which was applied after 10 samples and the final correction involved the international standards, whereby the calibration of the international standards was applied to calculate the final concentration of the isotopes.

#### *2.3.1.3 Nutrients*

Concentrations of $PO_4^{3-}$, $NO_3^-$ and $NH_4^+$ were determined by spectrophotometric methods and measured on the Thermo Scientific evolution 200 instrument on their specific wavelengths. A total of 291 samples were measured of which 70 samples are benthic flux samples and the remaining were porewater samples. For all analyses, the instrument was zeroed on a blank which was prepared from deionized water. All porewater samples were diluted with deionized water. Benthic flux samples were left undiluted. Final concentrations were calculated from regression lines obtained from measured absorbances and concentrations of the standards. The analytical methods for each compound are described below.

*Phosphate ($PO_4^{3-}$):*
Spectrophotometric determination of phosphate was adapted from the analytical methods outlined by Koroleff (1983). Prior to sample preparation 0.31M ascorbic and mixed reagent solutions were prepared and stored in the fridge, covered with aluminium foil and renewed every week.
The reagents were prepared as follows in accordance with the Handbook outlined by Brüchert (2023):

- Ammonium Molybdate solution: A 0.02 M solution was prepared by dissolving 7.5g of ammonium heptamolybdate tetrahydrate ($(NH_4)_6Mo_7O_{24}$ 4 $H_2O$) in 250mL of deionized water and is stored in bottle covered with aluminium foil.
- Potassium Antimonyl-tartrate solution: A 2.04 µM solution was prepared by dissolving 0.34g of Potassiumantimonyltartrate ($SbC_4H_4O_7$ ½H2O) in 250mL of deionized water and is stored in a bottle covered with aluminium foil.
- Diluted Sulfuric acid solution: A 2.91M $H_2SO_4$ solution was prepared by slowly adding 70mL of concentrated $H_2SO_4$ to 250mL of deionized water and was stored in dry and dark cabinet.
- Mixed reagent: The mixed reagent was prepared by adding 100mL of the ammonium molybdate solution and 50mL of the antimonyltartrate solution to 250mL of diluted sulfuric acid. The mixed reagent was kept in a glass bottle and stored in the fridge, covered with aluminium foil and renewed every week.
- Ascorbic acid solution: A 0.31M solution of ascorbic acid was prepared by diluting 1.35g of ascorbic acid in 25mL of deionized water and stored in the fridge, covered with aluminium foil and was renewed every week.
- Phosphate standard stock solution: A 0.01M phosphate solution was prepared by dissolving 1.36g of $KH_2PO_4$ in 1L of deionized water and was stored closed in the fridge.

After the preparation of the phosphate standard stock solution, a 100µM secondary standard phosphate solution was prepared by adding 1mL of the 0.01M phosphate solution to a 100mL

cylindrical volumetric flask and diluting it with deionized water to the meniscus. The 100µM secondary standard solution was used to make the following phosphate dilution series: 0.02, 0.05, 0.1, 0.5, 1.0, 2.5, 4.0, 5.0, 8.0, 10.0, 15.0 and 20.0 µM. Porewater samples were diluted 5 times with deinoized water and flux samples were left undiluted. 1cm cuvettes were prepared by adding 200µL of porewater sample and 800µL of deionized water, 1mL of benthic flux sample and 1mL of deionized water for the blank sample to their respective cuvettes. Thereafter, 100µL of ascorbic acid and 100µL of mixed reagents were added to the samples and no ascorbic acid or mixed reagent was added to the blanks. The wavelength of the instrument was set to a wavelength of 885nm and after 30 minutes, the samples were placed into the sample compartment of the instrument. The instrument was zeroed on the blank and absorbances for the standards and samples were obtained. Final concentrations of the samples were calculated from the regression line obtained from absorbances and known concentrations of the standards. Maximum concentrations for regression lines were chosen based on the highest absorbance ranges obtained for the samples. For samples K and L, which had the highest absorbances and concentrations the regression line was calculated with a maximum concentration of 20µM, the regression lines for the remaining samples were calculated to a maximum concentration of 5µM. The $r^2$ for the regression line of the standards ranged between 0.9118-0.9671 (table 3).

| **Phosphate ($PO_4^{3-}$) analysis** | | | | |
|---|---|---|---|---|
| **Date** | **Samples** | **Regression line (y)** | **$r^2$** | **Dilution** |
| 15/11/2023 | Porewater:A | 0.0205x | 0.9671 | x 20, 50µL sample+ 950µL deionized water |
| 16/11/2023 | Porewater:B | 0.0223x | 0.9118 | x 5, 200µL sample+ 800µL deionized water |
| 20/11/2023 | Porewater:C | 0.0218x | 0.9245 | x 5, 200µL sample+ 800µL deionized water |
| 21/11/2023 | Porewater:G | 0.0194x | 0.9806 | x 5, 200µL sample+ 800µL deionized water |
| 22/11/2023 | Porewater:H | 0.0175x | 0.9907 | x 5, 200µL sample+ 800µL deionized water |
| 23/11/2023 | Porewater:K | 0.018x | 0.998 | x 5, 200µL sample+ 800µL deionized water |
| 24/11/2023 | Porewater:L | 0.0166x | 0.9874 | x 5, 200µL sample+ 800µL deionized water |
| 07/12/2023 | Fluxes: All Samples | 0.0156x | 0.9629 | No dilution |

*Table 3: Date, descriptions and accuracy of regression lines of phosphate analysis.*

*Nitrate ($NO_3^-$):*

Spectrophotometric determination of nitrate was adapted from the analytical methods outlined by Schnetger & Lehners (2014). Prior to sample preparation a mixed reagent solution was prepared and stored in a glass bottle in the fridge, covered with aluminium foil and renewed every other day. The reagents were prepared as follows (Brüchert, 2023):

- Saturated reduced $VCl_3$ solution: A reduced $VCl_3$ solution was prepared by dissolving 800mg of $VCl_3$ in 20mL deionized water, followed by the addition of 8.4mL of concentrated HCl and diluting the mixture to 100mL.
- Sulfanilamide: The sulfanilamide solution was prepared by dissolving 5g of sulfanilamide in 50mL of concentrated HCl and adding 300mL of deionized water. The solution was then diluted to 500mL.
- NED: The NED solution was prepared by dissolving 0.5g of N-1 naphthyl ethylenediamine dihydrochloride in 500mL of deionized water.
- Mixed reagent: A mixed $VCl_3$ solution was prepared by combining 1 part of the $VCl_3$ solution, 1 part of the NED solution and 1 part of the sulfanilamide solution.

A 100mM primary standard stock solution was prepared by diluting 0.85g of sodium nitrate in 100mL of deionized water. The 100mM sodium nitrate primary stock solution was used to make the following dilution series: 1, 2.5, 3, 5, 10, 25 and 50 µM. Porewater samples were diluted 5 times with deionized water and flux samples were left undiluted. 1cm cuvettes were prepared by adding 120µL of sample

to 480µL of deionized water for the porewater samples and 600µL of flux sample and 600µL of deionized water for the preparation of the blank. Thereafter, 500µL of the mixed VCl3 solution was added to the samples and the sample box was covered in aluminium foil and placed in an oven for 1 hour at 50°C. No mixed reagent was added to the blank. The wavelength of the instrument was set to a wavelength of 543nm and the samples were placed into the sample compartment of the instrument. The instrument was zeroed on the blank and absorbances for the standards and samples were obtained. Final concentrations of the samples were calculated from the regression line obtained from absorbances and known concentrations of the standards. Maximum concentrations for regression lines were chosen based on the highest absorbance ranges obtained for the samples which was at a concentration of 25µM for all samples. The $r^2$ for the regression line of the standards ranged between 0.9952-0.9994 (table 4).

| Nitrate ($NO_3^-$) analysis | | | | |
|---|---|---|---|---|
| **Date** | **Samples** | **Regression line (y)** | **$r^2$** | **Dilution** |
| 05/12/2023 | Porewater A,B | 0.0216x | 0.9981 | x 5, 120uL of sample + 480µL of deionized water |
| 06/12/2023 | Porewater C,G,H,K,L | 0.0212x | 0.9952 | x 5, 120µL of sample + 480µL of deionized water |
| 08/12/2023 | Fluxes: All Samples | 0.0228x | 0.9994 | No dilution |

*Table 4: Date, descriptions and accuracy of regression lines of Nitrate analysis.*

*Ammonium ($NH_4^+$):*

Spectrophotometric determination of phosphate was adapted from the analytical methods outlined by Bower & Holm-Hansen (1980). Prior to sample preparation a 1:9 mixture of sodium hypochloride and alkali citrate solution as well as a salicylate nitroprusside solution were prepared. The reagents were prepared as follows (Brüchert, 2023):

- Reagent 1 - Salicylate nitroprusside solution: 440g of sodium salicylate ($C_7H_5NaO_3$) and 0.28g of sodium nitroprusside ($Na_2[Fe(CN)_5NO]2H_2O$) were diluted in 1L of deionized water. The solution was kept in a glass bottle covered in aluminium foil and is stable for 3 months.
- Reagent 2 – Alkali hypochlorite solution: 18.5g of sodium hydroxide (NaOH) and 100g of tri-sodium citrate (Na3C6H5O7) were diluted in 1L of deionized water. The solution was kept in a glass bottle with no expiration date.
- 5% Sodium hypochlorite solution: A 5% hypochlorite solution of household chlorine was used.

A solution containing one part of the 5% Sodium hypochlorite solution and 9 parts of Reagent 2 were made during sample preparation since the solution expires within 1 hour. A 100mM primary stock solution was prepared from $NH_4Cl$ for the standards. For the standard dilution series, the 100mM primary stock solution was used to make a 200µL secondary stock solution and used to make the following $NH_4Cl$ dilution series: 0.5,1.0, 2.5, 5.0, 10.0, 50.0 and 200µM. The upper 6cm of porewater samples were diluted 2 times and samples deeper than 6cm were diluted 20 times with deionized water. Benthic flux samples were left undiluted. 1cm cuvettes were prepared by adding 500 uL of sample and 500uL of deionized water for the upper 6cm and 50uL of porewater sample and 950uL of deionized water for porewater samples deeper than 6cm. 1mL of flux sample and 1mL of deionized water for the blank was transferred to the cuvette. Thereafter, 120uL of Reagent 1 and 200uL of the Reagent 2 mixture was added to the sample. No reagents were added to the blanks. Samples were placed in the dark for 1 hour until colour reaction was fully developed. Thereafter, the instrument wavelength was set to 640nm and samples were placed into the sample compartment of the instrument. The instrument was zeroed on the blank and absorbances for the standards and samples were obtained. Final concentrations of the samples were calculated from the regression line obtained from absorbances and known concentrations of the standards. Maximum concentrations for regression lines were chosen based on the highest absorbance ranges obtained for the samples which

was at a concentration of 200µM for all porewater samples and 50µM for benthic flux samples. The $r^2$ for the regression line of the standards ranged between 0.9882-0.9984 (table 5).

| Ammonium ($NH_4^+$) analysis | | | | |
|---|---|---|---|---|
| **Date** | **Samples** | **Regression line (y)** | **$r^2$** | **Dilution** |
| 13/12/2023 | Porewater:A | 0.0115x | 0.9882 | 0-6cm: x 2 dilution, 500µL sample + 500µL deionized water. 6-bottom: x 20 dilution, 50µL sample + 950µL deionized water |
| 14/12/2023 | Porewater:B,C,G,H,K,L | 0.01x | 0.9894 | 0-6cm: x 2 dilution, 500µL sample + 500µL deionized water. 6-bottom: x 20 dilution, 50µL sample + 950µL deionized water |
| 10/01/2024 | Fluxes: All Samples | 0.0141x | 0.9984 | No dilution |

*Table 5: Date, descriptions and accuracy of regression lines of Ammonium analysis.*

## *2.3.2 Sediments*

### *2.3.2.1 Sediment grain sizes and sedimentation rates*

Grain size data and sedimentation rates were obtained from sediments collected during the EL20-IGV03 cruise. Grainsizes were obtained from <0.5mL well-mixed sediments per slice and analysed using laser diffraction with a Malvern Mastersizer 3000. Grainsizes were calculated using the average of 2 subsamples. Grain size criteria are as follows: Clay (%): <2 µm, Fine silt (%): 2-10 µm, Sortable silt (%): 10-63 µm, Sand (%): 63 µm- 2mm, Gravel (%): 2-3.5 mm.
Sedimentation rates were obtained by applying the Constant Flux:Constant Sedimentation (CF:CS) rates to excess $^{210}Pb$ concentration profiles below the mixed layers whereby the average sediment accumulation rates for the last century were obtained by analyses done by gamma spectrometry at Edith Cook University, Australia. Since sediment layers within all localities are relatively mixed, they are subject to high uncertainties and sedimentation rates need to be considered with caution.

### *2.3.2.2 Particulate: TOC, $\delta^{13}C_{TOC}$, TC, TN, $\delta^{15}N_{totalN}$ and $\delta^{13}C_{totalC}$*

A total of 147 sediment samples were analysed which included 1 sediment core from locality A, K and L each and 2 replicate cores from locality B, C, G and H. Sediment samples were ground and freeze dried and prepared for isotope ratio mass spectrometry through combustion-GC-TCD (Thermal Conductivity Detector) detection on the Thermo Fisher Scientific EA IsoLink IRMS System with a CNSOH analyser for particulate TOC, $\delta13C_{TOC}$, TC, TN, $\delta15N_{totalN}$ and $\delta13C_{totalC}$ content. Standards and inhouse controls for each tray were prepared by weighing the following weights into tin capsules for each tray:

- x6 Inhouse control H (High organic content sediment IVA 338 02151): 7-8mg
- x6 Inhouse control L (Low organic content sediment IVA 33802153): 10 ± 0.5mg
- x4 IAEA 600 (caffeine): 195-235µg
- x4 IAEA CH3 (cellulose): 250-350µg
- x4 N-std (IAEA-N1):350 ± 50µg

The tin capsules were folded into squares and placed into their appropriate slots on the tray. One plate could accommodate 71 samples which were prepared as follows:
Each sample was weighed out twice into tin and silver capsules respectively. Sediments were weighed into tin capsules for samples designated to TC, TN, $\delta^{13}C$ and $\delta^{15}N$ analyses. Sediments were weighed in silver capsules designated to TOC and $\delta^{13}C_{TOC}$. To dissolve all inorganic $CaCO_3$, 100µL of a 2M HCl solution was added to the sediment samples in the silver capsules and dried in an oven set to 60°C for 2 hours; thereafter another 100µL of the HCl solution was added to the sediment samples and left in the oven overnight at 60°C. Sediments at locality K and L contained high $NH_4$ and DIC concentrations and sediment samples were weighed to 10 ± 1mg into tin and silver capsules respectively. Sediments

at locality A,B,C,G and H contained low $NH_4^+$ and DIC and 20 ± 1mg was weighed into tin and silver capsules respectively. All weights for samples and standards were recorded. Once all sediments were weighed out into both tin and silver capsules, the capsules were inserted into the carousel autosampler of the instrument. Capsules with their samples were combusted in an exothermic reaction within the elemental analyzer reaching a temperature of up to 1800°C (Thermo Fisher Scientific GmbH, 2010) and are oxidized within the first reactor leading to the oxidation of carbon to $CO_2$ and nitrogen to $N_2O$ and transported with a helium carrier gas (figure 10). Thereafter the combusted products are carried to the second reactor which contains a copper plate leading to the reduction of $N_2O$ to $N_2$. $H_2O$ is removed in a water trap column. $CO_2$ and $N_2$ are separated on an isothermal GC (Gas chromatography column) (Thermo Fisher Scientific GmbH, 2010). The different magnetic properties of the isotopes cause different curvature paths upon bombardment with high voltages leading them to their specific detectors in the isotope mass spectrometer.

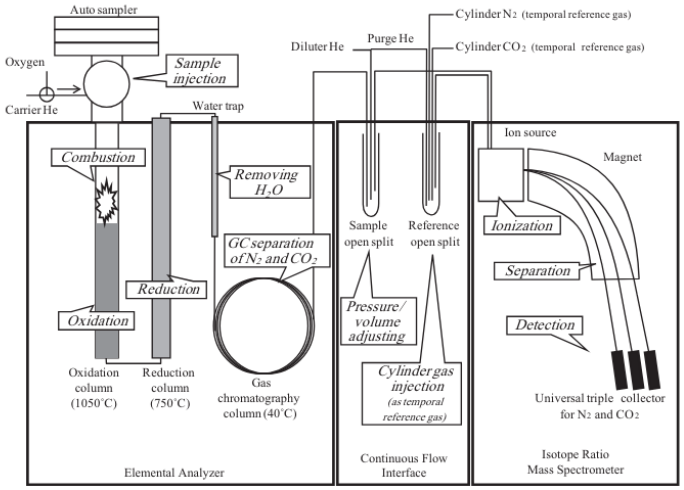



*Figure 10: An illustration of the workflow of a conventional EA-IRMS system from (Ogawa et al., 2010).*

### *2.3.2.3 Chlorophyll*

Triplicate subsamples of 1 mL sediment were taken from each thawed and homogenized sample and each mixed with 6 mL of 96% ethanol and left overnight in the dark at 4°C. The day after, samples were centrifuged for 5 min at 4000 rpm, the supernatant filtered on a GF/F filter and chlorophyll-a analysed on a Shimadzu spectrophotometer at 663 and 750 nm following the method of HELCOM (1988).

## 2.4 Data processing and calculations

### *2.4.1 Calculations of diffusive fluxes*

*Diffusive fluxes from Benthic Flux incubations:*

A total of 70 flux samples were analysed (10 for each site) for DIC, $PO_4^{3-}$, $NO_3^-$ and $NH_4^+$. $O_2$ concentrations were measured directly from the minicores with a multimeter. For each site, 4 samples were allocated to $t_0$ analyses, 2 duplicate samples for bottom water reserve tank and 4 $t_1$ samples collected 13-24hours after $t_0$. Field sampling and analytical methods are described above in section 2.2 and 2.3 respectively. Fluxes were calculated based on concentration changes in the sediments of the benthic fluxes over time. The equation to calculate benthic diffusive fluxes from sediments is as follows:

$$\frac{\Delta c}{\Delta t} = \frac{A\,J}{V}$$

$$Flux\ (J) = ((c_1 - c_2) \times V)/(t \times A)$$

Where J is the diffusive flux (units mass per unit area per unit time: mol $m^{-2}s^{-1}$). V is the volume of water overlying sediment of area A (Aller et al., 2023). Δc is the concentration change ($c_1$-$c_0$) over Δt, the change in time ($t_1$-$t_0$). Positive fluxes are indicative of greater sediment outflow and net production (Bratek et al., 2020). $T_0$ concentrations were corrected for the volume (~15mL) replaced by tank water.

*Diffusive fluxes calculated from porewater gradients by Fick´s law:*

Diffusive fluxes of porewaters are calculated by Fick´s first law of diffusion. This law states that the flux is proportional to the change in concentration of a substance over the change in distance, i.e. flux is proportional to the concentration gradient under steady state conditions (Burdige, 2006; Schulz & Zabel, 2006). The equation according to Fick´s first law is given by:

$$J = -\emptyset \cdot D_{sed} \cdot \frac{\Delta C}{\Delta z}$$

Where J is the diffusive flux (units mass per unit area per unit time), C is the concentration (mass per unit volume), z is the direction of the maximum concentration gradient, Ø is the average surface sediment porosity (dimensionless) of the 3 core replicates at a depth of 0-1cm and $D_{sed}$ is the diffusion coefficient ($cm^2s^{-1}$). Increasing concentrations at depth will yield negative gradients within the sediment with a positive upwards flux (Schulz & Zabel, 2006). Porosity has to be taken into account in this equation since the diffusion coefficient would yield much lower values in porewater sediments compared to a free solution (Schulz & Zabel, 2006). Porosity was calculated as follows:

$$\emptyset = \frac{ww - dw}{5}$$

Where $w_w$ is the wet weight in grams and $d_w$ is the dry weight in grams divided by the volume of the wet sediment sample ($5cm^3$).

Since diffusion within sediments does not follow a straight path as in a free solution, the tortuosity (θ) was calculated to account for this deviation around the grains according to the equation by Boudreau (1996):

$$\theta^2 = 1 - \ln(\emptyset^2)$$

The diffusion coefficient in the sediments ($D_{sed}$) was calculated by the ratio of the diffusion coefficient in free solutions of seawater ($D^{sw}$) and the dimensionless tortuosity (θ) (table 6,7,8):

$$D_{sed} = D^{sw} / \theta^2$$

The concentration gradient can be calculated either through the best fit curve of the first derivative or from Δc/Δz (change in concentration over change in depth) where Δc is the difference between the bottom water concentration and the first pore water sample collected and Δz is the depth of the porewater sample (Burdige, 2006). In this study concentration gradients were calculated from Δc/Δz between the overlying water (-0.5cm) to a depth of 2.5cm below the sediment surface.

| Compound | $D_{sw}$ ($m^2s^{-1}$) at 5°C |
|---|---|
| $NH4^+$ | 1.10E-09 |
| $NO3^-$ | 1.08E-09 |
| $PO4^{3-}$ | 3.16E-10 |
| $HCO3^-$ | 6.09E-10 |

*Table 6: $D_{sw}$ diffusive coefficients for components from Schulz & Zabel, 2006.*

| Property | Average A | Average B | Average C | Average G | Average H | Average K | Average L |
|---|---|---|---|---|---|---|---|
| **Porosity (∅)** | 0.80 | 0.65 | 0.76 | 0.73 | 0.75 | 0.90 | 0.89 |
| **Tortuosity ($\theta^2$)** | 1.44 | 1.87 | 1.55 | 1.64 | 1.58 | 1.22 | 1.24 |

*Table 7: Average porosities from upper sediments (0-1cm) and calculated Tortuosity from $\theta^2 = 1-\ln(\emptyset^2)$. Porosities were calculated from wet weight and dry weight of sediments.*

| $D_{sed}$ ($m^2s^{-1}$) | | | | | | | |
|---|---|---|---|---|---|---|---|
| **Compound** | **Average A** | **Average B** | **Average C** | **Average G** | **Average H** | **Average K** | **Average L** |
| $NH4^+$ | 7,65E-10 | 4,08E-10 | 2,64E-10 | 1,61E-10 | 1,02E-10 | 8,31E-11 | 6,71E-11 |
| $NO3^-$ | 7,51E-10 | 4,01E-10 | 2,59E-10 | 1,58E-10 | 9,97E-11 | 8,16E-11 | 6,59E-11 |
| $PO4^{3-}$ | 2,20E-10 | 1,17E-10 | 7,57E-11 | 4,62E-11 | 2,92E-11 | 2,39E-11 | 1,93E-11 |
| $HCO3^-$ | 4,23E-10 | 2,26E-10 | 1,46E-10 | 8,89E-11 | 5,62E-11 | 4,60E-11 | 3,72E-11 |

*Table 8: $D^{sed}$ (Diffusive coefficients within sediments calculated from components individual tortuosities and diffusive coefficients in seawater.*

## 2.5 Statistical analyses

ANOVA (analysis of variance) analyses were performed with the JMP statistical software on the average concentrations of separate porewater variables ($NH_4^+$, $PO_4^{3-}$, $NO_3^-$, DIC and $\delta^{13}C_{DIC}$), whereby depth as a categorical variable was compared to high and low trawling intensities. High trawling intensities were set to an SAR of $6y^{-1}$ and low trawling intensities were set to an SAR of $1y^{-1}$. Localities B and C displayed normally distributed data on untransformed $NH_4^+$, $PO_4^{3-}$ and $\delta^{13}C_{DIC}$ concentrations and normally distributed data on log transformed DIC and $NO_3^-$ concentrations. Localities G and H displayed normally distributed data on untransformed $NH_4^+$, DIC and $\delta^{13}C_{DIC}$ concentrations and on log transformed $NO_3^-$ and $PO_4^{3-}$ concentrations. Localities K and L only displayed normally distributed data on untransformed $NO_3^-$ concentrations. All variables displayed homogeneous variance on both transformed and untransformed data for all localities. All variables of locality B/C, G/H and K/L displayed a good fit with the Anova predicted models, whereby sample points fall into the confidence intervals predicted by the models.

# 3. Results

## 3.1 Physio-chemical characteristics of the bottom water

Samples were collected at depths ranging from 51- 65 metres below sea level, deepening toward the Northeast of the study area. CTD measurements were taken at approximately 0.5m above the seabed. Oxygen concentrations range from 2.58-4.95 mL/L and are indicative of oxic conditions according to the ranges of oxygen regimes outlined by (Tyson & Pearson, 1991) (oxic conditions: 8.0-2.0mL/L) and show a general decrease with depth (table 9). Salinities at the different localities range from 9.13-13.42 PSU, temperatures range from 6.55-8.34 °C and conductivities range from 10.19 -15.26mS/cm increasing systematically with increasing salinities.
Less saline and cooler waters at Locality A are characterized by the highest oxygen concentrations of 4.95 mg/L, a salinity of 9.13 PSU, a conductivity of 10.19 mS/cm and a temperature of 6.55°C close to the seabed. Lowest oxygen concentrations of 2.58mL/L were observed at Locality L, consistent with deeper more saline waters with a salinity of 13.42 PSU, conductivity of 15.26 mS/cm and a temperature of 8.34°C. Salinity and oxygen concentrations for the remaining stations are largely dependent on their depths and temperatures.

| Site | Locality | Trawling Intensity | Sampling Date | Coordinates CTD (Lat N, Long E) | Depth CTD (m) | Temperature (°C) | Conductivity (mS/cm) | Salinity (PSU) | $O_2$ (mL/L) | $O_2$ sat. (mL/L) | Turbidity Wet Labs ECO (NTU) |
|---|---|---|---|---|---|---|---|---|---|---|---|
| 1 | A | High | 11/06/2023 | 55.46 N 14.60 E | 59.75 | 6.55 | 10.19 | 9.13 | 4.95 | 8.09 | 0.44 |
| 2 | B | Low | 08/06/2023 | 55.33 N 14.44 E | 50.25 | 8.64 | 14.63 | 12.72 | 4.12 | 7.51 | 0.53 |
| | C | High | 07/06/2023 | 55.35 N 14.45 E | 48.75 | 8.44 | 14.96 | 13.11 | 3.84 | 7.53 | 1.01 |
| 3 | G | Low | 06/06/2023 | 55.40 N 14.51 E | 55.5 | 7.49 | 12.74 | 11.33 | 4.55 | 7.79 | 0.40 |
| | H | High | 05/06/2023 | 55.40 N 14.55 E | 60.5 | 7.57 | 13.85 | 12.36 | 3.96 | 7.72 | 1.28 |
| 4 | K | High | 13/06/2023 14/06/2023 | 55.50 N 14.71 E | 62.75 | 8.46 | 14.63 | 12.79 | 3.28 | 7.54 | 0.59 |
| | L | Low | 13/06/2023 15/06/2023 | 55.49 N 14.71 E | 63.25 | 8.34 | 15.26 | 13.42 | 2.58 | 7.53 | 1.05 |

*Table 9: Physiochemical properties of waters overlying bottom sediments and location description of individual sites. Depth, Temperatures, Conductivities, Salinities, Oxygen concentrations and Turbidity were taken from CTD (Conductivity, Temperature, Depth) during the 2023 EL23 IGV-2 cruise.*

## 3.2 Physical properties of sediments

Sediments become significantly finer grained towards the northeast of the basin as coarser fine-sands are deposited closer to the inlet source of the submarine channel through the Arkona basin toward the south where turbidity and currents are stronger (Christoffersen et al., 2007). The sediments in the study area were mainly composed of varying proportions of clay (<2µm), fine silts (2-63µm) and fine sands (63µm-2mm) and rarely gravels (2-3.5mm) that displayed a gradual change in grainsize and colour within the core (gradually grading from dark grey sediments to light/orange brown with increasing stratigraphic height) with no prominent sedimentary structures (table 10). Some of the cores contained small ~1mm in diameter and ~4mm long worm tubes/crustaceans sticking out of the sediments (locality B) as well as ~3cm long burrows (locality C) see figure 6e. Sediments at locality A,

B and G were normally graded with a slight coarsening and higher proportion of fine sands with depth. In contrast, sediments at locality C and H display reverse grading and a significant decrease in grain size with depth. K and L display a significantly higher proportion of fine organic rich, smelly sediments compared to other localities and the grainsize does not change significantly with depth and is relatively homogeneous; these are the only sites that contained very low proportions of gravels (0.39-0.74%). Sedimentation rates were obtained by applying the Constant Flux:Constant Sedimentation (CF:CS) rates to excess $^{210}$Pb concentration profiles below the mixed layers and average sediment accumulation rates for the last century were obtained . Since sediment layers within all localities were relatively mixed, they were subject to high uncertainties and sedimentation rates need to be considered with caution. Locality K and L are contrasted in the lowest and highest ranges of sedimentation rates with regards to all localities ranging from 0.021 to 0.141 g/cm$^3$yr respectively.

| Site | Locality | Trawling Intensity | Sedimentation rates from 210Pb (mm/yr) | Sedimentation rates from 210Pb (g/cm$^2$yr) | Average Grain size (%) from 0,5-12,5cm | Grain size distribution |
|---|---|---|---|---|---|---|
| 1 | A | High | A1: 1.9 ± 0.2<br>A2: 0.82± 0.06<br>A3: 0.84 ± 0.06 | A1: 0.102 ± 0.011<br>A2: 0.057 ± 0.004<br>A3: 0.050 ± 0.004 | Clay: 3,14%<br>Fine silt: 8.37%<br>Sortable silt: 24,32%<br>Sand: 64.17%<br>Gravel: 0% | Sediments display normal grading, ~9% increase in sands from 0,5 – 12,5cm. |
| 2 | B | Low | Very mixed<br>n.d. | Very mixed<br>n.d. | Clay: 1.79%<br>Fine silt: 5.89%<br>Sortable silt: 14.75%<br>Sand: 77.57%<br>Gravel: 0% | Grain size relatively homogeneous, normal grading. ~2% increase in sands from 0,5-12,5cm. |
| | C | High | Very mixed<br>n.d. | Very mixed<br>n.d. | Clay: 5.55%<br>Fine silt: 18.33%<br>Sortable silt: 15.93%<br>Sand: 60.17%<br>Gravel: 0.02% | Sediments are significantly finer with depth, ~71% decrease in sands from 0,5-12,5cm. |
| 3 | G | Low | G1: 0.98 ± 0.05<br>G2: 0.53 ± 0.04<br>G3: 0.92 ± 0.05 | G1: 0.087 ± 0.004<br>G2: 0.040 ± 0.003<br>G3: 0.074 ± 0.004 | Clay: 1.27%<br>Fine silt: 4.06%<br>Sortable silt: 11.61%<br>Sand: 83.05%<br>Gravel: 0.01% | Sediments display normal grading, with a ~18,5% increase in fine sands from 0,5-12,5cm. |
| | H | High | Very mixed, high uncertainty.<br>0.6-0.7 | Very mixed, high uncertainty.<br>0.04 | Clay: 12.95%<br>Fine silt: 14.10%<br>Sortable silt: 22.37%<br>Sand: 50.57%<br>Gravel: 0% | Sediments are significantly fining with depth. ~45,43% decrease in fine sands from 0,5-7,5cm. |
| 4 | L | Low | L1:4.2 ± 0.2 (4-20cm)<br>L2: 5.3 ± 0.3 (5-25cm)<br>L3a: 5.6 ± 0.4 (2-20cm)<br>L3b: 3.8 ± 0.4 (20-37cm) | L1: 0.093 ± 0.006 (4-20cm)<br>L2: 0.141 ± 0.008 (5-25cm)<br>L3a: 0.131 ± 0.010 (2-20cm)<br>L3b: 0.134 ± 0.013 (20-37cm) | Clay: 12.53%<br>Fine silt: 37.09%<br>Sortable silt: 40.60%<br>Sand: 9.04%<br>Gravel: 0.74% | Relatively homogeneous grain size distribution with depth. |
| | K | High | K1: 1.40 ± 0.08<br>K2: 0.72 ± 0.08<br>K3: 1.21 ± 0.16 | K1: 0.042 ± 0.002<br>K2: 0.021 ± 0.002<br>K3: 0.030 ± 0.004 | Clay: 11.91%<br>Fine silt: 33.43%<br>Sortable silt: 43.39%<br>Sand: 10.87%<br>Gravel: 0.39% | Relatively homogeneous grain size distribution with depth. |

*Table 10: Sediment descriptions of individual localities. Average grain size data and sedimentation rates are obtained from the 2020 Electra cruise (EL20- IGV03). Average grain sizes were calculated until a 12,5cm depth of the core. Grainsize criteria are as follows:* Clay (%) <2 µm, Fine silt (%) 2-10 µm, Sortable silt (%) 10-63 µm, Sand (%) 63 µm- 2mm, Gravel (%) 2-3.5 mm.

Grain size distributions with regard to depth are shown in figure 11. The grain size distributions of core A, B, K and L remain relatively homogeneous with depth with only minor changes. Core A displayed the most gradual change in grainsize distribution with a minor increase in fine sands with depth (56-69%), Core B displayed a small increase in fine sands with depth (81-83%). Core B contained the overall largest proportion of fine sands (80-83%) compared to core K and L containing the lowest proportion of fine sands (0-1%) with depth. Core G displayed a sharp increase in fine sands at a depth of approximately 2.5cm where the fine sand fraction increases ~10%, the fraction of fine sands continues to increase with depth (72%-90% for the whole core). Core C and H, which are situated in highly trawled locations; displayed a sharp decrease in grainsize at a depth of approximately 6.5cm (56% and 20 % decrease in fine sands respectively), whereby the fine sand fraction is overall decreased from 79%-9% for core C and from 67%-22% for core H with increasing depth. Porosities generally increase with decreasing grainsize (see Table 7).

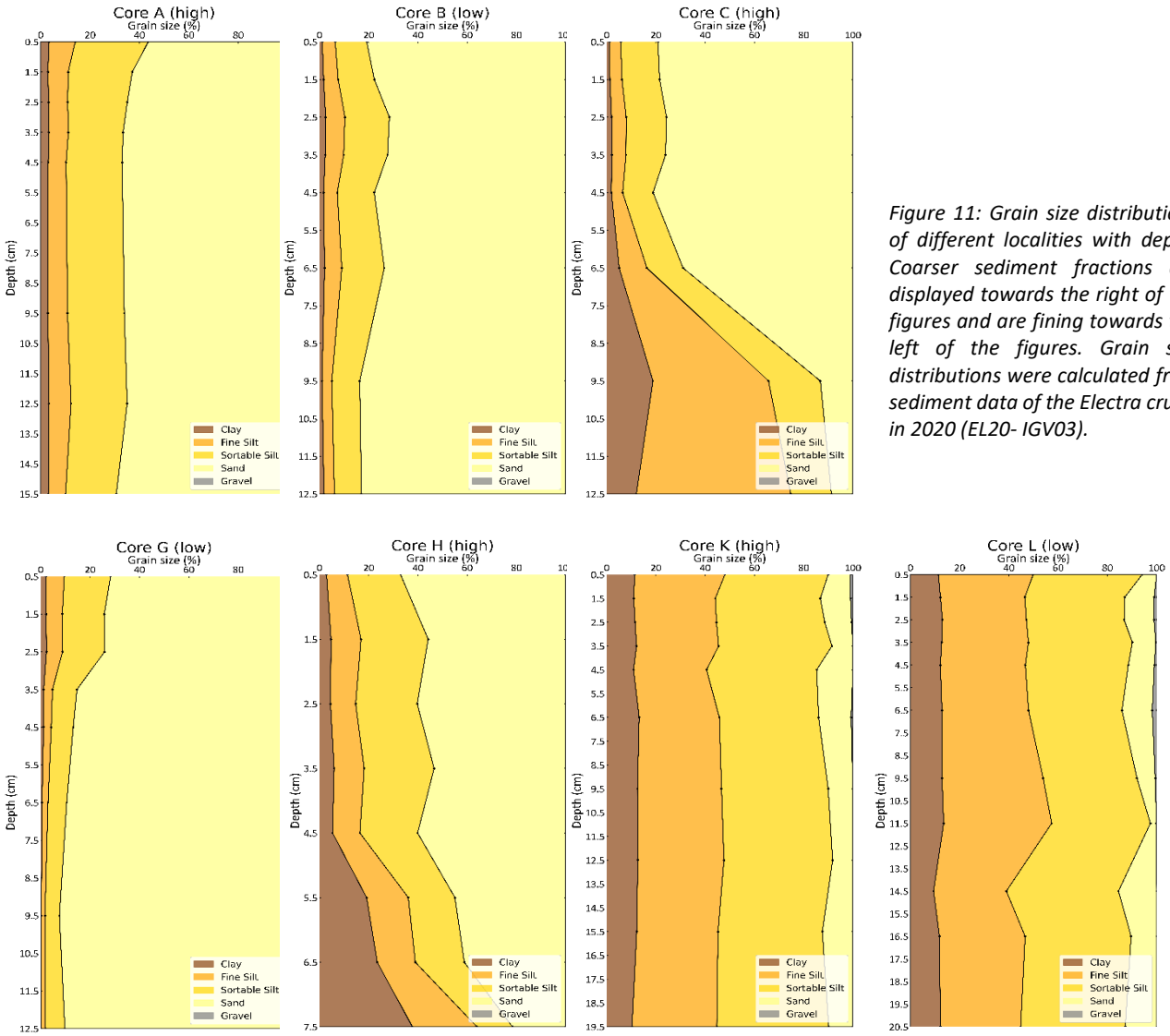



*Figure 11: Grain size distributions of different localities with depth. Coarser sediment fractions are displayed towards the right of the figures and are fining towards the left of the figures. Grain size distributions were calculated from sediment data of the Electra cruise in 2020 (EL20- IGV03).*

## 3.3 Biogeochemical properties of sediments and porewaters

All calculations and datatables can be found in Appendix A and B at the very end of the document.

### *3.3.1 Sediment solid-phase concentration profiles*

#### *3.3.1.1 Variability by localities:*

*TOC, $\delta^{13}C_{TOC}$ and C/N ratios in sediments:*

C/N ratios discussed in this section refer to the ratio between TOC and N.

All localities display a general decrease in TOC content with depth ranging from 0.45% to 5.63%. Localities K and L display the highest TOC concentrations where the averages ranged from 2.71-5.63% and 0.86%-5.24% respectively, followed by localities H (0.45%-3.53%), A (0.89% -3.23%), G (0.55% -1.40%), C (0.47% -1.28%) and B (0.88% -1.43%) (figure 12). Standard deviations for replicates of TOC contents range from 0 to 0.81%. Locality A, and H show the most gradual changes in concentrations with depth compared to the other localities which show a lot of variability. These observations are generally consistent with trends observed by $\delta^{13}C_{TOC}$ ratios. $\delta^{13}C_{TOC}$ ratios are slightly more negative with sediment depth, where localities with higher TOC contents are indicative of more negative, lighter $\delta^{13}C_{TOC}$ ratios due to an enrichment of the lighter 12C isotope in organic matter. The most negative $\delta^{13}C_{TOC}$ ratios at the sediment surface are characterised by the high TOC contents at locality L and K with $\delta^{13}C_{TOC}$ ratios ranging from -24.61‰ to -26.39‰ and -22.81‰ to -26.56‰ respectively. Standard deviations for replicates of $\delta^{13}C_{TOC}$ ratios range from 0 to 1.05 ‰. The TOC content generally increases with decreasing grainsize and increasing porosities at the different localities. High sedimentation rates at locality L and A likely lead to an increase in recently deposited material and may thus explain the relatively high TOC contents within sediments.

For all localities, $\delta^{13}C_{TOC}$ range from -22.81‰ to -26.71‰, δ 15N range from 0.89‰ to 5.13‰ and C/N ratios range from 1.44 to 12.09 (figure 13 a,b). These concentrations point to a mixture of a marine and terrestrial organic matter source whereby marine phytoplankton physically exhibit $\delta^{13}C$ values ranging from -19 ‰ to - 22‰, $\delta^{15}N$ values of 3‰ to 12 ‰ and C/N ratios of 5-8. In Terrestrially derived organic matter typically exhibits $\delta^{13}C$ values ranging between -35‰ to -25‰, $\delta^{15}N$ values of 5‰ to 8‰ and C/N ratios >15 (Boutton, 1991; Gao et al., 2012; Meyers, 1994; Wada & Hattori, 1991). There is no clear correlation between TOC and C/N (figure 13 c). C/N ratios remain relatively constant with depth with some fluctuations at specific depth intervals. The average C/N ratios for all depth intervals for the individual localities are: A (7.50), B (7.73), C (7.03), G (7.05), H (7.05), L (6.87) and K (6.66). The C/N ratios for L and K are closest to the Redfield ratio (C/N=6.6), whereas the remaining localities display C/N ratios slightly above.

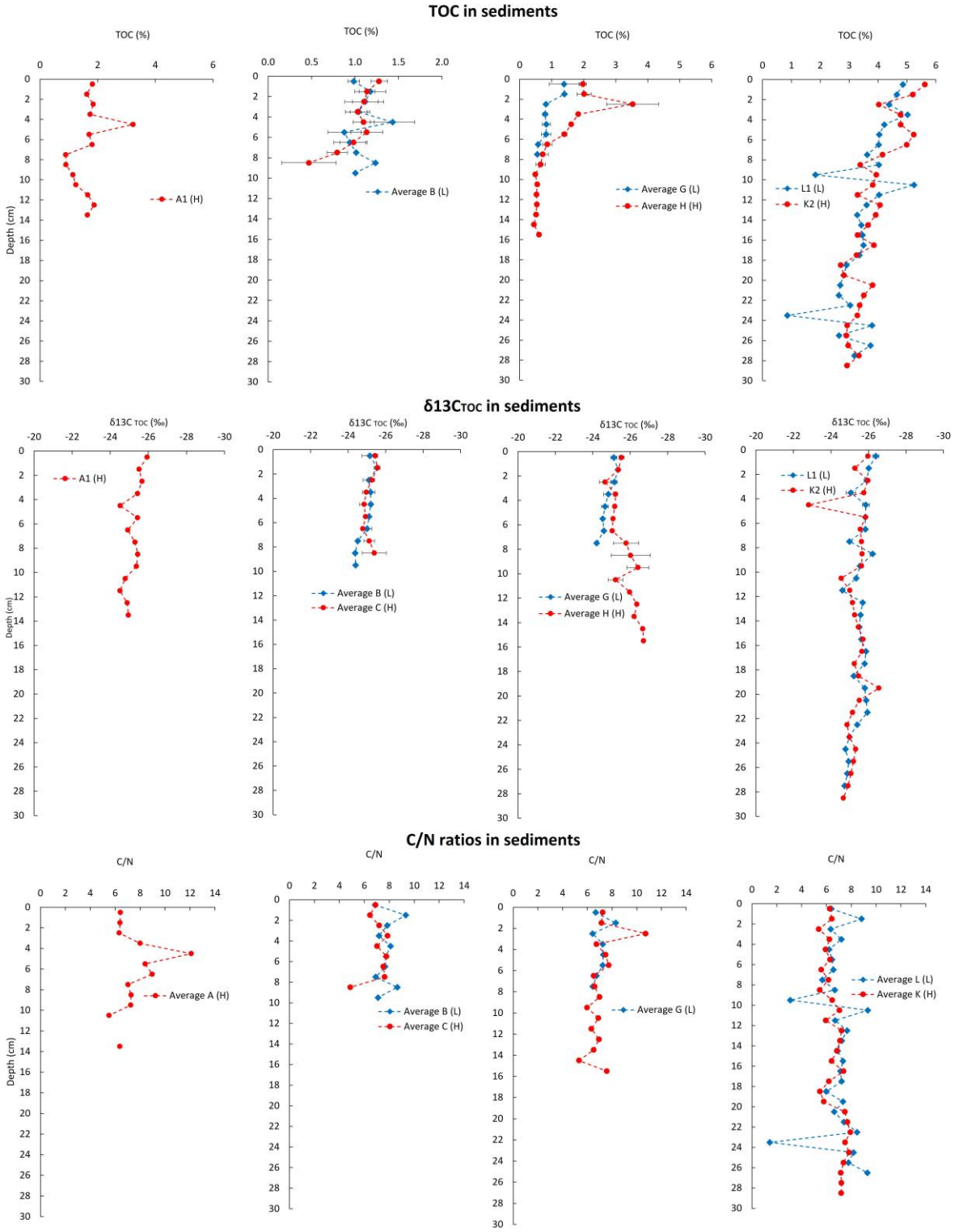



*Figure 12: Sediment profiles for Average TOC, $\delta 13C_{TOC}$ and $C_{TOC}/N$ contents displaying relationships between High (H) and Low (L) trawled pairs at different localities. Error bars display the standard deviations between sample replicates. No replicates were analysed for locality A, K and L.*

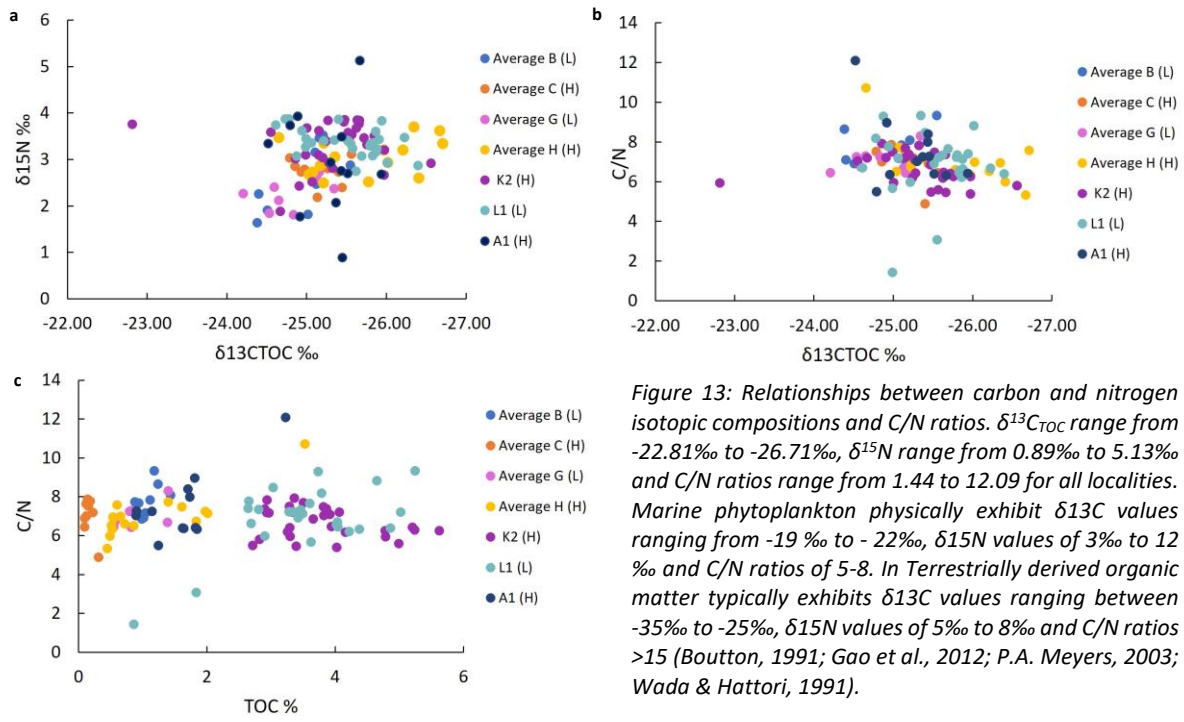



*Figure 13: Relationships between carbon and nitrogen isotopic compositions and C/N ratios. $\delta^{13}C_{TOC}$ range from -22.81‰ to -26.71‰, $\delta^{15}N$ range from 0.89‰ to 5.13‰ and C/N ratios range from 1.44 to 12.09 for all localities. Marine phytoplankton physically exhibit δ13C values ranging from -19 ‰ to - 22‰, δ15N values of 3‰ to 12 ‰ and C/N ratios of 5-8. In Terrestrially derived organic matter typically exhibits δ13C values ranging between -35‰ to -25‰, δ15N values of 5‰ to 8‰ and C/N ratios >15 (Boutton, 1991; Gao et al., 2012; P.A. Meyers, 2003; Wada & Hattori, 1991).*

*TC and $\delta^{13}C_{total}$ in sediments:*

The TC concentrations display a general decrease in concentration for all localities apart for locality H, which displays a gradual increase from a depth of 10.5cm, likely as a result of a higher inorganic carbon fraction within the sediments (figure 14). Locality G and H show the most gradual concentrations with depth compared to the other localities which show a lot of variability with depth. The TC concentration for all the cores including all depth intervals ranged between 0.02% to 6.60%. The highest concentrations were found at locality K with averages of 3.29% to 6.60%, followed by locality L (2.88% - 5.68%), H (0.70% - 2.51%), A (0.02% - 2.15%), G (0.53% - 1.54%), C (0.33% - 1.48%) and B (0.52% - 1.51%), displaying the same order as described for the TOC concentrations. The standard deviation of all localities ranges from 0% to 0.76%.

$\delta^{13}C_{total}$ concentrations show variable trends within the different profiles likely as a result of different inorganic carbon fractions within individual localities at different depths, refractory organic carbon content as well as variabilities in bioturbation and bioirrigation potentials. $\delta^{13}C_{total}$ contents range from -8.66‰ to -24.44‰ for all localities but generally range from -20-28‰ to 24.44‰. Overall, the average $\delta^{13}C_{total}$ concentrations for all depth intervals range from: A (-24.17‰ to -23.42‰), B (-24.14‰ to -23.15‰), C (-24.26‰ to -20.28‰), H (-24.13‰ to -8.66‰), G (-24.44‰ to -21.13‰), K (-24.34‰ to -22.52‰) and L (-24.43‰ to -22.83‰). The standard deviations for the localities range from 0‰ to 2.98‰.

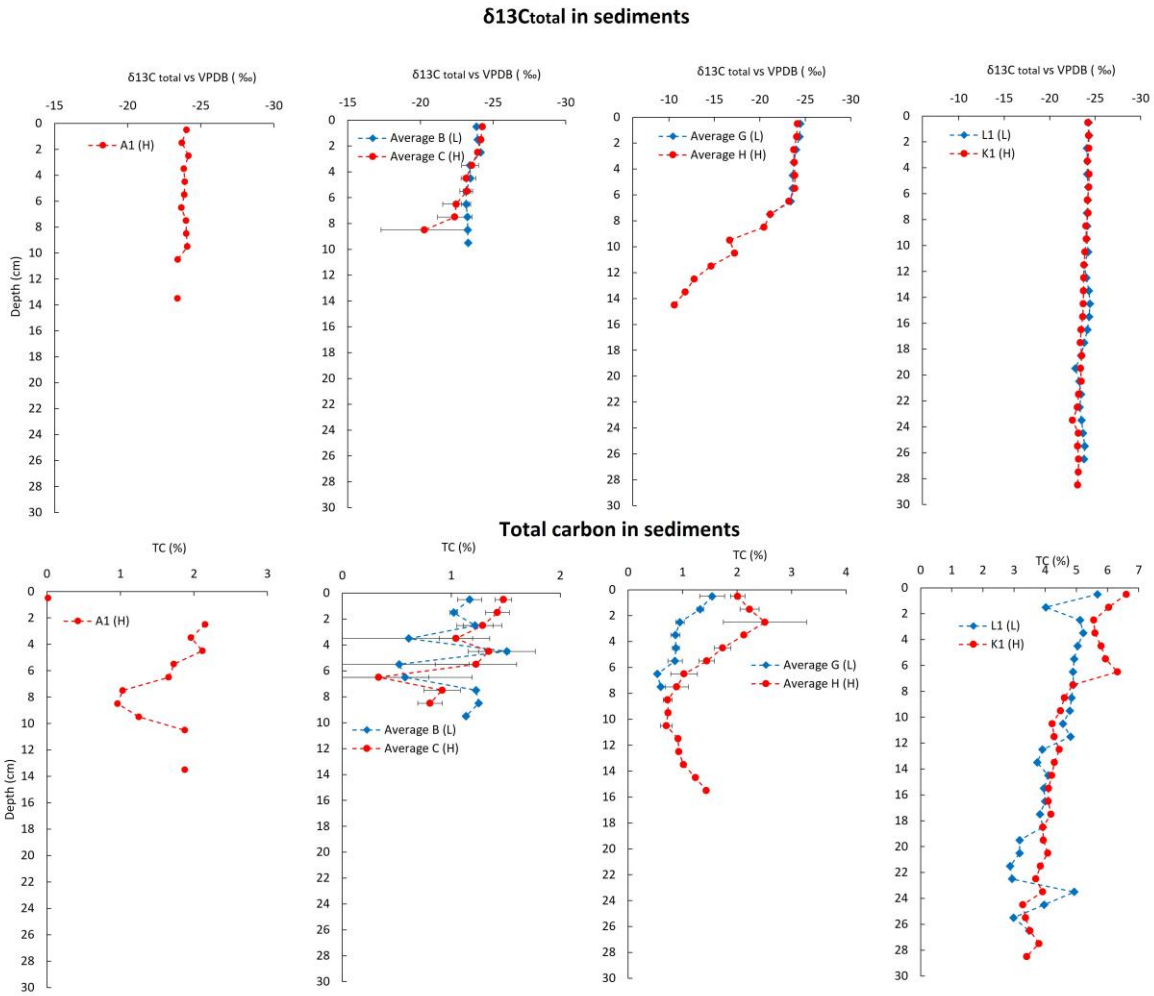



*Figure 14: Sediment profiles for average δ13C$_{total}$ and TC contents displaying relationships between High (H) and Low (L) trawled pairs at different localities. Error bars display the standard deviations between sample replicates. No replicates were analysed for locality A, K and L.*

### *δ$^{15}$N and TN in sediments:*

The TN concentrations display a general decrease in concentration for all localities (figure 15). Locality B, C, G and H display the most gradual concentrations with depth compared to locality A, K and L which display a lot of variability within their profiles. The TN concentrations for all localities ranged from 0.08% to 0.90%. Locality K displayed the highest TN concentrations with average concentrations ranging between 0.38% to 0.90% at all depth intervals, followed by locality L (0.34% – 0.76%), H (0.08% – 0.33%), A (0.12% – 0.29%), C (0.10% – 0.19%) and B (0.11% – 0.18%). The standard deviations for all localities range between 0% to 0.11%. TN and TOC show high to very high positive linear correlations for locality C ($r^2$=0.81), G ($r^2$=0.92), H ($r^2$=0.91) and K ($r^2$=0.85). TN and TOC show low to moderate positive correlations for locality L ($r^2$=0.22), followed by A ($r^2$=0.46) and B ($r^2$=0.56). The TN and TC profiles show a moderate positive correlation between locality B ($r^2$=0.59) and C ($r^2$=0.52). In comparison TN and TC show a high to very high positive correlation for locality H ($r^2$=0.88), G($r^2$=0.98), K ($r^2$=0.99); L ($r^2$=0.97) and A ($r^2$=0.93). Locality B therefore shows the lowest correlation between both TOC and TN as well as TC and TN. At the majority of the sites the clear correlation of TN and TC suggests that the TN within the sediments is mostly derived from organic matter.

The δ$^{15}$N profiles display more fluctuating profiles for all localities in comparison to δ$^{13}C_{TOC}$ and δ$^{13}C_{total}$ profiles. The δ$^{15}$N profiles display a general increase with depth for locality A, C, H and L. In comparison the δ$^{15}$N profiles display a general decrease with depth for locality B, G and K.

The average $\delta^{15}N$ concentrations range from 0.89‰ to 5.13‰ for all the localities. The highest $\delta^{15}N$ concentrations are found at locality A with averages ranging from 0.89‰ to 5.13‰ including all depth intervals, followed by locality L (2.75‰ – 3.88‰), K (1.88‰ – 3.86‰), H (2.49‰ – 3.69‰), B (1.64‰ – 3.52‰), C (2.18‰ – 3.12‰) and G (1.81‰ – 2.73‰). The standard deviations for all localities range from 0‰ to 1.13‰.

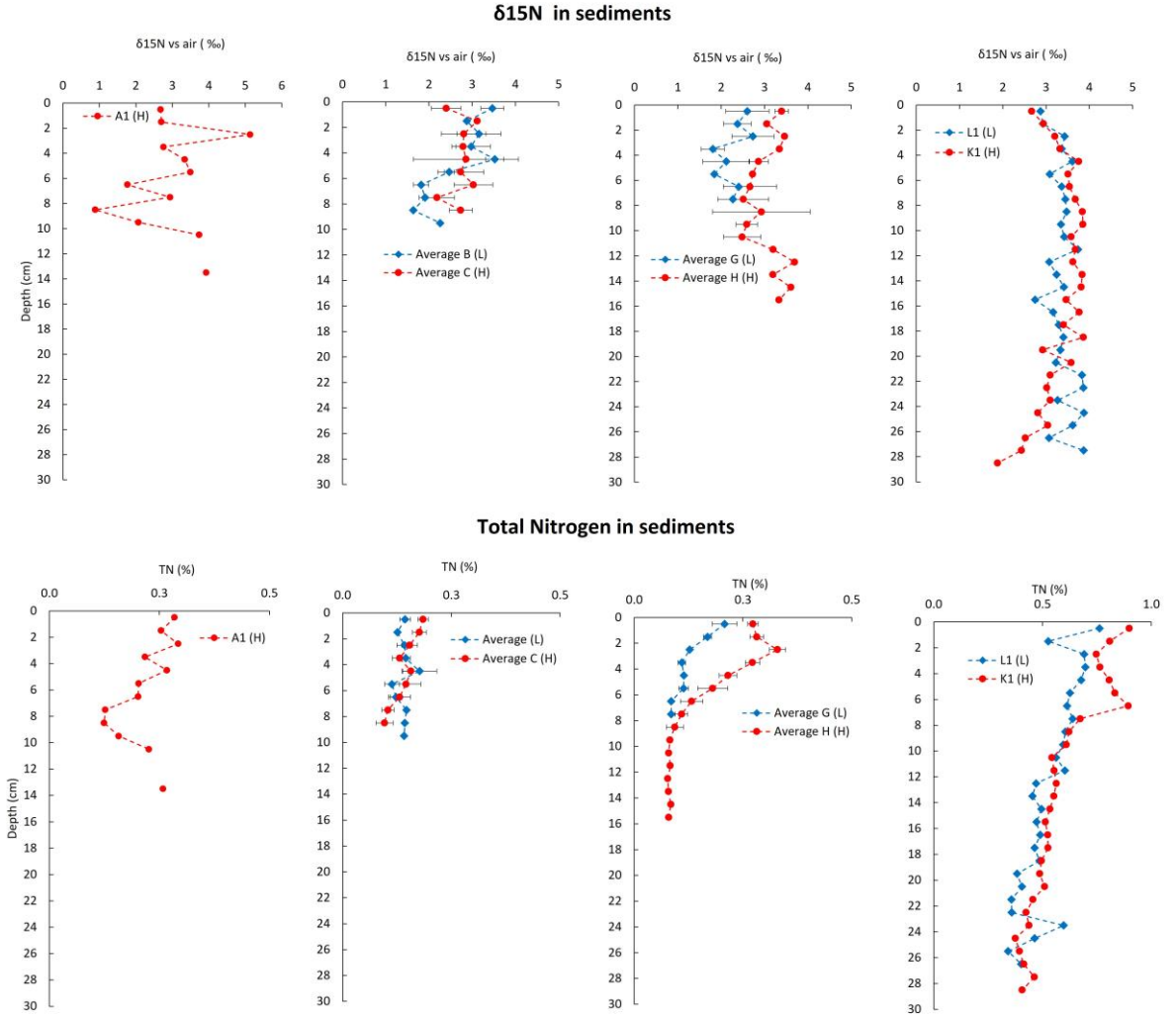



*Figure 15: Sediment profiles for average $\delta^{13}N_{total}$ and TN contents displaying relationships between High (H) and Low (L) trawled pairs at different localities. Error bars display the standard deviations between sample replicates. No replicates were analysed for locality A, K and L.*

*Chlorophyll in sediments:*

The chlorophyll concentrations display a sharp decrease with depth for all localities as a result of degradation by microbial activity, readily consumption by macro-/meiofauna and mixing by bioturbation from the sediment surface where it was recently deposited after the spring bloom (figure 16). High concentrations at the sediment surface can be attributed to freshly deposited organic matter that has settled on the seabed from the water column. Variability of chlorophyll concentrations between different localities are dependent on water currents, water depths and sediment compositions. At all localities the chlorophyll profiles display a sharp decrease to about 2.5cm as a result of rapid degradation by microbial activity near the sediment surface. Thereafter the chlorophyll concentration decreases gradually at different rates for each locality. The average chlorophyll concentrations range from 0 µg/cm$^3$ to 11.73 µg/cm$^3$ at all depth intervals. The highest chlorophyll concentrations were found at locality H with average concentrations ranging from 0 µg/cm$^3$ to 11.73

µg/cm$^3$, followed by locality A (2.11 µg/cm$^3$ – 11.61 µg/cm$^3$), C (1.08 µg/cm$^3$ – 9.88 µg/cm$^3$), K (1.66 µg/cm$^3$ – 8.57 µg/cm$^3$), G (1.48 µg/cm$^3$ – 8.02 µg/cm$^3$), L (1.73 µg/cm$^3$ – 5.61 µg/cm$^3$) and B (1.99 µg/cm$^3$ – 5.25 µg/cm$^3$). Chlorophyll and TN show a strong to very strong positive correlation for locality G ($r^2$=0.97), C ($r^2$=0.76) and H ($r^2$=0.61). Chlorophyll and TN show a weak to moderate positive correlation for locality A ($r^2$=0.42) and K ($r^2$=0.31). There is almost no correlation for chlorophyll and TN for locality B ($r^2$=0.0027) and L ($r^2$=0.0091). Chlorophyll and TOC shows a strong positive correlation for locality G ($r^2$=0.88). Chlorophyll and TOC shows a weak to moderate positive correlation for locality K ($r^2$=0.3), H ($r^2$=0.43) and C ($r^2$=0.51). Chlorophyll and TOC show almost no to very weak correlations for locality L ($r^2$=0.002), B ($r^2$=0.0131) and A ($r^2$=0.11). All localities displayed positive correlations for chlorophyll and TN and TOC, apart for locality L which displayed a very weak negative correlation between chlorophyll, TN and TOC. The standard deviations for chlorophyll ranged from 0 µg/cm$^3$ to 3.75 µg/cm$^3$ for all localities.

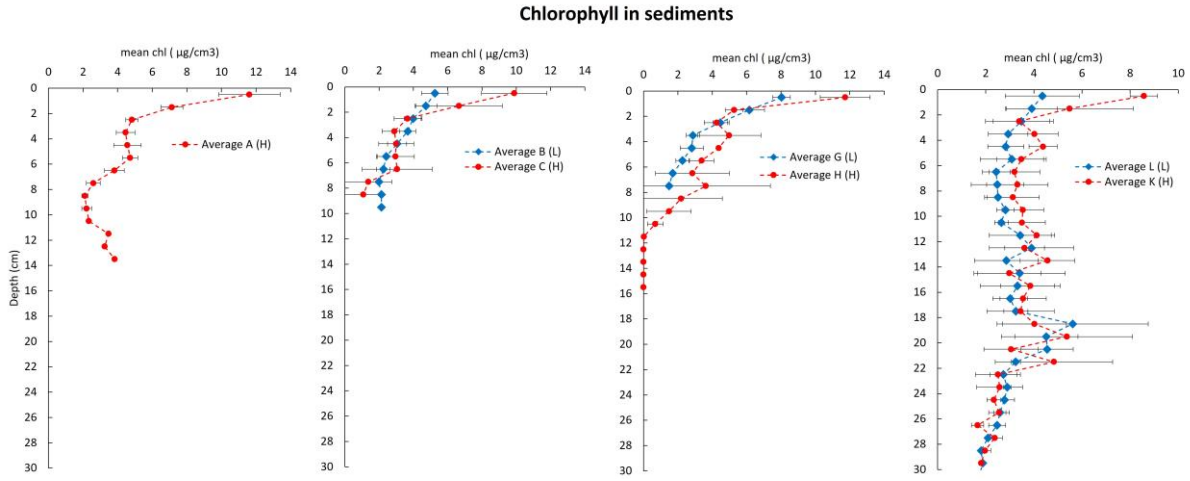



*Figure 16: Sediment profiles for chlorophyll contents displaying relationships between High (H) and Low (L) trawled pairs at different localities. Error bars display the standard deviations between sample replicates. Localities A, B, C, G, H and K had 3 replicate cores, whereas locality L only had 2 replicate cores.*

### *3.3.1.2 Variability of sediment profiles by trawling intensity between high- and low-trawled pairs:*

See calculated differences at each depth between high- and low-trawled pairs in Appendix A.
TOC, TC and TN concentrations are higher for all high-trawled sites close to the sediment-water interface until a depth of about 2.5cm, whereafter the TOC and TN concentration profiles differ greatly between sites. Low- and high-trawled locality pairs G/H displayed the greatest difference in the TOC, TC, TN and δ15N concentrations with regards to all sites, where the concentrations are higher for high-trawled locality H, close to the sediment surface until a depth of about 6.5cm, whereafter the concentrations of TOC, TN and TC between low- and high-trawled pairs G/H, decrease to near-constant values. Low- and high-trawled localities B/C and K/L do not show pronounced differences and trends between their pairs, below 2.5cm; although generally showing consistent trends and systematic relationships between TOC, TN, $\delta^{15}N$ and TC. $\delta^{13}C_{TOC}$ concentrations did not show any significant differences between high- and low-trawled localities in any of the sites, and had relatively constant concentrations with depth, apart for locality H, which became slightly more negative below a depth of 6.5cm. The $\delta^{13}C_{total}$ concentration for locality A, K and L had constant concentrations throughout the core and did not show any significant differences between high- and low-trawled localities. For sites B/C and G/H, the $\delta^{13}C_{total}$ concentration did not show any significant differences between the pairs until a depth of 4.5cm and 6.5cm respectively. Below 4.5 and 6.5cm, high-trawled localities C and H showed an increase (less negative) in their $\delta^{13}C_{total}$ concentrations.

The chlorophyll concentrations are significantly higher for all high-trawled localities close to the sediment surface until a depth of about 2.5cm, whereafter the chlorophyll concentrations of the site-specific pairs approach similar concentrations and lower differences.

### *3.3.2 Porewater concentration profiles*

#### *3.3.2.1 Variability by localities:*

*Nutrients ($NH_4^+$, $PO_4^{3-}$ and $NO_3^-$) of porewaters:*

The $NH_4^+$ concentrations generally show distinct increases in concentration with depth from the sediment-water interface for all localities (figure 17). Lower $NH_4^+$ concentrations at the sediment surface may be related to anoxic oxidation of ammonium by either manganese or nitrate.
The $NH_4^+$ concentrations for all localities range from 0µM to 2649µM. The highest $NH_4^+$ concentrations ranges were observed at locality K with concentrations ranging from 10.20µM to 2649µM, followed by Locality L (8.90-2417µM), A (4.52-766.96µM), G (0-334µM), H (32.27-359µM), B (0.80-129.33µM) and C (4.53-155.70µM).

The $PO_4^{3-}$ concentrations show a general increase from the sediment-water interface with depth for all localities apart for locality A and H which display a decrease with depth. The $PO_4^{3-}$ concentrations ranged from 0µM to 90.21µM for all localities. The highest $PO_4^{3-}$concentrations were observed at locality L with concentrations ranging from 0µM to 90.21µM, followed by locality K (0.46-81.11µM), A (11.71-57.56µM), G (1.63-23.07µM), B (0.60-15.81µM), C (1.99-10.55µM) and H (0-6.19µM). The standard deviation ranged from 0µM to 44.73µM. $PO_4^{3-}$ and $NH_4^+$ show a moderate to strong positive correlation for locality C ($r^2$=0.69), B ($r^2$=0.66) and G ($r^2$=0.51). $PO_4^{3-}$ and $NH_4^+$ show a weak positive correlation for locality L ($r^2$=0.19) and a weak negative correlation for locality H ($r^2$= 0.18). Locality K ($r^2$= 0.03) and A ($r^2$= 0.08) show almost no correlation between $NH_4^+$ and $PO_4^{3-}$. The N:P ratios for all localities show large variabilities with regards to different depth intervals (see Appendix A, table 12). Locality B (17.44), C (15.12) and G (16.04) have average N:P ratios closest to the Redfield ratio (N:P = 16). Locality A, L and K have average N:P ratios of 11.14, 20.34 and 25.82 respectively. Locality H shows the highest N:P ratios of 125.88. At Low N:P ratios it is expected that the uptake rates for $NH_4^+$ are higher in comparison to $PO_4^{3-}$.

The $NO_3^-$ concentrations display a general decrease from the sediment-water interface and generally become exhausted at approximately 5.5cm likely displaying zones of denitrification. $NO_3^-$ concentrations display a lot of variability between localities. Higher $NO_3^-$ concentrations at the sediment surface are likely related to nitrification leading to a conversion of ammonium into nitrates in oxidizing conditions which occurs until a depth of approximately 0.5cm for all localities, thereafter the $NO_3^-$concentration generally decreases with depth with some minor fluctuations. The $NO_3^-$ concentrations range from 0µM to 30.05µM for all localities. The highest $NO_3^-$ concentrations were observed at locality G with concentration ranges of 0µM to 30.05µM, followed by locality A (0-20.14µM), C (2.22-16.58µM), K (2.38-13.46µM), H (0.49-12.81µM), B (0-10.26µM) and L (2.83-9.61µM). Only locality K ($r^2$=0.52), L ($r^2$=0.33), G ($r^2$=0.29) and B ($r^2$=0.27) show weak to moderate negative correlations between $NH_4^+$ and $NO_3^-$. The remaining localities show no correlations between $NH_4^+$ and $NO_3^-$, A ($r^2$= 0.0043), C ($r^2$=0.05) and H ($r^2$=0.0024). The standard deviations range from 0µM to 28.48µM. Higher nutrient concentrations in the porewaters are generally associated with higher TOC, TN and chlorophyll concentrations within the sediments.

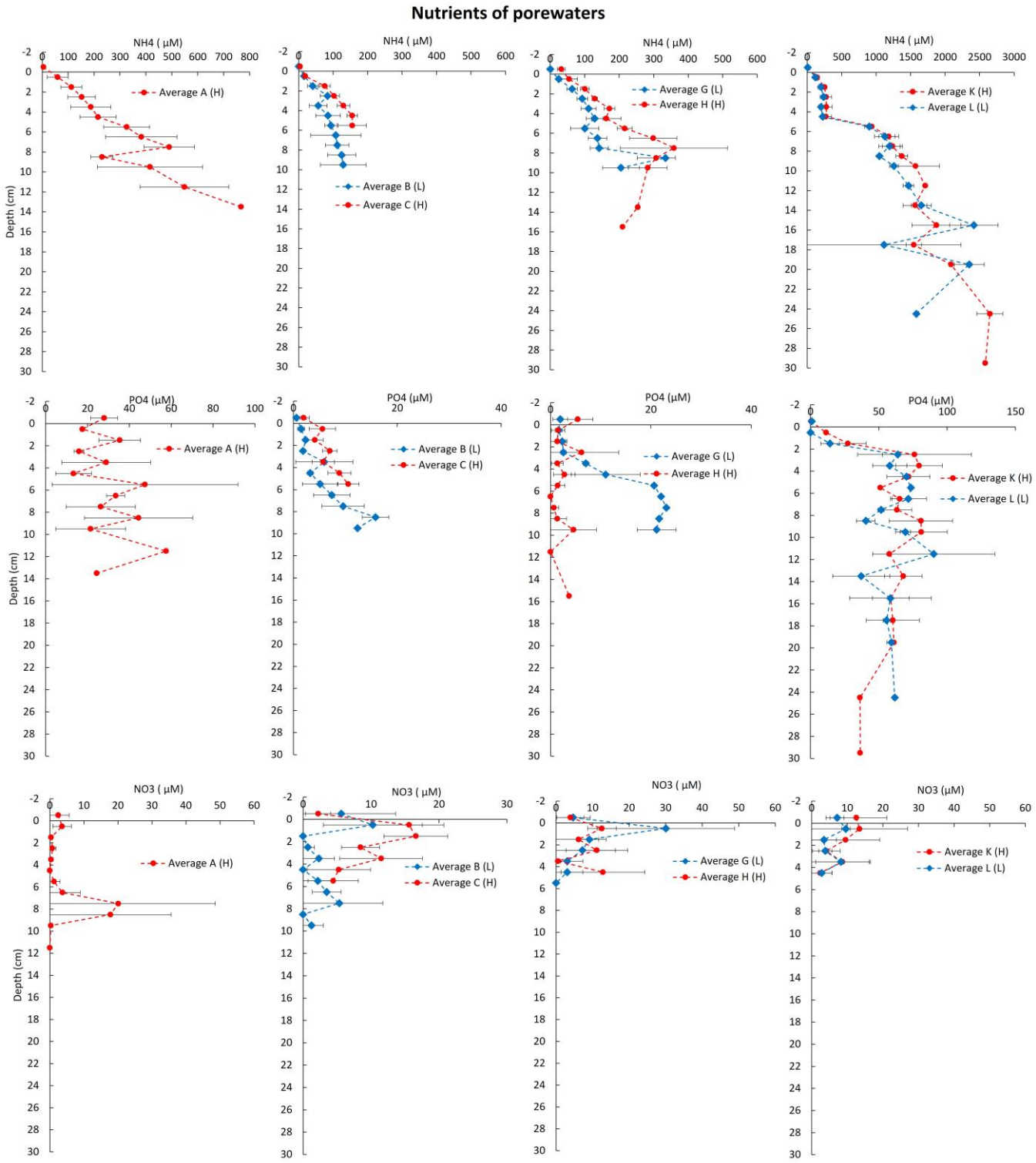



*Figure 17: Porewater profiles for nutrients ($NH_4^+$, $PO_4^{3-}$ and $NO3^-$) displaying relationships between High (H) and Low (L) trawled pairs at different localities. Error bars display the standard deviations between sample replicates. All localities had 3 replicates, apart for locality L which only had 2 replicates. The -0.5cm depth interval is representative of the overlying water of the sediment core. The depth interval at 0.5cm is representative of the first sample collected from sediment porewater of sediment sliced from the sediment surface with a 1cm thickness (0-1cm).*

*DIC and $\delta^{13}C$ of DIC in porewaters:*

The DIC concentrations display an increase from the sediment water interface with depth for all the localities (figure 18). The DIC concentrations range from 1.95mM to 23.48mM. The highest DIC concentrations were observed at locality L with concentrations ranging from 2.29mM to 23.48mM, followed by locality K (2.27-22.11mM), A (2.06-7.33mM), H (2.37-4.12mM), G (2.03-3.56mM), B (1.95-3.40mM) and C (2.10-3.30mM). The standard deviations range from 0mM to 2.52mM. All localities display a gradual decrease in TOC concentration within the sediments which is consistent with an increase in DIC and $NH_4^+$ with depth in the porewater profiles indicative of mineralization after sediment burial. C:N ratios display a significant decrease with depth and likely present the most accurate ratios from 5.5cm after $NO_3^-$ concentrations have generally been exhausted (See Appendix A, table 13). C:N ratios in this section refer to the ratio between DIC and $NH_4^+$. C:N ratios for all localities are well above the Redfield ratio (C:N = 106:16). The C/P ratios are also well above the redfield ratio for all localities and may relate to retention of phosphates adsorbing to iron oxyhydroxides (Van De Velde et al., 2018).

DIC and $NH_4^+$ show moderate to very strong positive correlations for all localities. Strong to very strong positive correlations between DIC and $NH_4^+$ are observed at locality A ($r^2$= 0.97), K ($r^2$=0.93), H ($r^2$=0.91), L ($r^2$=0.83) and B ($r^2$=0.8). Moderate to strong correlations between DIC and $NH_4^+$ are observed at locality C ($r^2$=0.64) and G ($r^2$=0.51). DIC and $PO_4^{3-}$ show weak to very strong positive correlations between all localities. Strong to very strong positive correlations between DIC and $PO_4^{3-}$ are observed at locality G ($r^2$=0.9), B ($r^2$= 0.89) and C ($r^2$=0.79). Low positive correlations between DIC and $PO_4^{3-}$ were observed at locality K ($r^2$=0.11), H ($r^2$=0.15) and L ($r^2$=0.31). There is no clear correlation between DIC and $PO_4^{3-}$ at locality A ($r^2$=0.07).

Compared to the $\delta 13_{TOC}$ and $\delta 13_{total}$ concentrations within the sediment profiles, the $\delta^{13}C_{DIC}$ isotopes of the porewaters shows more variability and trends with depth and are heavier and less negative compared to isotope signatures in the sediments. The $\delta^{13}C_{DIC}$ concentrations lead to more negative isotope ratios from the sediment water interface with depth for all localities, apart for locality K and L which show a decrease in $\delta^{13}C_{DIC}$ values (more negative) until about 9.5cm followed by a sharp increase in the $\delta^{13}C_{DIC}$ values (less negative with depth). The $\delta^{13}C_{DIC}$ concentrations range from -22.60‰ to -1.60‰ for all localities. The most negative $\delta^{13}C_{DIC}$ ratios were observed at locality L with concentrations ranging from -22.60‰ to -3.77‰ with regards to all depth intervals, followed by locality K (-20.78‰ to -3.41‰), A (-15.39‰ to -2.94‰), H (-11.48‰ to -2.42‰), B (-9.12‰ to -1.65‰), G (-9‰ to -1.93‰) and C (-8.87‰ to -1.60‰). The standard deviation for all localities ranges between 0‰ to 4.07‰. The $\delta^{13}C_{DIC}$ profiles are generally mirrored to the DIC profiles. $\delta^{13}C_{DIC}$ and DIC show a strong correlation for locality A ($r^2$=0.87), B ($r^2$=0.78), C ($r^2$=0.74), G ($r^2$=0.6) and H ($r^2$=0.87) with regards to all depth intervals. There is almost no correlation between $\delta^{13}C_{DIC}$ and DIC for locality K ($r^2$=0.025) and L ($r^2$=0.01) with regards to all depth intervals.

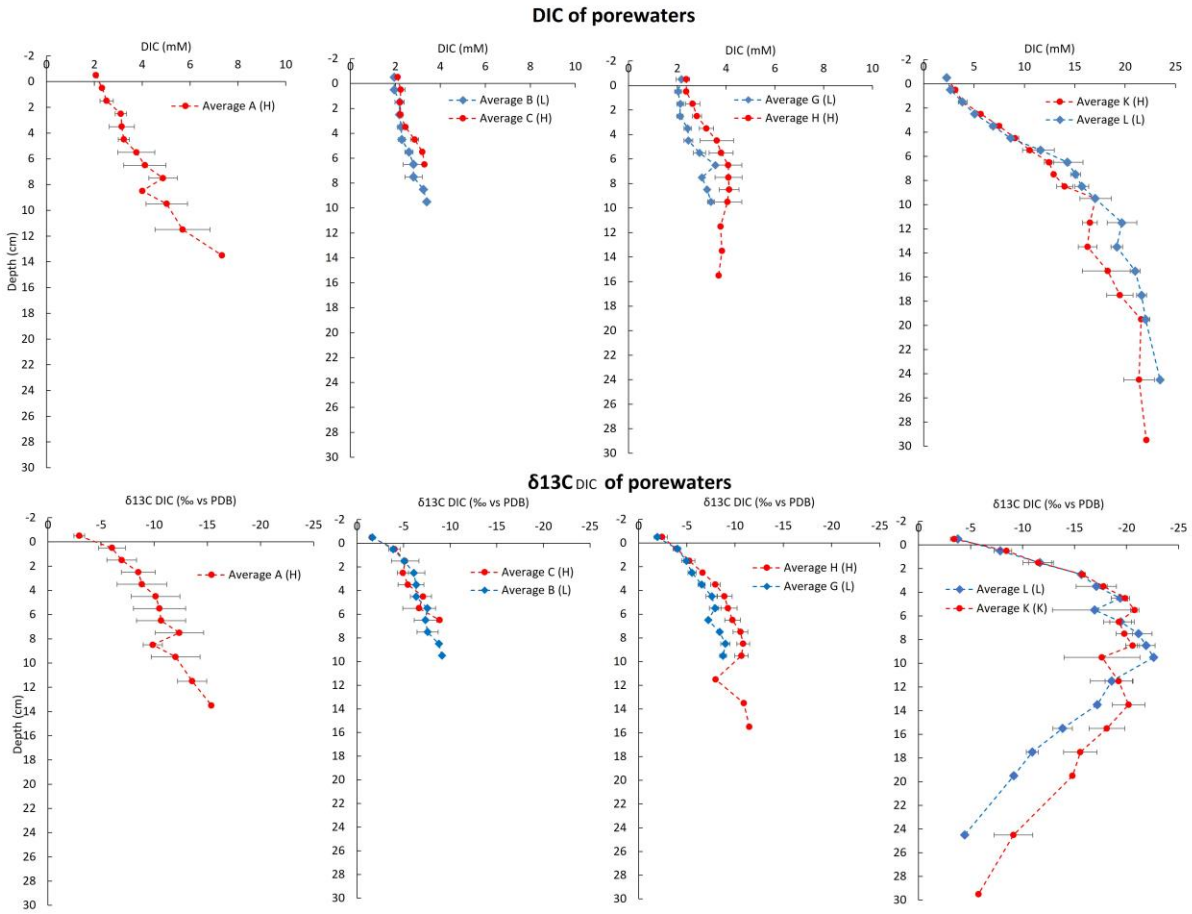



*Figure 18: Porewater profiles for DIC and δ13C$_{DIC}$ displaying relationships between High (H) and Low (L) trawled pairs at different localities. Error bars display the standard deviations between sample replicates. All localities had 3 replicates, apart for locality L which only had 2 replicates. The -0.5cm depth interval is representative of the overlying water of the sediment core. The depth interval at 0.5cm is representative of the first sample collected from sediment porewater of sediment sliced from the sediment surface with a 1cm thickness (0-1cm).*

### *3.3.2.2 Variability of porewater profiles by trawling intensity between high- and low-trawled pairs:*

See calculated differences at each depth between high and low trawled pairs in Appendix A.
The porewater difference show much more pronounced differences between high- and low-trawled localities compared to the solid-phase sediment profiles. With regards to all sites, low- and high-trawled locality B/C and G/H showed the greatest difference between high- and low-trawled pairs. High-trawled localities C and H contained higher concentrations of $NH4^+$ and DIC, as well as more negative $\delta^{13}C_{DIC}$ concentrations. The concentration difference between low- and high-trawled localities B/C and G/H showed a greater difference from a depth of about 3.5/4.5cm, compared to concentration differences between low- and high-trawled localities above 3.5cm, closer to the sediment-water interface, where concentrations approach near-constant values. Sites B/C show consistent, systematic changes between DIC, $NH_4^+$, $PO_4^{3-}$ and $NO_3^-$, which always had higher concentrations for high-trawled locality C. Sites G/H displayed the highest concentration differences of $NH_4^+$ and DIC with regards to all sites, consistent with observations in the solid-phase sediment profiles. Surprisingly, the $PO_4^{3-}$ concentration at low-trawled locality G is lower than at H, which is inconsistent to the $NH_4^+$ profiles. $NO_3^-$ concentrations do not show significant differences between locality G and H. Furthermore, locality G and H are distinctive since they display a sharp decrease in the $NH_4^+$ concentration at 8.5cm and 7.5cm respectively. A sharp decrease in $NH_4^+$ at locality G and H

may be as a result of sulfate reducing ammonium oxidation (Yang et al., 2023). K and L did not show any pronounced differences between high- and low-trawled pairs and $NH_4^+$, $PO_4^{3-}$, $NO_3^-$, DIC and $\delta^{13}C_{DIC}$ follow similar trends and concentration ranges for both profiles. Locality K and L, on average had the highest $NH_4^+$, $PO_4^{3-}$ and DIC concentrations as well as the most negative $\delta 13C_{DIC}$ concentrations.
Localities B and C display linear, near-constant DIC concentrations with very low differences between the pairs until a depth of about 3.5cm. Below 3.5cm low-trawled locality B, displays a concave-up DIC profile with depth. In comparison to low-trawled locality B, high-trawled locality C, displays a concave-down DIC profile below 3.5cm. Concave-up profiles represent, advective dominated processes by mixing of bottom waters by bioturbation, whereas concave-down profiles represent the combined effects between production and upward diffusion (Morys et al., 2021; Van De Velde et al., 2018).

Similar patterns are observed between low- and high-trawled localities G and H. Low-trawled locality G, displays near-constant DIC concentrations until a depth of 3.5cm, whereafter it displays a general concave-up profile with depth. High-trawled locality H, on the other hand displays a concave-up DIC profile until a depth of 3.5cm, whereafter it follows a concave-down, diffusive dominated profile. Localities K and L display advective dominated processes until deeper depths compared to the other localities, marked by a concave-up profile until a depth of about 5.5cm. Below 5.5cm, localities K and L show concave-down DIC, diffusive dominated profiles. The discontinuities in concentration gradients within the study area strongly suggest disturbances of the sediments (Vanderborght et al., 1977).

### *3.3.3 Fluxes*

See Appendix A for numerical values and calculations of fluxes.

#### *3.3.3.1 Fluxes calculated from benthic incubation experiments:*

The benthic incubation fluxes display a lot of variability between replicates for each locality as well as a lot of variation between the different localities with no clear differences between high- and low-trawled pairs for $NH_4^+$, $NO_3^-$ and $PO_4^{3-}$ (figure 19). The concentration ranges of the over lying waters from the Gemini cores generally fall in the same ranges as the t0 concentrations measured from the benthic incubation cores for all parameters. The $NH_4^+$ fluxes particularly displayed a lot of variability between replicates. The best discriminators for benthic fluxes within this study are oxygen and DIC. The $O_2$ fluxes are generally negative for locality A, B, C, G, H and K and indicate a decrease in the oxygen concentration in the overlying water with time (t1-t0) indicative of oxygen consumption within the sediments. Only locality L generally displayed positive oxygen concentration, likely induced by measurement errors. With regards to all localities, the $O_2$ fluxes are higher (more negative for locality C, H, K) for areas identified as high-trawled areas compared to their low-trawled pairs. Between locality B and C, the average $O_2$ fluxes are 3808 µmol/$m^2$d more negative for locality C than locality B. Between locality H and G, the average $O_2$ fluxes are 10242 µmol/$m^2$d more negative for locality H than locality G. The DIC fluxes are generally negative and decrease with time in the overlying water for locality A, B, C, K and L. The DIC fluxes for locality G and H are on the other hand positive, indicative of increasing DIC concentrations in the water column with time. The DIC fluxes are on average 17.45mmol/$m^2$d lower (less negative) for locality C compared to locality B. The DIC fluxes between G and H are on average 24.24mmol/$m^2$d lower (less positive) for locality H compared to locality G. The DIC fluxes between K and L are on average 4.76mmol/$m^2$d lower (less negative) for locality K compared to locality L. In summary, DIC fluxes are generally lower for high-trawled areas and $O_2$ fluxes are generally higher for high-trawled areas. The high variability between replicates and localities are likely caused by changes in micro-/macrofauna within each core as well as changes between bioturbation and bioirrigation between the different sites. Unfortunately, the macrofauna within the incubation cores have not been analysed in time for this study and benthic incubation fluxes are therefore only described briefly.

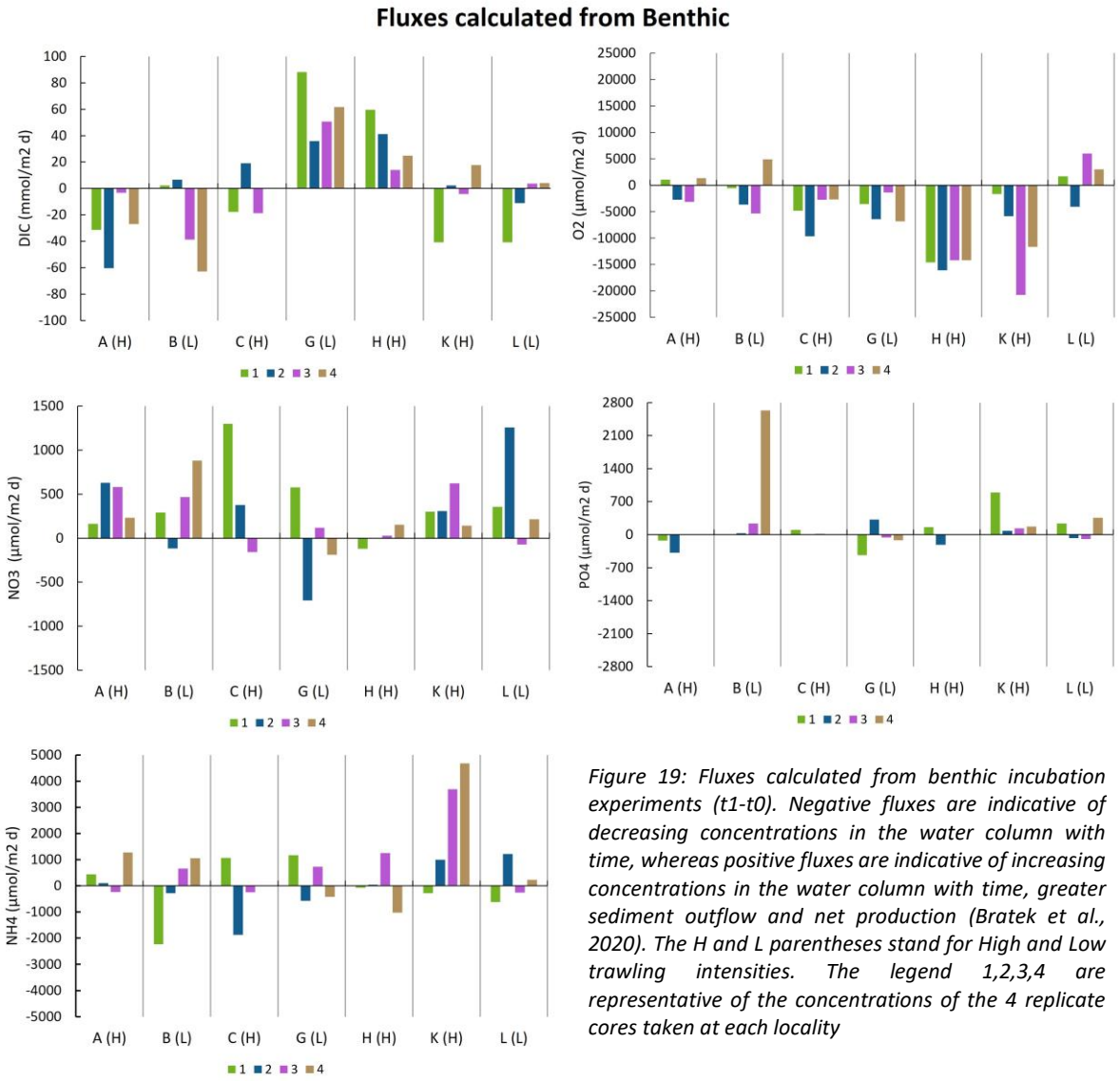



*Figure 19: Fluxes calculated from benthic incubation experiments (t1-t0). Negative fluxes are indicative of decreasing concentrations in the water column with time, whereas positive fluxes are indicative of increasing concentrations in the water column with time, greater sediment outflow and net production (Bratek et al., 2020). The H and L parentheses stand for High and Low trawling intensities. The legend 1,2,3,4 are representative of the concentrations of the 4 replicate cores taken at each locality*

### *3.3.3.2 Fluxes calculated from porewater gradients through Fick's law:*

The fluxes were calculated from the porewater concentration gradients of the overlying water (-0.5cm) until a depth of 2.5cm from the sediment surface. The fluxes calculated from the porewater gradients show much less variability and significantly lower standard deviations compared to the fluxes calculated from the benthic incubation experiments (see Appendix A). DIC and $NH_4^+$ show positive fluxes for all localities indicative of increasing concentrations with depth, negative gradients and positive upwards fluxes (figure 20). The highest DIC fluxes were observed at locality A (0.54 – 1.36mmol/$m^2$d) and the lowest at locality G (0.01 – 0.09mmol/$m^2$d). The highest $NH_4^+$ fluxes were observed at locality A (207.23 – 393.32 µmol/$m^2$d) and the lowest at H (17.75 – 25.57 µmol/$m^2$d). $PO_4^{3-}$ generally shows positive upward fluxes for all localities apart for locality A, which is distinctive in showing negative downwards fluxes. The highest $PO_4^{3-}$ fluxes were observed at locality K (2.26 to 8.03 µmol/$m^2$d) and the lowest at H (-0.47 to 0.58 µmol/$m^2$d).

$NO_3^-$ shows the most variability between sample replicates and displays both positive upwards fluxes as well as negative downwards fluxes. On average (average of replicates), $NO_3^-$ shows positive upward

fluxes for locality C and H and and negative downwards fluxes for the remaining localities.
The highest $NO_3^-$ fluxes were observed at locality B (-11.35 to -1.97 µmol/m$^2$d), followed by A (-14.11 to 2.41 µmol/m$^2$d), C (1.05 to 6.74 µmol/m$^2$d), K (-3.39 to -1.06 µmol/m$^2$d), G (-4.22 to 5.24 µmol/m$^2$d), H (-2.16 to 4.99 µmol/m$^2$d) and L (-1.16 to -0.47 µmol/m$^2$d). Locality B on average (average fluxes of replicates) displayed higher DIC and $NH_4^+$ fluxes than its high-trawled pair C (DIC: 0.084 mmol/m$^2$d higher for B, $NH_4^+$: 3.71 µmol/m$^2$d higher at B). In contrast, locality G displayed lower DIC fluxes compared to its high-trawled pair H but higher $NH_4^+$ fluxes (DIC: 0.037 mmol/m$^2$d lower for G, $NH_4^+$: 10.75 µmol/m$^2$d higher for G). Locality L on average displayed lower DIC and $NH_4^+$ fluxes than its high-trawled pair K (DIC: 0.118 mmol/m$^2$d lower for locality L, $NH_4^+$: 18.11 µmol/m$^2$d lower for locality L). The $PO_4^{3-}$ concentration of high- and low-trawled pairs is higher for high-trawled locations C ($PO_4^{3-}$: 0.47 µmol/m$^2$d higher for C compared to B) and K ($PO4^{3-}$: 1.48 µmol/m$^2$d higher for K compared to L), whereas the $PO_4^{3-}$ concentration is lower for high-trawled location H ($PO_4^{3-}$: 0.08 µmol/m$^2$d lower for H compared to G).

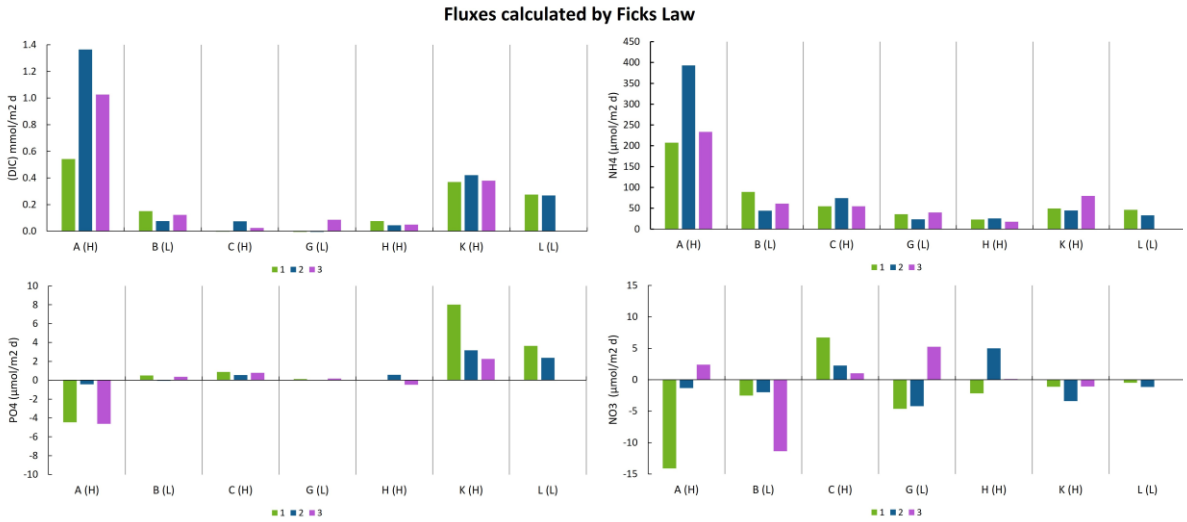



*Figure 20: Fluxes calculated by Fick's law only taking account molecular diffusion. Fluxes were calculated from gradients of porewater concentrations from overlying water -0.5cm until a depth 2.5cm below the sediment surface. Increasing concentrations with depth yield negative gradients within the sediment with a positive upwards flux (Schulz & Zabel, 2006) and flow out of the sediment upwards into the overlying water column. The H and L parentheses stand for High and Low trawling intensities. The legend 1,2,3 is representative of the concentrations of the 3 replicate cores taken at each locality.*

## 3.4 Macrofauna

The macrofauna from 2023, differs only slightly from macrofauna that was observed in 2019 and 2020 with the addition of some new species at localities in 2023 (see figure 21 for onsite macrofauna observations). The community bioturbation potential (BPc) and the bioirrigation potential (IPc) was calculated from the wet weights of different taxa in 2019 and 2020 and their burrowing and feeding traits, with higher values indicative of more mixing of particles (BPc) or solutes (IPc).

The highest IPc were observed at locality L and K respectively with regards to all localities (table 11). These 2 sites contained the highest abundances of *Macoma balthica* bivalves, *Oligochaeta* worms and *Scoloplos armiger* worms (apart for locality A which contains a higher abundance of *Scoloplos armiger* than K) both in the macrofauna dataset from 2023 and 2019/2020. The highest BPc was observed at locality B which contains a higher abundance of *Astarte borealis* bivalves and *Diastylis rathkei* crustaceans compared to other localities both in the macrofauna dataset from 2023 and 2019/2020. Pairs B/C and G/H both showed lower BPc and IPc for the high-trawled counterparts.

Similar to macrofaunal abundances in 2019, the priapulid worm *Halycryptus spinulosus* and the bivalve *Macoma baltica* were more abundant at high-trawled localities C and K. Furthermore, the *Diastylis rathkei* crustacean had much higher abundances in 2023 compared to 2019, whereby the abundance is higher for high-trawled locality H compared to low-trawled locality G but these species are not very mobile and likely do not affect the BPc and IPc significantly. Although not significant, the deep burrowing, polychaete *Scoloplos armiger* was similar in abundance for both high- and low-trawled localities in 2023. Localities G and H had the lowest summed biomass, showing not much difference between the 2 pairs (1.44g and 2.58 g respectively). Localities B and C showed the largest difference of summed biomasses between the pairs (38.75g and 12.54 g respectively). The biomass of locality A was relatively low, 3.33g and sites K/L ranged from 22.99 g to 12.8 g respectively.

| Localites | A | B | C | G | H | K | L |
|---|---|---|---|---|---|---|---|
| Bioturbation Potential (BPc) | 37.72 | 207.93 | 70.85 | 67.32 | 24.39 | 98.46 | 178.43 |
| Bioirrigation Potential (IPc) | 15.51 | 44.14 | 27.69 | 38.30 | 12.91 | 48.40 | 93.79 |

*Table 11: Bioturbation Potential (BPc) and Bioirrigation Potential (IPc) at different localities calculated from macrofauna dataset from 2019/2020.*

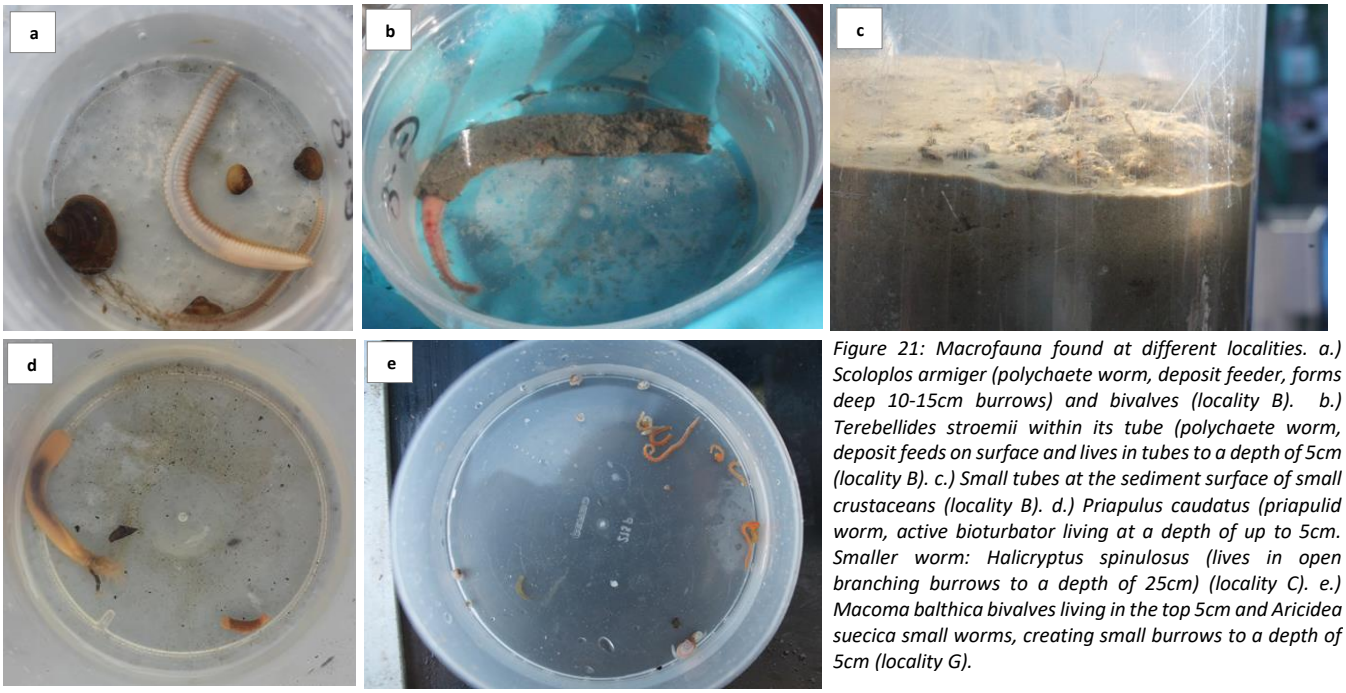



*Figure 21: Macrofauna found at different localities. a.) Scoloplos armiger (polychaete worm, deposit feeder, forms deep 10-15cm burrows) and bivalves (locality B). b.) Terebellides stroemii within its tube (polychaete worm, deposit feeds on surface and lives in tubes to a depth of 5cm (locality B). c.) Small tubes at the sediment surface of small crustaceans (locality B). d.) Priapulus caudatus (priapulid worm, active bioturbator living at a depth of up to 5cm. Smaller worm: Halicryptus spinulosus (lives in open branching burrows to a depth of 25cm) (locality C). e.) Macoma balthica bivalves living in the top 5cm and Aricidea suecica small worms, creating small burrows to a depth of 5cm (locality G).*

# 4. Discussion and Interpretation

## 4.1 Variabilities across study sites and considerations for upscaling the effects of trawling

To study the effects of trawling on carbon mineralization by means of on-site sampling, it is important to conduct a sampling campaign comparing localities with similar hydrographic, sedimentary, physio-chemical and biological conditions paired into high- and low-trawled intensities based on high-resolution SAR (swept-area ratio) and fishing intensity maps interpolated from detailed information from fishing log books and fishing vessels equipped with VMS (vessel monitoring systems). On a global scale, detailed information from fishing log books and VMS may be incomplete. This shows only one of the major challenges associated with identifying the impacts of trawling on carbon mineralization globally and locally. Another challenge is to accurately discriminate whether mixing and chemical variations in sediment and porewater profiles occur as a result of bioturbation/bio-irrigation and/or disturbances (including disturbances caused by trawling and/or high turbidity currents) in the overlying waters and sediments. To discriminate natural biogeochemical variations within sediments from trawling-associated disturbances, large datasets on porewater and sediment profile concentrations are required, particularly in locations that may display a mixture of physical disturbances and natural biogeochemical variations. In addition, data of the physio-chemical bottom water properties, sediment grain size distributions, macrofauna, bioturbation/bioirrigation potential and fluxes are required. CT scans of sediment cores to identify structural changes, multi-beam and sidescan sonar analyses may provide evidence for sediment resuspension and redeposition related to trawling, which should be coupled to biogeochemical and compositional observations. Lastly, transport models of porewater profiles, simulating different scenarios of mixing and advection effects of natural variabilities and/or disturbances or obtaining mixing coefficient by bioturbation through experiments with artificial tracers, may be useful to quantify the extent of disturbances and mixing related to trawling.

The results from the current study highlight the challenges to discriminate natural from induced biogeochemical variability. Sites 1 to 4 display a lot of variability in their physio-chemical properties, sediment grain size distributions, sediment and porewater concentration profiles and fluxes as well as abundances in macrofauna and their associated bioturbation/ bioirrigation potentials. Comparisons between sites for all measured properties show greater differences than those observed between their high- and low-trawled locality pairs.

## 4.2 Trawling and its effect on the seafloor and sediment properties

Seabed alterations can be seen in the linear morphological depression (trawl marks on the seabed) from multibeam and sidescan sonar analyses and are more pronounced and frequent in areas that have been classified as high-trawled, whereby trawl marks are more pronounced in muddy and finer-grained sediment as observed at locality K and L, which show the highest proportion of silts and clays. The trawl track marks with regards to all localities, displayed no prominent direction. Trawl marks on soft and fine-grained sediment beds, similar to those observed in this study area may persist for longer than one year (Palanques et al., 2001); since this study area has not been trawled since 2019, trawl marks may even persist for more than 4 years. Localities A, G, H, K and L in particular show a lot of ridges and are situated in localities with higher SAR trawling intensities compared to locality B and C, whereby trawling seems to be related to change the roughness of the seabed (Bruns et al., 2023). The persistence of trawl track marks on the seabed are highly dependent on the complex relationships between natural disturbances and sediment transport processes (turbidity currents and wave action), sediment composition, hydrodynamic conditions, frequency and trawling intensity as well as the type of trawling gear that has been used and may furthermore influence the organic carbon content and bioturbation potential within the sediments (Bruns et al., 2020, 2023; Jones, 1992; Mérillet et al.,

2018). The sedimentation rates of the study sites displayed highly variable results with large ranges and are subject to high uncertainties since sediments displayed a lot of mixing. Sedimentation rates of all localities ranged between ± 0.021 to 0.141 g/cm$^2$yr, which fall into similar $^{210}$Pb accumulation rates in the Bornholm basin found by Christoffersen et al. (2007), ranging between 0.0129-0.1144 g/cm$^2$yr. Locality K and H, both classified as high-trawled sites, have lower sedimentation rates compared to their low-trawled locality pairs. Lower sedimentation rates could be related to high mixing, resuspension and erosion of newly deposited material, whereas higher sedimentation rates at locality A, G and L may be related to redeposited material that was suspended after trawling (Bruns et al., 2023; Christoffersen et al., 2007; Paradis et al., 2021).

Locality C and H, classified as high-trawled localities, showed a significant decrease in grainsize with depth and an upward coarsening as well as an overall higher proportion of clays and silts with lesser sands and gravels compared to their low-trawled locality pairs which displayed a relatively homogeneous grain size distribution and indicated a higher degree of sorting. Similar observations of upward coarsening in trawled areas have been described by Palanques et al. (2014), who attributed the upward coarsening and increase in silt fractions to winnowing of resuspended sediments during continuous scraping and ploughing of the seabed (Palanques et al., 2014). Furthermore, the grading of the sediments in high-trawled areas may be affected by tides and currents, whereby fine-grained materials settle on coarser material when currents are absent (Bruns et al., 2020). Locality A, B and G displayed normally graded beds with lower turbidities than locality C, H and L. In the presence of tides and currents the fine-grained material would be transported away, leading to a decrease in fine particles on the sediment surface (Bruns et al., 2023). Locality C, H and L displayed higher turbidity in their bottom waters and likely represent areas where currents are stronger leading to the transportation of finer fractions to adjacent localities and could explain the inverse grading observed at these localities.

## 4.3 Trawling and its effect on solid-phase sediment concentration profiles

The TOC, TN, TC and chlorophyll concentrations for all localities displayed a general decrease with depth indicative of ongoing organic matter remineralization and degradation. The highest TOC concentrations were observed at locality K and L, which are the deepest sampling sites with the lowest oxygen concentrations. The spatial variation in TOC contents therefore also depend on their water depths, whereby poorer degradation in the deeper parts of the basin may be a function of less frequent oxygen supply by inflow waters (Christoffersen et al., 2007).

With regard to all localities, locality G and H showed the greatest and most distinct differences between high- and low-trawled pairs, whereby high-trawled locality H displayed higher and stronger upward increasing gradients for TOC, TN, TC, $\delta^{13}C_{TOC}$ and chlorophyll concentrations compared to its low-trawled locality pair G, specifically close to the sediment surface from 0.5 to 6.5cm. For the remaining high and low-trawled locality pairs (B/C and K/L), the concentration differences between TOC, TN, TC and $\delta^{13}C_{TOC}$ were lower and less pronounced, although generally displaying higher concentrations for TOC, TN and TC at high-trawled localities C and K specifically in the upper 3.5cm and 6.5cm respectively. Higher TOC concentrations in trawled areas have also been observed in the Thermaikos Gulf and in the northwestern Mediterranean by Palanques et al. (2014) and Pusceddu et al. (2005), who have related these trends to geopolymeric carbon that have been surfaced from deeper sediments (bottom-up transfer) during reworking and/or decreased carbon and nitrogen uptake by benthic organisms. In this case, surfaced geopolymeric carbon is transformed to biopolymeric organic carbon, which may be utilized by benthic organisms leading to an increased bacterial activity in trawled sediments and increased oxygen availability which leads to enhanced degradation of refractory compounds (Pusceddu et al., 2005). The most applicable hypothesis in this study area points to decreased carbon and nitrogen uptake by benthic organisms, leading to higher

TOC concentrations in trawled areas, since these localities contained lower biomasses and bioturbation (BPc) and bioirrigation (IPc) potentials. Furthermore, sediment disturbances have been related to release large nutrient loads, contributing to primary production, specifically during phytoplankton blooms leading to an increase in the TOC concentration within sediments (Palanques et al., 2014; Pusceddu et al., 2005), since this study area has not been trawled since 2019, this hypothesis is unlikely in this study and a much larger study area would be required to test this hypothesis.

Locality G and H, had lower bioturbation and bioirrigation potentials and lower biomasses compared to high- and low-trawled BPc and IPc of B/C and K/L and could explain the greater concentration differences seen between high-trawled locality H and low-trawled locality G, due to lower microbial activity, lower degradation rates and reduced carbon and nitrogen uptake by benthic organisms (Pusceddu et al., 2005). Lower bioturbation potentials in sediments are largely dependent on dissolved oxygen and the quality of organic matter, whereby high-quality organic carbon and low dissolved oxygen concentrations favour tube building, surface-feeding organisms which have lower bioturbation potentials (Gutiérrez et al., 2000). Furthermore, trawling modifies and disturbs the structure of benthic habitats since trawling induced changes in the porosity, sediment composition and water content largely affect the benthic community structure and benthic fluxes (Ellingsen, 2002; Morys et al., 2021). Trawled areas are dominated by opportunistic species, showing a higher abundance of burrowing epifaunal feeders and deep burrowing infauna (De Juan et al., 2007; Pusceddu et al., 2005). In contrast, untrawled regions have a greater abundance of bottom-dwelling, tube building infauna, suspension feeders and predatory fish (De Juan et al., 2007; Pusceddu et al., 2005). Differences between epifauna and infauna in trawled and untrawled regions result in different BPc and IPc and may affect the texture and carbon content in the sediments (Pusceddu et al., 2005). The lower BPc and IPc at high-trawled localities and lower macrofaunal biomass are likely caused as a secondary response to trawling induced changes, rather than environmental factors that have not completely recovered in a 4-year time span, since high- and low-trawled pairs had similar sediment compositions, similar depths and hydrographic conditions. Therefore, the effects of trawling and the ability to detect differences between carbon mineralization of high and low-trawled pairs, is largely dependent and a factor of biological activity, sediment compositions and natural variabilities within the water column and the sediments.

Chlorophyll is an important indicator of fresh high quality organic matter and in determining periods of high productivity and phytoplankton blooms and preservation and anoxic conditions in marine and freshwater systems (Szymczak-Zyła et al., 2011). The chlorophyll concentrations displayed higher concentrations for all high-trawled localities specifically close to the sediment surface from a depth of ~0.5- 1.5cm, displaying recent chlorophyll deposition with a lower degree of degradation compared to deeper sediments (Buat-Menard, 1986). The fresh organic matter likely settled on the seabed by mid-April/early May during the phytoplankton bloom season (Bradshaw et al., 2024). Sciberras et al. (2016) has related high levels of TOC and chlorophyll in frequently trawled areas to decreased consumption due to a reduction in biomass and/or the accumulation of resuspended particles. High chlorophyll concentrations at trawled sites are likely not controlled by elevated nutrient concentrations in the sediments since light penetration is too low, but rather settled on the seabed from the water column during the recent spring bloom. Differences in chlorophyll and TOC concentrations between high and low-trawled sites are likely controlled by benthic macrofauna, by controlling TOC mineralization through redox processes and organic matter from phytoplankton through bioturbation (Sciberras et al., 2016). High-trawled sites within this study contained a high abundance of *Halicryptus spinulosis* and *Scoloplos armiger* which are deep-burrowing, gallery building worms which degrade fresh organic carbon more slowly compared to surface feeders, thus resulting in decreased reworking and sediment processing, leading to higher chlorophyll concentrations (Bradshaw et al., 2024). The variabilities of chlorophyll concentrations seen at the various sites are

furthermore highly dependent on transport by water currents, their hydrodynamic conditions and depth of the seabed. Localities that show higher bioturbation and bioirrigation potential, situated at low-trawled localities, display lower chlorophyll concentrations and likely represent areas of higher productivity with faster degradation rates and higher consumption of chlorophyll and nutrients leading to overall lower chlorophyll and nutrient concentrations compared to high-trawled localities. Moreover, high chlorophyll concentrations at depth, as seen at locality K and L, are linked to localities with finer grain sizes, higher TOC contents and higher sedimentation rates leading to hypoxic/anoxic conditions within the sediment column and enhanced preservation and lower degradation of chlorophyll (Szymczak-Zyła et al., 2011). Anoxic conditions greatly inhibit aerobic organisms and largely reduces or even eliminates bioturbation in sediments (Szymczak-Zyła et al., 2011). Localities with lower sedimentation rates, higher proportions of coarser sediments such as fine sands and more mixing leads to more oxic conditions and increased chlorophyll degradation with depth (Burdige, 2006). More favourable water column exchange between the water column and sediments in localities with higher proportions of courser sediments likely lead to increases in oxygen conditions favouring aerobic processes and bioturbation leading to a higher degree of chlorophyll degradation (Burdige, 2006).

The $\delta^{13}C_{TOC}$ and the $\delta^{13}C_{total}$, generally did not display significant differences between high- and low-trawled locality pairs B/C, G/H and K/L and are thus not the best discriminators to differentiate differences related to low- and high-trawled sites, specifically in areas that display organic matter sources derived from a mixture of terrestrial material and marine material, as was the case within this study area. Products of organic matter degradation such as $NH_4^+$, DIC, and $\delta^{13}C_{DIC}$ in sediment porewaters are much more sensitive discriminators of carbon mineralization between high- and low-trawled locality pairs, since small changes in porewater composition occur against a low background, e.g., $NH_4^+$ and $PO_4^{3-}$, or are isotopically distinct, such as DIC produced by carbon mineralization (Hesse & Schacht, 2011; Schulz & Zabel, 2006).

The organic matter content of sediments within the study area mainly point to a mixture of a terrestrial source and marine algae with $\delta^{13}C$ values falling into the ranges of Rubisco carbon isotope fractionation ranging from -19.9‰ to -24.8‰, with a preferential uptake of the lighter $^{12}C$ isotope (Bauer et al., 2002; Silori et al., 2021). The C/N ratios within the sediments remain relatively constant with depth and generally decrease with decreasing grain size as can be seen for locality K and L, which have higher clay fractions as a result of degradation of nitrogen metabolites, which are usually associated with coarse vascular plant material, leading to higher C/N ratios in coarser materials in comparison to finer grained material (Burdige, 2006).

The general decrease in TOC and TN concentrations with depth at all localities are likely related to increased mineralization by microorganisms and metazoans (Escobar-Briones & García-Villalobos, 2009). Fluctuating profiles in $\delta^{13}C_{TOC}$ and $\delta^{13}C_{total}$ at all localities are possibly related to variable sedimentation rates due to mixing (Yang et al., 2023). The sharp decreases in TOC concentrations at locality C, G and H may be related to lower bioturbation potentials seen at these locations, leading to an exponential decrease in TOC concentrations and its rate of mineralization with depth (Burdige, 2006). More gradual TOC concentrations at locality B, K and L are likely related to high bioturbation potentials, whereby higher biological activity mixes surface sediments rich in TOC with deeper sediments lower in organic carbon that has been remineralized (Burdige, 2006).
Fluctuations and shifts in $\delta^{15}N$ profiles may be related to early diagenesis of organic matter during microbial processes which can shift $\delta^{15}N$ ratios to more positive values at around 3 in oxic environments (Cartigny & Busigny, 2018). Furthermore, higher and heavier $\delta^{15}N$ values are generally related to denitrification within the sediments, which discriminates against the heavier 15N isotope, preferentially incorporating the lighter 14N isotope leading to heavier signals with $\delta^{15}N$ values of approximately 0‰ (Quan & Falkowski, 2009; Yang et al., 2023). Most nitrogen reactions preferentially

incorporate the lighter 14N isotope into their product leaving the reactants enriched in 15N, leading to heavier isotope signals. Only nitrogen fixation preferentially incorporates the heavier isotope 15N, leading to lower isotope signals (Quan & Falkowski, 2009). $\delta^{15}N$ values for sediments dominated by nitrogen fixation yield values ranging between -2‰ to 2‰ with lighter isotope signals (Quan & Falkowski, 2009). In general, most of the $\delta^{15}N$ within all study locations are enriched in the heavy 15N isotope (>2‰), with relatively large and heavy isotope signals indicative of denitrification, specifically at locality A, C, H and L. $\delta^{15}N$ values < 2‰ are observed only at specific depth intervals at locality A at 6.5cm and 8.5cm, locality B from a depth of 6.5cm, locality G at 3.5cm and locality K at 28.5cm and may have occurred as a result of nitrogen fixation specific to individual depth intervals.

## 4.4 Statistical significance of high- and low-trawled pairs of porewater profiles

At trawling pairs B and C, the effect of trawling intensity is significant for $NH_4^+$, $PO_4^{3-}$ and DIC whereby higher trawling intensities are associated with increased concentrations of $NH_4^+$, $PO_4^{3-}$ and DIC (p-values of trawling intensity: 0.0167, 0.009 and 0.016, respectively) indicating that trawling activities significantly impact sediment biogeochemistry by potentially increasing the concentrations of nutrients and DIC in the porewaters; $NO_3^-$ and $\delta^{13}C$ showed no significant effects with trawling intensity (p-values: 0.21 and 0.33). Depth shows a significant effect for $NH_4^+$, DIC and $\delta^{13}C$ (p-value: 0.007, 0.01 and 0.0004, respectively), where shallower depths (-0.5 to ~ 2.5cm) display significant negative effects (at these depths, the concentrations are lower relative to the intercept modelled by JMP) for $NH_4^+$ and DIC and significant positive effects at deeper depths (4.5cm) (at these depths, the concentrations are higher relative to the intercept, modelled by JMP).The opposite trends are observed in $\delta^{13}C$, displaying positive effects at shallower depths (-0.5 and 0.5cm) and negative effects at deeper depths (4.5cm).

For trawling pairs G and H, the trawling intensity is significant for $NH_4^+$, $PO_4^{3-}$, DIC and $\delta^{13}C$ (p-values: 0.0071, 0.0331, <0.0001 and 0.0003), whereby an increase in trawling intensity is associated with an increase in $NH_4^+$ and DIC and a decrease in $PO_4^{3-}$ and $\delta^{13}C$ (more negative). Depth had a significant effect for $NH_4^+$, DIC and $\delta^{13}C$ (p-values: 0.0034, <0.0001 and <0.0001, respectively), where shallower depths (-0.5 to ~1.5cm) display strong negative effects and deeper depths ~6.5 to 9.5cm display strong positive effects for $NH_4^+$ and DIC. The opposite trend is observed for $\delta^{13}C$ which shows strong positive effects at shallower depths (-0.5 to 2.5cm) and strong negative effects from 7.5 to 9.5cm. $NO_3^-$ does not show strong effects for neither trawling intensity, nor depths for both locality B/C (p-value; 0.21 and 0.60, respectively) and G/H (p-value: 0.63 and 0.15, respectively).

For trawling pairs K and L, the trawling intensity is significant only for DIC (p-value: 0.0049), where higher trawling intensities are associated with a decrease in DIC concentration. Depth displays a significant effect for all variables, $NH_4^+$, $PO_4^{3-}$, $NO_3^-$, DIC and $\delta^{13}C$ (p-value: <0.0001, 0.0006, 0.0386, <0.0001 and <0.0001, respectively), showing significant negative effects at shallow depths (-0.5cm to ~4.5cm) for $NH_4^+$, $PO_4^{3-}$, and DIC and significant positive effects at deeper depths (11.5 to 25.5cm). The opposite trend is observed for $\delta^{13}C$ which shows strong positive effects at shallower depths (-0.5 to 1.5cm) and strong negative effects from 4.5 to 13.5cm.

The variability in significance at different depths suggest that trawling disturbances and its associated changes to bioturbation and bioirrigation potential impacts nutrient, DIC and isotopic distributions differently throughout the sediment column and is largely dependent on biological species and biological activity in the sediments. In all localities, negative effects for $NH_4^+$, $PO_4^{3-}$, DIC were generally observed at shallower depths whereas positive effects were observed at deeper depths. In contrast, $\delta^{13}C$ generally displayed positive effects at shallower depths and negative effects at deeper depths. These observations could be related to higher biological activity at the sediment surface, which play a crucial role in carbon cycling at shallower depths leading to an increased consumption of the nutrients

and DIC resulting in lower concentrations. Furthermore, higher organic matter content at the surface of the sediments, promotes microbial respiration leading to a further drawdown in nutrients and DIC, whereas deeper sediments have lower TOC contents and slower metabolic rates leading to the accumulation of DIC over time. Higher redox potential in shallower sediments and oxidizing conditions favour aerobic microbial respiration, whereby deeper sediments are more reduced, enhancing anaerobic processes like bacterial sulfate reduction releasing DIC as a byproduct.

## 4.5 Trawling and its effect on carbon mineralization products in porewaters:

The porewater profiles for mineralisation end-products ($NH_4^+$, $PO_4^{3-}$ and DIC) displayed distinct differences for all high- / low-trawled locality pairs and are much more sensitive to diagenetic changes compared to solid-phase sediment concentration profiles. Localities B/C and G/H displayed higher $NH_4^+$, DIC and more negative $\delta^{13}C_{DIC}$ for high-trawled localities, whereby the differences between high and low-trawled concentrations increased from a depth of about 3.5 to 4.5cm (statistical significance is described below).

The DIC, $\delta^{13}C_{DIC}$ profiles for locality pairs B/C, G/H and K/L follow similar trends and all point to a remineralized $\delta^{13}C_{DIC}$ source of marine origin. The higher concentrations observed in the high-trawled localities are thus likely not a consequence of natural compositional differences, but rather show an increased quantity of DIC that has accumulated and retained in the pore space, largely due to differences in BPc and IPc of the individual localities. Concave-up DIC porewater profiles with increasing depth can be interpreted to indicate the effect of mixing with bottom waters by bioirrigation, whereas concave-down profiles display the combined effects of production due to organic matter mineralisation and transport limitation by upward diffusion (Morys et al., 2021; Van De Velde et al., 2018).

The porewater concentration profiles for low- and high-trawled locality pairs B/C and G/H displayed near-constant values, approaching the concentrations of the overlying water column in the upper ~3.5cm for DIC, $NH_4^+$ and $PO_4^{3-}$, suggesting effective mixing of the upper 3.5cm, by advection through bioturbation and bioirrigation (Van De Velde et al., 2018). Sediments below 3.5cm at high-trawled localities C and H may not have had the time to effectively re-equilibrate with overlying waters due to slow diffusive transport rates and lower biological activity leading to lower BPc and IPc compared to their low-trawled pairs, resulting in concave-down profiles and higher DIC concentrations. Thus, it is interpreted that the sediment mineralization rates between high-/low-trawled locality pairs B/C and G/H are likely similar, but the different concentrations in DIC and nutrients are due to differences in advective and diffusive transport processes, mainly influenced by BPc and IPc, whereby the total transport rates are higher at low-trawled localities, since they are dominated by both advection and diffusion due to higher BPc and IPcs and lower at low-trawled localities since they are dominated by slow diffusive processes leading to higher DIC and nutrient retention. Higher $NH_4^+$, $PO_4^{3-}$ and $NO_3^-$ concentrations at high-trawled site locality C and H are related to lower BPc and IPc, since oxygen penetration is reduced due to reduced reworking of sediments with waters from the overlying water column (Langlet et al., 2023). $PO_4^{3-}$ is released from iron-bound complexes under anoxic conditions and $NH_4^+$ accumulates in pore spaces due to decomposition of organic matter and suppressed nitrification.

Sciberras et al. (2016) hypothesized that the effects of trawling are greater in muddy sediments compared to sandy sediments as a result of oxygenation of sediment porewaters during resuspension. Since localities K and L contained the highest proportion of muddy sediments compared to the remaining localities, it was expected that these would also show trawling related differences. The porewater concentration profiles for the high-/low-trawled pair K/L differ from the other data pairs. Here the $NH_4^+$concentrations in the upper 4.5cm of the sediments were almost constant and indicative

of $NH_4^+$ oxidation and release of DIC close to the sediment-water interface. However, the $NH_4^+$ profile differed from the concave-up profiles of $PO_4^{3-}$ and DIC, which suggests that the concentration differences of $NH_4^+$, $PO_4^{3-}$ and DIC at locality K and L are mainly driven by the respective bioturbation and bioirrigation potentials and not related to trawling intensity, since locality K and L are likely situated in an area with similar trawling intensities. Below 3.5-4.5cm, the $NH_4^+$ and DIC profiles for all localities generally display distinct concave down profiles indicating higher mineralisation rates in deeper sediments as opposed to the sediment surface.

## 4.6 Trawling and its effect on fluxes:

The interpretation of fluxes is complex, because they are the result of the interplay between organic matter distribution, community size, temporal related disturbance effects and sediment compositions affecting the biogeochemical processes within the sediments. Trawling-induced changes in sediment composition, water content, porosity and biogeochemical processes cause significant alterations in the benthic community structure and therefore the BPc and IPc in the sediments (Duplisea et al., 2001). Since these processes are governed by microbial metabolic pathways and are influenced by the interaction of carbon and the oxygen in the sediments during mixing, it is inevitable that trawling-related disturbances affect the biogeochemistry of the system since physical and chemical trawling effects do not contribute to community metabolism (Duplisea et al., 2001), causing both temporal and long-term changes in the biogeochemical fluxes in the system. Trawling also induces changes in ecosystem functioning, through indirect changes in the biodiversity over time (Bradshaw et al., 2024). Therefore, although immediate biogeochemical effects caused by trawling may have recovered, differences observed at the different localities are largely influenced by macrofaunal abundances and their associated bioturbation potentials affecting the carbon retention within these sediments, which have changed due to trawling and have not completely recovered over a 4-year time span.

The fluxes calculated from benthic flux incubations show a lot of variability between replicates of each locality. Since macrofaunal data from incubation cores are lacking, interpretations of the benthic flux incubations in terms of bioturbation and bioirrigation effects can only be made tentatively. Generally, the initial $t_0$ concentrations of DIC, $\delta^{13}C$, $NO_3^-$, $PO_4^{3-}$ and $NH_4^+$ of the benthic flux incubations were approximately in agreement with concentration ranges measured from replicates in the overlying waters of the porewaters for all localities, apart for locality H which showed higher concentrations in $NH_4^+$ and $PO_4^{3-}$ in their overlying porewaters. Oxygen consumption rates were on average higher for high trawled localities C, H, and K compared to their low-trawled counterparts. The nutrient and oxygen fluxes are influenced by a combination of microbial activity, respiration by meio- and macrofauna and the biogeochemical processes (Bradshaw et al., 2024), whereby the fluxes are influenced by the activities of different organisms (Olsgard et al., 2008). Bioturbators play a crucial role in maintaining equilibrium in ecosystems, as their biomass, carbon input and associated chemical fluxes and storages are strongly related (Duplisea et al., 2001).

High oxygen consumption at high-trawled localities, although having lower BPc and IPc compared to low trawled localities, may be linked to generally high abundances of *Halicryptus spinulosus*, *Scoloplos armiger*, *Pontopeira femorata* and *Macoma balthica* in sedimients from van Veen grabs, leading to higher $NH_4^+$ effluxes and higher $O_2$ consumption rates (Bradshaw et al., 2024). Although these might be high in abundance for high-trawled sites, *Halicryptus spinulosis* and *Scoloplos armiger*, degrade newly deposited carbon more slowly in comparison to organisms that bioturbate and graze close to the sediment surface (Bradshaw et al., 2024; Josefson et al., 2012). Sediment oxygen uptake can be higher in disturbed areas where organic matter has been redistributed by trawling and metabolized (Bradshaw et al., 2024). $NH_4^+$ fluxes were higher in comparison to all other fluxes measured and generally consistent with nitrate fluxes, but showed no significant correlation between high- and low-trawled pairs. Lower DIC benthic fluxes at high-trawled localities C, H and K, compared to their low-

trawled locality pairs are also attributed to lower bioturbation and bioirrigation potentials at these localities. DIC and $\delta^{13}C_{DIC}$ show systematic changes in the fluxes, whereby the final carbon isotope composition of DIC is more negative when there is a greater increase in DIC.
Previous studies by Morys et al. (2021) have attributed increased $NH_4^+$ fluxes to removal of surface sediments and readjustment of porewater gradient to a new steady state. High ammonium fluxes from sediments decrease the ammonium reservoir for sediment nitrification and potentially result in a reversal of $NO_3^-$ fluxes (Morys et al., 2021), as can be seen in the benthic fluxes of the current study. Disturbances caused by trawling and reduction in benthic organisms lead to disruptions in the sediment system, affecting the fluxes of $NO_2^-$ and $NO_3^-$ from the sediment to the water column, processes that involve anaerobic carbon mineralization by denitrification and aerobic oxidation of $NH_4^+$ (Duplisea et al., 2001).

In theory fluxes calculated from benthic flux incubations should yield more accurate results than fluxes calculated from porewater gradients by Fick´s first law (Burdige, 2006). This may be the result of inaccurate porewater concentrations close to the sediment water interface (Burdige, 2006). Furthermore, Fick´s first law assumes that the overlying water at the sediment water interface is homogeneous (Burdige, 2006) and only takes molecular diffusion into account as transport process and thus can underestimate the fluxes significantly. Diffusive fluxes from benthic flux incubation measures both fluxes from bioirrigation/bioturbation as well as molecular diffusion. Some limitations and inaccuracies for diffusive fluxes from benthic incubations may arise during sampling, causing porewater to be expelled upward as tube is pushed into the sediment.
The diffusive fluxes calculated by Fick's law in general do not show systematic correlations between high-and low-trawled pairs. Higher DIC, $NH_4^+$, $PO_4^{3-}$ and $NO_3^-$ fluxes result from a strengthening in the diffusive gradient within the sediments. In general, the sediments within the study area are a source of DIC, $NH_4^+$ and $PO_4^{3-}$ within the study area of all localities, in accordance with observations made in the Bornholm basin by Lengier et al. (2021). The DIC fluxes in this study ranged from 0.02 to 0.98 mmol/$m^3$d which are lower than previously reported fluxes during the stagnation period (DIC ± 0.21 ± 0.07 mmol/$m^3$d) (Winogradow & Pempkowiak, 2014), which may relate to recent major Baltic inflows (Lengier et al., 2021).

# 5. Conclusion

- Comparisons between sites for all measured properties show greater differences than those observed between their high- and low-trawled locality pairs. Variabilities between study sites lead to differences in concentration ranges in porewaters and sediments causing an overall variability in carbon mineralization and porewater constituent concentrations between sites. Variabilities caused by trawling need to be explained in the context of environmental variabilities.
- To identify the spatial effects of trawling on carbon mineralization and porewater geochemistry, it is crucial to compare locality pairs categorized into high- and low-trawling intensities at locations with similar sediment compositions, depths and hydrographic conditions to minimize the effect of total concentration ranges between study sites.
- Trawling-induced changes to porosities, sediment composition and water content lead to significant changes in the benthic community structures and bioturbation and bioirrigation potentials. Changes of the macrobiological activity within trawled regions likely cause the largest effects in nutrient and carbon cycling, carbon degradation rates and fluxes whereby more DIC and nutrients are retained in high-trawled areas with lower advection and consumption by macrofauna, whereby transport is mainly controlled by slow diffusive processes within the sediments.
- Short-term effects in the biogeochemistry are likely influenced by physical processes such as trawling, whereas long-term effects in the biogeochemical system are mainly influenced by variabilities caused by benthic communities influenced by trawling induced variabilities of benthic habitats.
- Porewater profiles were the best discriminators to identify trawling related effects as opposed to solid-phase sediment profiles, since these display greater sensitivities to diagenetic changes.
- Locality G and H showed the largest differences and significantly higher TOC concentrations and chlorophyll of the solid-phases for its high-trawled pair. High-trawled locality H also showed higher nutrient concentrations and DIC, with more negative $\delta^{13}C_{DIC}$ of its porewaters indicative of greater carbon mineralization rates and DIC production compared to its low-trawled locality pair, specifically from a depth of ~4.5cm. Locality B and C showed similar trends for their porewater profiles and chlorophyll concentrations to G and H, with higher nutrient concentrations and DIC for high-trawled locality C, although with smaller differences between the pairs likely resulting from higher biomasses and bioturbartion/bioirrigation potentials in the sediments of locality B and C.
- The differences observed between high- and low-trawled pairs were interpreted to result from lower bioturbation and bioirrigation potentials found at high-trawled localities, leading to a greater retention of nutrients and DIC in the sediments due to lower advective; diffusive dominated transports compared to their high-trawled locality pairs. Closer to the sediment surface, the concentrations of the porewater profiles approach nearing concentrations between high- and low-trawled pairs, since the biological activity and its associated bioturbation and bioirrigation potential are higher for both high- and low-trawled localities, with higher, advective dominated transport rates close to the sediment surface. Furthermore, closer to the sediment surface, porewaters approach the concentrations of overlying waters, leading to similar concentration ranges between high/low -trawled pairs.
- Although immediate biogeochemical effects from trawling may have recovered, differences observed at the different localities are largely influenced by macrofaunal abundances and their associated bioturbation potential affecting carbon retention within the sediments.
- High chlorophyll concentrations at the sediment surface represent recently settled fresh organic material from the spring phytoplankton bloom. Higher chlorophyll concentrations at high-trawled localities likely resulted from reduced grazing activity of macrofauna and microorganisms, confirmed with generally lower biomasses at high-trawled localities.

Future recommendations:

- Obtain macrofaunal abundances and bioturbation/bioirrigation potentials in benthic incubation cores to interpret benthic fluxes more accurately. Furthermore, long-term benthic macrofauna surveys could possibly be used in the future to constrain bioturbation potentials in different areas for larger studies.
- Evaluate seasonal variations of solid-phase profiles and porewater profiles as well as chlorophyll concentrations within the study area. Seasonal variations could be obtained by deploying sediment porewater dialysis passive samplers (peepers), to obtain annual averages of chemicals within sediment porewaters. These may be useful to study the recovery rates by comparing concentrations of trawled areas and concentration changes after the trawling events with time.
- Information on CT scans, multi-beam and sidescan sonar analyses may provide further evidence on sediment resuspension and redeposition and should be coupled to biogeochemical interpretations.
- Simulated porewater transport-reaction models may be helpful in constraining natural biogeochemical variabilities from trawling associated disturbances. Furthermore, experiments with artificial tracers are useful in obtaining mixing coefficients. Furthermore, it can be useful to quantify organic matter processes and carbon storages within sediments.
- Measure manganese, dissolved iron and sulphate concentrations in sediments to identify the dominant mineralization pathways. On site, porewaters should be treated with zinc acetate for $H_2S$ analyses as well as ferrozine for Fe(III) analyses.

# 6. References


Aller, R. C., Dwyer, I. P., Perger, D. A. S., Heilbrun, C., Volkenborn, N., & Wehrmann, L. M. (2023). Estimating benthic Fe and reactive solute fluxes. In *Marine Chemistry* (Vol. 249). https://doi.org/10.1016/j.marchem.2023.104221

Amoroso, R. O., Pitcher, C. R., Rijnsdorp, A. D., McConnaughey, R. A., Parma, A. M., Suuronen, P., Eigaard, O. R., Bastardie, F., Hintzen, N. T., Althaus, F., Baird, S. J., Black, J., Buhl-Mortensen, L., Campbell, A. B., Catarino, R., Collie, J., Cowan, J. H., Durholtz, D., Engstrom, N., … Jennings, S. (2018). Bottom trawl fishing footprints on the world's continental shelves. *Proceedings of the National Academy of Sciences of the United States of America*, *115*(43), E10275–E10282. https://doi.org/10.1073/pnas.1802379115

Bauer, J. E., Druffel, E. R. M., Wolgast, D. M., & Griffin, S. (2002). Temporal and regional variability in sources and cycling of DOC and POC in the northwest Atlantic continental shelf and slope. In *Deep-Sea Research II* (Vol. 49).

Benn, A. R., Weaver, P. P., Billet, D. S. M., van den Hove, S., Murdock, A. P., Doneghan, G. B., & le Bas, T. (2010). Human activities on the deep seafloor in the North East Atlantic: An assessment of spatial extent. *PLoS ONE*. https://doi.org/10.1371/journal.pone.0012730

Binczewska, A., Moros, M., Polovodova Asteman, I., Sławińska, J., & Bąk, M. (2018). Changes in the inflow of saline water into the Bornholm Basin (SW Baltic Sea) during the past 7100 years – evidence from benthic foraminifera record. *Boreas*, *47*(1), 297–310. https://doi.org/10.1111/bor.12267

Boudreau, B. P. (1996). Diagenetic models and their implementation: modelling transport and reactions in aquatic sediments. In *Diagenetic models and their implementation: modelling transport and reactions in aquatic sediments* (Issue June).

Boutton, T. W. (1991). Stable Carbon Isotope Ratios of Natural Materials: II. Atmospheric, Terrestrial, Marine, and Freshwater Environments. In *Carbon Isotope Techniques*. ACADEMIC PRESS, INC. https://doi.org/10.1016/b978-0-12-179730-0.50016-3

Bower, C. E., & Holm-Hansen, T. (1980). A Salicylate–Hypochlorite Method for Determining Ammonia in Seawater. *Canadian Journal of Fisheries and Aquatic Sciences*, *Aquat. Sci. 37*, 794–798. https://doi.org/10.1139/f80-106

Bradshaw, C., Iburg, S., Morys, C., Sköld, M., Pusceddu, A., Ennas, C., Jonsson, P., & Nascimento, F. J. A. (2024). Effects of bottom trawling and environmental factors on benthic bacteria, meiofauna and macrofauna communities and benthic ecosystem processes. *Science of the Total Environment*, *921*(November 2023). https://doi.org/10.1016/j.scitotenv.2024.171076

Bradshaw, C., Jakobsson, M., Brüchert, V., Bonaglia, S., Mörth, C. M., Muchowski, J., Stranne, C., & Sköld, M. (2021). Physical Disturbance by Bottom Trawling Suspends Particulate Matter and Alters Biogeochemical Processes on and Near the Seafloor. *Frontiers in Marine Science*, *8*(August). https://doi.org/10.3389/fmars.2021.683331

Bratek, A., E. E. Van Beusekom, J., Neumann, A., Sanders, T., Friedrich, J., Emeis, K. C., & Dähnke, K. (2020). Spatial variations in sedimentary N-transformation rates in the North Sea (German Bight). *Biogeosciences*, *17*(10), 2839–2851. https://doi.org/10.5194/bg-17-2839-2020

Brüchert, V. (2023). *Handbook: Geochemical field sampling, analysis, and data evaluation - Course:GG7030*.

Bruns, I., Bartholomä, A., Menjua, F., & Kopf, A. (2023). Physical impact of bottom trawling on seafloor sediments in the German North Sea. *Frontiers in Earth Science*, *11*. https://doi.org/10.3389/feart.2023.1233163

Bruns, I., Holler, P., Capperucci, R. M., Papenmeier, S., & Bartholomä, A. (2020). Identifying trawl marks in north sea sediments. *Geosciences (Switzerland)*, *10*(11), 1–31. https://doi.org/10.3390/geosciences10110422

Buat-Menard, P. (1986). The Role of Air-Sea Exchange in Geochemical Cycling. In *NATO Scientific Affairs Division* (Vol. 4, Issue 1). NATO Scientific Affairs Division.

Burdige, D. J. (2006). *Geochemistry of Marine Sediments*. Princeton University Press.
Cartigny, P., & Busigny, V. (2018). *Nitrogen Isotopes* (pp. 1–13). https://doi.org/10.1007/978-3-319-39193-9_197-1
Christoffersen, P. L., Christiansen, C., Jensen, J. B., Leipe, T., & Hille, S. (2007). Depositional conditions and organic matter distribution in the Bornholm Basin, Baltic Sea. *Geo-Marine Letters*, *27*(5), 325–338. https://doi.org/10.1007/s00367-007-0054-6
Corell, H., Bradshaw, C., & Sköld, M. (2023). Sediment suspended by bottom trawling can reduce reproductive success in a broadcast spawning fish. *Estuarine, Coastal and Shelf Science*, *282*(January). https://doi.org/10.1016/j.ecss.2023.108232
De Borger, E., Tiano, J., Braeckman, U., Rijnsdorp, A. D., & Soetaert, K. (2021). Impact of bottom trawling on sediment biogeochemistry: A modelling approach. *Biogeosciences*, *18*(8), 2539–2557. https://doi.org/10.5194/bg-18-2539-2021
De Juan, S., Thrush, S. F., & Demestre, M. (2007). Functional changes as indicators of trawling disturbance on a benthic community located in a fishing ground (NW Mediterranean Sea). *Marine Ecology Progress Series*, *334*, 117–129. https://doi.org/10.3354/meps334117
Duplisea, D. E., Jennings, S., Malcolm, S. J., Parker, R., & Sivyer, D. B. (2001). Modelling potential impacts of bottom trawl fisheries on soft sediment biogeochemistry in the North Sea. *Geochemical Transactions*, *2*(1). https://doi.org/10.1186/1467-4866-2-112
Durrieu De Madron, X., Ferré, B., Le Corre, G., Grenz, C., Conan, P., Pujo-Pay, M., Buscail, R., & Bodiot, O. (2005). Trawling-induced resuspension and dispersal of muddy sediments and dissolved elements in the Gulf of Lion (NW Mediterranean). *Continental Shelf Research*, *25*(19–20), 2387–2409. https://doi.org/10.1016/j.csr.2005.08.002
Eero, M., MacKenzie, B. R., Karlsdóttir, H. M., & Gaumiga, R. (2007). Development of international fisheries for the eastern Baltic cod (Gadus morhua) from the late 1880s until 1938. In *Fisheries Research* (Vol. 87, Issues 2–3, pp. 155–166). https://doi.org/10.1016/j.fishres.2007.02.015
Eigaard, O. R., Bastardie, F., Hintzen, N. T., Buhl-Mortensen, L., Buhl-Mortensen, P., Catarino, R., Dinesen, G. E., Egekvist, J., Fock, H. O., Geitner, K., Gerritsen, H. D., González, M. M., Jonsson, P., Kavadas, S., Laffargue, P., Lundy, M., Gonzalez-Mirelis, G., Nielsen, J. R., Papadopoulou, N., … Rijnsdorp, A. D. (2017). The footprint of bottom trawling in European waters: Distribution, intensity, and seabed integrity. *ICES Journal of Marine Science*, *74*(3), 847–865. https://doi.org/10.1093/icesjms/fsw194
Ellingsen, K. E. (2002). Soft-sediment benthic biodiversity on the continental shelf in relation to environmental variability. *Marine Ecology Progress Series*, *232*, 15–17. https://doi.org/10.2307/24865148
Escobar-Briones, E., & García-Villalobos, F. J. (2009). Distribution of total organic carbon and total nitrogen in deep-sea sediments from the southwestern Gulf of Mexico. *Boletin de La Sociedad Geologica Mexicana*, *61*(1), 73–86. https://doi.org/10.18268/BSGM2009v61n1a7
European Commission. (2019). Commission Implementing Regulation (EU) 2019/1248 of 22 July 2019, establishing measures to alleviate a serious threat to the conservation of the eastern Baltic cod (Gadus morhua) stock. *Official Journal of the European Union*, *L195/2*.
Gao, X., Yang, Y., & Wang, C. (2012). Geochemistry of organic carbon and nitrogen in surface sediments of coastal Bohai Bay inferred from their ratios and stable isotopic signatures. *Marine Pollution Bulletin*, *64*(6), 1148–1155. https://doi.org/10.1016/j.marpolbul.2012.03.028
Gutiérrez, D., Gallardo, V., Mayor, S., Neira, C., Vásquez, C., Sellanes, J., Rivas, M., Soto, A., Carrasco, F., & Baltazar, M. (2000). Effects of dissolved oxygen and fresh organic matter on the bioturbation potential of macrofauna in sublittoral sediments off Central Chile during the 1997/1998 El Niño. *Marine Ecology Progress Series*, *202*, 81–99.
HELCOM. (1988). *Baltic Sea Environment Proceedings No. 27 D: Guidelines For The Baltic Monitoring Programme For The Third Stage*.
HELCOM. (2002). Environment of the Baltic Sea area 1994-1998. *HELCOM: Baltoc Marine Environment Protection Comission*, *82B*.

Hendriks, K., Gubbay, S., Arets, E., Janssen, J., Dige, G., & Erhard, M. (2020). Carbon stocks and sequestration in terrestrial and marine ecosystems: a lever for nature restoration? *European Environment Agency*, 1–66.

Herbert, R. A. (1999). Nitrogen cycling in coastal marine ecosystems. *FEMS Microbiology Reviews*, *23*(5), 563–590. https://doi.org/10.1016/S0168-6445(99)00022-4

Hesse, R., & Schacht, U. (2011). *Chapter 9: Early Diagenesis of Deep-Sea Sediments* (H. HüNeke & T. Thierry Mulder, Eds.; Vol. 63). Elsevier. https://doi.org/10.1016/S0070-4571(11)63009-4

Hiddink, J. G., Jennings, S., Sciberras, M., Szostek, C. L., Hughes, K. M., Ellis, N., Rijnsdorp, A. D., McConnaughey, R. A., Mazor, T., Hilborn, R., Collie, J. S., Pitcher, C. R., Amoroso, R. O., Parma, A. M., Suuronen, P., & Kaiser, M. J. (2017). Global analysis of depletion and recovery of seabed biota after bottom trawling disturbance. *Proceedings of the National Academy of Sciences of the United States of America*, *114*(31), 8301–8306. https://doi.org/10.1073/pnas.1618858114

Jones, J. B. (1992). Environmental impact of trawling on the seabed: A review. *New Zealand Journal of Marine and Freshwater Research*, *26*(1), 59–67. https://doi.org/10.1080/00288330.1992.9516500

Josefson, A. B., Norkko, J., & Norkko, A. (2012). Burial and decomposition of plant pigments in surface sediments of the Baltic Sea: Role of oxygen and benthic fauna. *Marine Ecology Progress Series*, *455*, 33–49. https://doi.org/10.3354/meps09661

Koroleff, F. (1983). Determination of phosphorous. In Grasshoff, M. Ehrhardt, & K. Kremling (Eds.), *Methods of seawater analysis. Verlag Chemie, Weinheim* (pp. 125–139).

Langlet, D., Mermillod-Blondin, F., Deldicq, N., Bauville, A., Duong, G., Konecny, L., Hugoni, M., Denis, L., & Bouchet, V. M. P. (2023). Single-celled bioturbators: benthic foraminifera mediate oxygen penetration and prokaryotic diversity in intertidal sediment. *Biogeosciences*, *20*(23), 4875–4891. https://doi.org/10.5194/bg-20-4875-2023

Legge, O., Johnson, M., Hicks, N., Jickells, T., Diesing, M., Aldridge, J., Andrews, J., Artioli, Y., Bakker, D. C. E., Burrows, M. T., Carr, N., Cripps, G., Felgate, S. L., Fernand, L., Greenwood, N., Hartman, S., Kröger, S., Lessin, G., Mahaffey, C., … Williamson, P. (2020). Carbon on the Northwest European Shelf: Contemporary Budget and Future Influences. *Frontiers in Marine Science*, *7*(March). https://doi.org/10.3389/fmars.2020.00143

Lengier, M., Szymczycha, B., Brodecka-Goluch, A., Kłostowska, Ż., & Kuliński, K. (2021). Benthic diffusive fluxes of organic and inorganic carbon, ammonium and phosphates from deep water sediments of the Baltic Sea. *Oceanologia*, *63*(3), 370–384. https://doi.org/10.1016/j.oceano.2021.04.002

Martín, J., Puig, P., Palanques, A., & Giamportone, A. (2014). Commercial bottom trawling as a driver of sediment dynamics and deep seascape evolution in the Anthropocene. In *Anthropocene* (Vol. 7, pp. 1–15). Elsevier Ltd. https://doi.org/10.1016/j.ancene.2015.01.002

Mérillet, L., Kopp, D., Robert, M., Salaün, M., Méhault, S., Bourillet, J. F., & Mouchet, M. (2018). Are trawl marks a good indicator of trawling pressure in muddy sand fishing grounds? *Ecological Indicators*, *85*, 570–574. https://doi.org/10.1016/j.ecolind.2017.11.016

Meyers, P. A. (1994). Preservation of elemental and isotopic source identification of sedimentary organic matter. *Chemical Geology*, *114*(3–4), 289–302. https://doi.org/10.1016/0009-2541(94)90059-0

Morys, C., Brüchert, V., & Bradshaw, C. (2021). Impacts of bottom trawling on benthic biogeochemistry in muddy sediments: Removal of surface sediment using an experimental field study. *Marine Environmental Research*, *169*(December 2020), 105384. https://doi.org/10.1016/j.marenvres.2021.105384

Oberle, F. K. J., Puig, P., & Martin, J. (2016). Submarine Geomorphology: Bottom trawling and other Fishing activities. *Geotechnical, Geological and Earthquake Engineering*, *16*(July), 129–145. https://doi.org/10.1007/978

Olsgard, F., Schaanning, M. T., Widdicombe, S., Kendall, M. A., & Austen, M. C. (2008). Effects of bottom trawling on ecosystem functioning. *Journal of Experimental Marine Biology and*

*Ecology*, *366*(1–2), 123–133. https://doi.org/10.1016/j.jembe.2008.07.036
Ouyang, X., Lai, D. Y. F., Marchand, C., & Lee, S. Y. (2022). Carbon Mineralization in coastal Wetlands. In *Chapter 1*. Elsevier, Volume 2. https://doi.org/10.4324/9781315609621-5
Palanques, A., Guillén, J., & Puig, P. (2001). Impact of bottom trawling on water turbidity and muddy sediment of an unfished continental shelf. *Limnology and Oceanography*, *46*(5), 1100–1110. https://doi.org/10.4319/lo.2001.46.5.1100
Palanques, A., Puig, P., Guillén, J., Demestre, M., & Martín, J. (2014). Effects of bottom trawling on the Ebro continental shelf sedimentary system (NW Mediterranean). *Continental Shelf Research*, *72*, 83–98. https://doi.org/10.1016/j.csr.2013.10.008
Paradis, S., Lo Iacono, C., Masqué, P., Puig, P., Palanques, A., & Russo, T. (2021). Evidence of large increases in sedimentation rates due to fish trawling in submarine canyons of the Gulf of Palermo (SW Mediterranean). *Marine Pollution Bulletin*, *172*. https://doi.org/10.1016/j.marpolbul.2021.112861
Pusceddu, A., Bianchelli, S., Martín, J., Puig, P., Palanques, A., Masqué, P., & Danovaro, R. (2014). Chronic and intensive bottom trawling impairs deep-sea biodiversity and ecosystem functioning. *Proceedings of the National Academy of Sciences of the United States of America*, *111*(24), 8861–8866. https://doi.org/10.1073/pnas.1405454111
Pusceddu, A., Fiordelmondo, C., Polymenakou, P., Polychronaki, T., Tselepides, A., & Danovaro, R. (2005). Effects of bottom trawling on the quantity and biochemical composition of organic matter in coastal marine sediments (Thermaikos Gulf, northwestern Aegean Sea). *Continental Shelf Research*, *25*(19–20), 2491–2505. https://doi.org/10.1016/j.csr.2005.08.013
Quan, T. M., & Falkowski, P. G. (2009). Redox control of N:P ratios in aquatic ecosystems. *Geobiology*, *7*(2), 124–139. https://doi.org/10.1111/j.1472-4669.2008.00182.x
Schnetger, B., & Lehners, C. (2014). Determination of nitrate plus nitrite in small volume marine water samples using vanadium(III)chloride as a reduction agent. *Marine Chemistry*, 91–98. https://doi.org/10.1016/j.marchem.2014.01.010
Schulz, H. D., & Zabel, M. (2006). Marine Geochemistry. In *Marine Geochemistry* (2nd ed.). Springer. https://doi.org/10.1007/3-540-32144-6_11
Sciberras, M., Parker, R., Powell, C., Robertson, C., Kröger, S., Bolam, S., & Geert Hiddink, J. (2016). Impacts of bottom fishing on the sediment infaunal community and biogeochemistry of cohesive and non-cohesive sediments. *Limnology and Oceanography*, *61*(6), 2076–2089. https://doi.org/10.1002/lno.10354
Silori, S., Sharma, D., Chowdhury, M., Biswas, H., Bandyopadhyay, D., Shaik, A. U. R., Cardinal, D., Mandeng-Yogo, M., & Narvekar, J. (2021). Contrasting phytoplankton and biogeochemical functioning in the eastern Arabian Sea shelf waters recorded by carbon isotopes (SW monsoon). *Marine Chemistry*, *232*. https://doi.org/10.1016/j.marchem.2021.103962
Snoeijs-Leijonmalm, P., Schubert, H., & Radziejewska, T. (2017). Biological Oceanography of the Baltic Sea. In *Elsevier Oceanography Series* (Vol. 30).
Szymczak-Zyła, M., Kowalewska, G., & Louda, J. W. (2011). Chlorophyll-a and derivatives in recent sediments as indicators of productivity and depositional conditions. *Marine Chemistry*, *125*(1–4), 39–48. https://doi.org/10.1016/j.marchem.2011.02.002
Thermo Fisher Scientific GmbH. (2010). *Manual:Thermo Scientific Flash HT Plus Elemental Analyzer for IRMS*. https://static.thermoscientific.com/images/D01818~.pdf
Tyrrell, T. (2001). Redfield Ratio. In *Encyclopedia of Ocean Sciences* (pp. 2377–2387). Elsevier. https://doi.org/10.1006/rwos.2001.0271
Tyson, R. V., & Pearson, T. H. (1991). Modern and ancient continental shelf anoxia. *Modern and Ancient Continental Shelf Anoxia*, *58*, 1–24. https://doi.org/10.2307/3515153
Van De Velde, S., Van Lancker, V., Hidalgo-Martinez, S., Berelson, W. M., & Meysman, F. J. R. (2018). Anthropogenic disturbance keeps the coastal seafloor biogeochemistry in a transient state. *Scientific Reports*, *8*(1), 1–10. https://doi.org/10.1038/s41598-018-23925-y
Van Denderen, P. D., Bolam, S. G., Friedland, R., Hiddink, J. G., Norén, K., Rijnsdorp, A. D., Sköld, M.,

Törnroos, A., Virtanen, E. A., & Valanko, S. (2020). Evaluating impacts of bottom trawling and hypoxia on benthic communities at the local, habitat, and regional scale using a modelling approach. *ICES Journal of Marine Science*, *77*(1), 278–289. https://doi.org/10.1093/icesjms/fsz219

Vanderborght, J. -P, Wollas, R., & Bitten, G. (1977). Kinetic models of diagenesis in disturbed sediments. Part 1. Mass transfer properties and silica diagenesis. *Limnology and Oceanography*, *22*(5), 787–793. https://doi.org/10.4319/lo.1977.22.5.0787

Wada, E., & Hattori, A. (1991). *Nitrogen in the Sea: Forms, Abundances and Rate Processes* (208th ed.). Boca Raton CRC Press.

Watson, R., Revenga, C., & Kura, Y. (2006). Fishing gear associated with global marine catches. II. Trends in trawling and dredging. *Fisheries Research*, *79*(1–2), 103–111. https://doi.org/10.1016/j.fishres.2006.01.013

Winogradow, A., & Pempkowiak, J. (2014). Organic carbon burial rates in the Baltic Sea sediments. *Estuarine, Coastal and Shelf Science*, *138*, 27–36. https://doi.org/10.1016/j.ecss.2013.12.001

Yang, X., Zhang, Y., Sun, X., Xu, L., & Chen, T. T. (2023). Marine sediment nitrogen isotopes and their implications for the nitrogen cycle in the sulfate-methane transition zone. *Frontiers in Marine Science*, *9*. https://doi.org/10.3389/fmars.2022.1101599

Zacharia, P. U., Krishnan, A. A., Durgekarz, R. N., & Krishnakumar, P. K. (2006). Immediate effects of experimental otter trawling on the physico-chemical parameters of seawater off Mangalore. *J.Mar.Biol.Ass.India*, *48*(2), 200–205.

# 7. Appendices

## 7.1 Appendix A: Tables with calculations

| N/P | | | | | | | |
|---|---|---|---|---|---|---|---|
| **Depth (cm)** | **A** | **B** | **C** | **G** | **H** | **K** | **L** |
| -0.5 | 0.25 | 10.76 | 3.40 | 2.42 | 6.67 | 49.17 | 17.75 |
| 0.5 | 5.41 | 17.70 | 6.20 | 33.44 | 44.21 | 14.10 | n.d. |
| 1.5 | 3.18 | 17.46 | 22.41 | 31.18 | 80.02 | 9.61 | 14.46 |
| 2.5 | 9.62 | 45.29 | 15.87 | 38.86 | 22.66 | 3.66 | 3.79 |
| 3.5 | 6.49 | 9.95 | 24.63 | 16.25 | 129.12 | 3.63 | 3.61 |
| 4.5 | 16.16 | 26.27 | 18.14 | 12.00 | 63.46 | 3.84 | 3.27 |
| 5.5 | 6.89 | 18.57 | 15.18 | 4.85 | 151.20 | 18.35 | 12.23 |
| 6.5 | 11.53 | 15.07 | | 6.22 | PO4=0 | 18.13 | 15.71 |
| 7.5 | 19.38 | 12.26 | | 6.16 | 538.50 | 19.53 | 23.11 |
| 8.5 | 5.59 | 7.91 | | 15.43 | 230.50 | 16.97 | 25.84 |
| 9.5 | 19.38 | 10.59 | | 9.70 | 61.83 | 19.36 | 18.13 |
| 11.5 | 9.53 | | | | $PO_4$=0 | 29.63 | 16.28 |
| 13.5 | 31.45 | | | | n.d. | 23.04 | 44.49 |
| 15.5 | | | | | 56.54 | 31.90 | 41.36 |
| 17.5 | | | | | | 25.68 | 19.99 |
| 19.5 | | | | | | 34.13 | 39.70 |
| 24.5 | | | | | | 73.08 | 25.65 |
| 29.5 | | | | | | 71.01 | |
| **Average** | **11.14** | **17.44** | **15.12** | **16.04** | **125.88** | **25.82** | **20.34** |

*Table 12: Approximation of N/P ratios calculated from the average sum of $NH_4^+$ and $NO3^-$ concentrations divided by the concentration of* $PO_4^{3-}$ in porewater profiles.

| Depth (cm) | A | | B | | C | | G | | H | | K | | L | |
|---|---|---|---|---|---|---|---|---|---|---|---|---|---|---|
| | **C/N** | **C/P** | **C/N** | **C/P** | **C/N** | **C/P** | **C/N** | **C/P** | **C/N** | **C/P** | **C/N** | **C/P** | **C/N** | **C/P** |
| -0.5 | 456.41 | 73.79 | 2434.56 | 3257.44 | 463.17 | 1056.32 | $NH_4$=0 | 1123.12 | 73.37 | 436.12 | 222.18 | 4895.15 | 256.99 | 2531.14 |
| 0.5 | 38.90 | 198.57 | 120.38 | 1304.67 | 117.69 | 400.65 | 82.81 | 1244.63 | 43.26 | 1555.65 | 21.40 | 276.38 | 22.23 | $PO_4$=0 |
| 1.5 | 22.42 | 70.94 | 53.29 | 930.30 | 29.11 | 535.34 | 33.54 | 913.89 | 26.15 | 1971.48 | 15.30 | 141.70 | 18.87 | 268.24 |
| 2.5 | 20.39 | 195.12 | 25.99 | 1167.38 | 21.53 | 315.71 | 22.70 | 818.62 | 21.73 | 453.28 | 20.68 | 74.49 | 21.33 | 79.50 |
| 3.5 | 16.79 | 108.78 | 39.80 | 380.43 | 18.87 | 426.87 | 21.79 | 344.75 | 18.61 | 2396.60 | 26.75 | 94.19 | 34.41 | 119.21 |
| 4.5 | 15.00 | 242.48 | 26.81 | 704.15 | 18.39 | 322.73 | 19.05 | 223.25 | 22.28 | 1310.49 | 33.21 | 126.35 | 38.06 | 122.99 |
| 5.5 | 11.53 | 79.12 | 27.84 | 505.38 | 20.57 | 303.61 | 29.17 | 141.36 | 17.58 | 2658.03 | 11.24 | 206.35 | 12.92 | 157.99 |
| 6.5 | 10.75 | 122.77 | 25.97 | 379.09 | | | 26.00 | 161.64 | 13.69 | $PO_4$=0 | 10.52 | 190.71 | 12.68 | 199.16 |
| 7.5 | 9.93 | 184.96 | 25.08 | 293.59 | | | 21.19 | 130.44 | 11.42 | 6148.55 | 10.45 | 204.02 | 12.63 | 291.86 |
| 8.5 | 17.38 | 90.20 | 25.96 | 205.27 | | | 9.65 | 148.86 | 13.42 | 3093.38 | 10.21 | 173.23 | 15.00 | 387.62 |
| 9.5 | 12.09 | 234.06 | 26.27 | 275.54 | | | 16.49 | 159.99 | 14.34 | 886.72 | 10.88 | 210.52 | 13.52 | 245.26 |
| 11.5 | 10.36 | 98.80 | | | | | | | n.d. | $PO_4$=0 | 9.64 | 285.63 | 13.40 | 218.24 |
| 13.5 | 9.56 | 300.63 | | | | | | | 15.08 | n.d. | 10.40 | 239.70 | 11.59 | 515.45 |
| 15.5 | | | | | | | | | 17.61 | 995.75 | 9.76 | 311.17 | 8.69 | 359.29 |
| 17.5 | | | | | | | | | | | 12.59 | 323.32 | 19.43 | 388.37 |
| 19.5 | | | | | | | | | | | 10.35 | 353.37 | 9.38 | 372.44 |
| 24.5 | | | | | | | | | | | 8.07 | 589.67 | 14.82 | 380.19 |
| 29.5 | | | | | | | | | | | 8.56 | 607.54 | | |
| **Average** | **50.12** | **153.86** | **257.45** | **854.84** | **98.48** | **480.18** | **28.24** | **491.87** | **23.73** | **1991.46** | **25.68** | **516.86** | **31.53** | **414.81** |

*Table 13: C/N and C/P ratios for individual localities calculated from average concentrations at each depth interval. C/N ratios were calculated from the average concentrations between DIC and $NH_4^+$ and C/P ratios were calculated from the average concentrations between DIC and $PO_4^{3-}$ in porewater profiles.*

**Differences in sediment concentrations between high and low trawled areas**

| Sediments: Difference between Average C (High)-B (Low) | | | | | | | | |
|---|---|---|---|---|---|---|---|---|
| **Depth (cm)** | **δ15N vs Air ‰** | **δ13Ctotal vs VPDB ‰** | **N%** | **C%** | **d13CTOC vs VPDB ‰** | **TOC%** | **C/N** | **Chlorophyll (µg/cm³)** |
| 0.5 | -1.07 | -0.40 | 0.04 | 0.31 | -0.29 | 0.29 | 0.04 | 4.63 |
| 1.5 | 0.24 | -0.22 | 0.05 | 0.40 | -0.01 | -0.04 | -2.88 | 1.93 |
| 2.5 | -0.35 | 0.19 | 0.01 | 0.07 | -0.16 | -0.01 | -0.65 | -0.33 |
| 3.5 | -0.19 | -0.12 | -0.01 | 0.43 | 0.23 | -0.01 | 0.69 | -0.78 |
| 4.5 | -0.67 | 0.28 | -0.02 | -0.17 | 0.35 | -0.33 | -1.08 | -0.05 |
| 5.5 | 0.27 | -0.05 | 0.03 | 0.70 | 0.19 | 0.26 | 0.04 | 0.54 |
| 6.5 | 1.21 | 0.69 | 0.01 | -0.24 | 0.23 | 0.04 | -0.15 | 0.80 |
| 7.5 | 0.27 | 0.88 | -0.04 | -0.31 | -0.62 | -0.22 | 0.73 | -0.61 |
| 8.5 | 1.09 | 2.97 | -0.05 | -0.45 | -1.02 | -0.77 | -3.76 | -1.05 |

| Sediments: Difference between Average H (High) -G (Low) | | | | | | | | |
|---|---|---|---|---|---|---|---|---|
| **Depth (cm)** | **δ15Nvs Air, ‰** | **δ13Ctotal vs VPDB ‰** | **N%** | **C%** | **d13CTOC vs VPDB ‰** | **TOC%** | **C/N** | **Chlorophyll (µg/cm³)** |
| 0.5 | 0.79 | 0.31 | 0.07 | 0.47 | -0.41 | 0.59 | 0.56 | 3.71 |
| 1.5 | 0.68 | 0.28 | 0.11 | 0.91 | -0.02 | 0.62 | -1.15 | -0.89 |
| 2.5 | 0.74 | 0.24 | 0.20 | 1.56 | 0.50 | 2.71 | 4.29 | -0.22 |
| 3.5 | 1.54 | -0.06 | 0.16 | 1.26 | -0.39 | 1.04 | -0.51 | 2.11 |
| 4.5 | 0.75 | -0.20 | 0.10 | 0.86 | -0.53 | 0.78 | 0.19 | 1.57 |
| 5.5 | 0.88 | -0.24 | 0.07 | 0.58 | -0.55 | 0.57 | 0.49 | 1.13 |
| 6.5 | 0.26 | 0.19 | 0.05 | 0.49 | -0.44 | 0.29 | -0.23 | 1.14 |
| 7.5 | 0.24 | -0.03 | 0.02 | 0.29 | -1.57 | 0.17 | 0.15 | 2.14 |

| Sediments: Difference between average K(High) - L (Low) | | | | | | | | |
|---|---|---|---|---|---|---|---|---|
| Depth (cm) | δ15Nvs Air, ‰ | δ13Ctotal vs VPDB ‰ | N% | C% | δ13CTOC vs VPDB ‰ | TOC% | C/N | Chlorophyll (µg/cm³) |
| 0.5 | -0.21 | 0.09 | 0.14 | 0.92 | 0.42 | 0.77 | -0.12 | 4.22 |
| 1.5 | 0.01 | 0.05 | 0.28 | 2.02 | 0.73 | 0.55 | -2.39 | 1.57 |
| 2.5 | -0.23 | -0.23 | 0.06 | 0.44 | -0.06 | -0.35 | -0.95 | -0.08 |
| 3.5 | -0.04 | 0.01 | 0.07 | 0.38 | -0.70 | -0.24 | -0.95 | 1.10 |
| 4.5 | 0.15 | -0.21 | 0.13 | 0.75 | 3.05 | 0.57 | -0.28 | 1.55 |
| 5.5 | 0.42 | -0.09 | 0.21 | 1.00 | -0.02 | 1.20 | -0.16 | 0.40 |
| 6.5 | 0.18 | 0.05 | 0.28 | 1.43 | 0.27 | 0.97 | -0.98 | 0.76 |
| 7.5 | 0.23 | -0.11 | 0.03 | -0.02 | -0.63 | 0.53 | 0.50 | 0.83 |
| 8.5 | 0.37 | 0.12 | 0.02 | -0.23 | 0.56 | -0.64 | -1.22 | 0.63 |
| 9.5 | 0.51 | 0.03 | 0.01 | -0.30 | -0.08 | 2.11 | 3.39 | 0.72 |
| 10.5 | 0.16 | 0.35 | -0.02 | -0.34 | 0.80 | -1.42 | -2.29 | 0.86 |
| 11.5 | -0.06 | 0.01 | -0.05 | -0.53 | -0.39 | -0.74 | -0.75 | 0.69 |
| 12.5 | 0.55 | 0.27 | 0.09 | 0.55 | 0.54 | 0.46 | -0.44 | -0.29 |
| 13.5 | 0.60 | 0.58 | 0.10 | 0.55 | 0.31 | 0.64 | -0.13 | 1.71 |
| 14.5 | 0.40 | 0.74 | 0.04 | 0.12 | 0.05 | 0.23 | -0.06 | -0.43 |
| 15.5 | 0.72 | 0.72 | 0.04 | 0.15 | -0.10 | -0.17 | -0.91 | 0.54 |
| 16.5 | 0.60 | 0.70 | 0.03 | 0.10 | 0.22 | 0.37 | 0.24 | 0.54 |
| 17.5 | 0.10 | 0.42 | 0.06 | 0.35 | 0.55 | -0.10 | -1.03 | 0.19 |
| 18.5 | 0.46 | -0.10 | 0.01 | 0.00 | -0.26 | -0.19 | -0.49 | -1.59 |
| 19.5 | -0.41 | -0.58 | 0.10 | 0.76 | -0.76 | 0.01 | -1.54 | 0.86 |
| 20.5 | 0.36 | -0.22 | 0.10 | 0.90 | 0.36 | 1.13 | 0.86 | -1.50 |
| 21.5 | -0.73 | 0.28 | 0.10 | 0.97 | 0.79 | 0.86 | 0.29 | 1.59 |
| 22.5 | -0.84 | 0.26 | 0.07 | 0.76 | 0.54 | 0.33 | -0.54 | -0.23 |
| 23.5 | -0.17 | 1.01 | -0.16 | -1.01 | 0.00 | 2.43 | 6.07 | -0.31 |
| 24.5 | -1.06 | 0.51 | -0.09 | -0.68 | -0.54 | -0.85 | -0.35 | -0.45 |
| 25.5 | -0.57 | 0.78 | 0.05 | 0.39 | -0.26 | 0.25 | -0.39 | -0.04 |
| 26.5 | -0.55 | 0.61 | 0.01 | 0.02 | -0.19 | -0.77 | -2.13 | -0.81 |
| 27.5 | -1.44 | 0.46 | 0.46 | 3.80 | -0.18 | 0.15 | 7.21 | 0.28 |

**Differences in porewater concentrations between high and low trawled areas**

| Porewaters: Difference between Average C (High)-B (Low) | | | | | |
|---|---|---|---|---|---|
| Depth (cm) | NH4 (µM) | PO4 (µM) | NO3 (µM) | DIC (mM) | δ13C (‰) |
| -0.5 | 3.73 | 1.39 | -3.42 | 0.15 | 0.05 |
| 0.5 | 2.80 | 4.09 | 5.34 | 0.29 | -0.15 |
| 1.5 | 34.83 | 1.77 | 16.58 | 0.02 | -0.09 |
| 2.5 | 19.20 | 5.17 | 7.76 | 0.04 | 1.16 |
| 3.5 | 72.93 | -0.21 | 9.18 | 0.19 | 0.87 |
| 4.5 | 70.20 | 5.62 | 5.25 | 0.57 | -0.74 |
| 5.5 | 62.10 | 5.39 | 2.27 | 0.60 | 0.88 |
| 6.5 | n.d | n.d | n.d | 0.49 | -1.53 |

| Porewaters: Difference between Average H (High) -G (Low) | | | | | |
|---|---|---|---|---|---|
| **Depth (cm)** | **NH4 (µM)** | **PO4 (µM)** | **NO3 (µM)** | **DIC (mM)** | **δ13C (‰)** |
| -0.5 | 32.27 | 3.50 | -0.74 | 0.20 | -0.49 |
| 0.5 | 30.27 | -0.11 | -17.49 | 0.34 | 0.06 |
| 1.5 | 37.33 | -0.99 | -2.96 | 0.51 | -0.30 |
| 2.5 | 36.20 | 3.61 | 3.94 | 0.70 | -1.11 |
| 3.5 | 60.20 | -5.71 | -2.55 | 0.77 | -1.45 |
| 4.5 | 33.60 | -8.23 | 9.77 | 1.16 | -1.32 |
| 5.5 | 116.07 | -19.19 | n.d | 0.88 | -1.33 |
| 6.5 | 161.67 | -22.04 | n.d | 0.53 | -2.52 |
| 7.5 | 217.00 | -22.40 | n.d | 1.09 | -2.16 |
| 8.5 | -26.67 | -20.32 | n.d | 0.90 | -1.85 |
| 9.5 | 77.67 | -16.56 | n.d | 0.67 | -1.91 |

| Porewaters: Difference between average K(High) - L (Low) | | | | | |
|---|---|---|---|---|---|
| **Depth (cm)** | **NH4 (µM)** | **PO4 (µM)** | **NO3 (µM)** | **DIC (mM)** | **δ13C (‰)** |
| -0.5 | 1.30 | -0.44 | 5.42 | -0.02 | 0.36 |
| 0.5 | 26.87 | 11.39 | 3.86 | 0.48 | -0.59 |
| 1.5 | 50.47 | 13.10 | 6.08 | 0.05 | 0.16 |
| 2.5 | 36.20 | 12.26 | 0.29 | 0.59 | -0.10 |
| 3.5 | 79.17 | 21.56 | 0.37 | 0.58 | -0.67 |
| 4.5 | 46.20 | 1.58 | -0.45 | 0.44 | -0.46 |
| 5.5 | 39.00 | -22.38 | n.d | -1.06 | -3.84 |
| 6.5 | 57.33 | -6.41 | n.d | -1.83 | 0.17 |
| 7.5 | 42.67 | 11.68 | n.d | -2.16 | 1.34 |
| 8.5 | 325.00 | 40.32 | n.d | -1.70 | 1.30 |
| 9.5 | 311.00 | 11.68 | n.d | 0.05 | 4.97 |
| 11.5 | 243.00 | -32.43 | n.d | -3.18 | -0.67 |
| 13.5 | -90.00 | 30.72 | n.d | -2.89 | -3.00 |
| 15.5 | -543.00 | 0.32 | n.d | -2.71 | -4.26 |
| 17.5 | 434.00 | 4.55 | n.d | -2.15 | -4.62 |
| 19.5 | -264.00 | 1.92 | n.d | -0.45 | -5.66 |
| 24.5 | 1065.00 | -25.50 | n.d | -2.10 | -4.68 |

**Benthic Incubation Fluxes**

| (DIC) mmol/m2 d | | | | | | | |
|---|---|---|---|---|---|---|---|
| | A (H) | B (L) | C (H) | G (L) | H (H) | K (H) | L (L) |
| 1 | -31.30 | 2.23 | -17.76 | 88.15 | 59.53 | -40.69 | -40.79 |
| 2 | -60.35 | 6.62 | 19.14 | 35.98 | 41.19 | 2.21 | -11.05 |
| 3 | -3.23 | -38.81 | -18.74 | 50.64 | 13.98 | -4.18 | 3.59 |
| 4 | -26.96 | -62.99 | n.d. | 61.65 | 24.76 | 17.58 | 4.12 |
| SD | 23.44 | 33.48 | 21.59 | 22.03 | 19.89 | 24.70 | 21.05 |

| O2 (µmol/m2 d) | | | | | | | |
|---|---|---|---|---|---|---|---|
| | A | B | C | G | H | K | L |
| 1 | 1070.50 | -582.20 | -4824.03 | -3561.04 | -14592.34 | -1657.57 | 1660.93 |
| 2 | -2731.78 | -3662.12 | -9671.22 | -6438.79 | -16086.77 | -5879.85 | -4091.96 |
| 3 | -3142.90 | -5360.32 | -2760.01 | -1341.72 | -14211.82 | -20734.52 | 5977.29 |
| 4 | 1365.70 | 4891.99 | -2689.80 | -6805.94 | -14224.13 | -11661.64 | 3005.49 |
| SD | 2408.03 | 4504.16 | 3276.44 | 2577.29 | 889.70 | 8257.56 | 4224.23 |

| NO3 (µmol/m2 d) | | | | | | | |
|---|---|---|---|---|---|---|---|
| | A | B | C | G | H | K | L |
| 1 | 162.76 | 289.11 | 1298.46 | 578.02 | -120.27 | 300.98 | 355.13 |
| 2 | 630.04 | -118.55 | 377.87 | -706.30 | 4.15 | 306.11 | 1257.98 |
| 3 | 580.20 | 467.86 | -157.15 | 117.26 | 27.24 | 621.91 | -70.59 |
| 4 | 230.51 | 879.41 | n.d. | -189.87 | 153.69 | 141.79 | 215.91 |
| SD | 238.32 | 413.90 | 736.27 | 539.34 | 112.24 | 201.16 | 573.65 |

| PO4 (µmol/m2 d) | | | | | | | |
|---|---|---|---|---|---|---|---|
| | A | B | C | G | H | K | L |
| 1 | -126.79 | -10.45 | 97.19 | -431.82 | 158.34 | 890.30 | 235.03 |
| 2 | -386.35 | 27.71 | 0.00 | 321.67 | -215.29 | 78.91 | -73.02 |
| 3 | 0.67 | 235.12 | 15.42 | -58.40 | -12.51 | 132.31 | -93.22 |
| 4 | 0.00 | 2635.95 | n.d. | -119.86 | -12.54 | 173.22 | 357.44 |
| SD | 182.29 | 1280.47 | 52.23 | 309.26 | 152.81 | 383.03 | 224.80 |

| NH4 (µmol/m2 d) | | | | | | | |
|---|---|---|---|---|---|---|---|
| | A | B | C | G | H | K | L |
| 1 | 436.66 | -2231.57 | 1058.49 | 1164.85 | -69.62 | -281.04 | -620.14 |
| 2 | 101.15 | -286.60 | -1869.91 | -574.67 | 36.85 | 1000.30 | 1218.38 |
| 3 | -230.99 | 662.37 | -245.43 | 725.66 | 1255.12 | 3686.10 | -256.90 |
| 4 | 1276.51 | 1049.51 | n.d. | -419.14 | -1028.76 | 4678.48 | 225.17 |
| SD | 647.30 | 1465.12 | 1467.13 | 854.08 | 936.40 | 2304.06 | 796.97 |

## Calculated Diffusive Fluxes by Fick's Law: DIC and $NH_4^+$

| Fluxes Ficks Law DIC | | | | | | | | | | | | | |
|---|---|---|---|---|---|---|---|---|---|---|---|---|---|
| Locations | | Concentrations of porewaters (DIC - mmol/m3) | | | | Flux calculations | | | | | | | |
| Depth (m): | | 0.005 | -0.005 | -0.015 | -0.025 | Gradients of trendline Δc/Δz (mmol/m3 m) | Gradients Δc/Δz from max/min (mmol/m3 m) | SD (gradients trendline vs gradients max/min) | R2 of trendline | Flux DIC (mmol/m2s) | Flux DIC (mmol/m2d) | Average Flux DIC (mmol/m2d) | SD of Flux (individual cores) |
| A | A1 | 2154.12 | 2283.15 | 2132.46 | 2819.25 | -18447.05 | -22171.06 | 2633.27 | 0.55 | 6.27E-06 | 0.54 | 0.98 | 0.41 |
| | A2 | 1931.58 | 2348.73 | 2608.09 | 3392.51 | -46421.48 | -48697.67 | 1609.51 | 0.95 | 1.58E-05 | 1.36 | | |
| | A3 | 2105.55 | 2342.37 | 2803.53 | 3116.09 | -34927.55 | -33684.39 | 879.05 | 0.99 | 1.19E-05 | 1.03 | | |
| B | B1 | 1951.07 | 1929.03 | n.d. | 2281.82 | -11970.06 | -11025.16 | 668.14 | 0.86 | 1.75E-06 | 0.15 | 0.12 | 0.04 |
| | B2 | 1893.14 | 1883.01 | 1985.75 | 2060.41 | -6045.36 | -5575.51 | 332.23 | 0.87 | 8.83E-07 | 0.08 | | |
| | B3 | 1998.74 | 2038.49 | 2394.58 | 2201.40 | -9640.74 | -6755.36 | 2040.27 | 0.48 | 1.41E-06 | 0.12 | | |
| C | C1 | 2127.89 | 2075.91 | 2174.30 | 2083.44 | 349.67 | 1481.77 | 800.51 | 0.01 | -3.88E-08 | 0.00 | 0.03 | 0.04 |
| | C2 | 2010.32 | 2125.32 | 2324.09 | 2205.08 | -7830.48 | -6492.00 | 946.44 | 0.58 | 8.68E-07 | 0.08 | | |
| | C3 | 2160.94 | 2506.92 | 2131.96 | 2373.26 | -2619.82 | -7077.10 | 3151.77 | 0.04 | 2.91E-07 | 0.03 | | |
| G | G1 | 2385.82 | 2144.55 | 2308.79 | 2242.02 | 2671.60 | 4793.31 | 1500.27 | 0.11 | -1.73E-07 | -0.01 | 0.02 | 0.06 |
| | G2 | 1956.14 | 2113.13 | 1984.14 | 1944.60 | 1636.29 | 384.86 | 884.90 | 0.07 | -1.06E-07 | -0.01 | | |
| | G3 | | 1837.17 | 2066.65 | 2142.93 | -15287.81 | -15287.81 | 0.00 | 0.92 | 9.87E-07 | 0.09 | | |
| H | H1 | 2557.15 | 2463.72 | 3053.63 | 3065.40 | -21146.73 | -16941.81 | 2973.33 | 0.73 | 8.88E-07 | 0.08 | 0.06 | 0.02 |
| | H2 | 2290.37 | 2318.17 | 2415.55 | 2671.77 | -12415.99 | -12713.57 | 210.42 | 0.85 | 5.21E-07 | 0.05 | | |
| | H3 | 2255.06 | 2329.66 | 2416.76 | 2680.92 | -13647.00 | -14195.56 | 387.89 | 0.90 | 5.73E-07 | 0.05 | | |
| K | K1 | 2194.53 | 3003.26 | 3339.88 | 5537.67 | -103660.32 | -111437.94 | 5499.61 | 0.88 | 4.27E-06 | 0.37 | 0.39 | 0.03 |
| | K2 | 2208.62 | 3204.79 | 4411.10 | 5743.91 | -118121.80 | -117842.96 | 197.18 | 1.00 | 4.86E-06 | 0.42 | | |
| | K3 | 2395.67 | 3235.08 | 3899.54 | 5727.19 | -106590.23 | -111050.61 | 3153.96 | 0.94 | 4.39E-06 | 0.38 | | |
| L | L1 | 2262.57 | 2681.26 | 3726.47 | 5128.05 | -96416.54 | -95516.11 | 636.70 | 0.95 | 3.18E-06 | 0.27 | 0.27 | 0.00 |
| | L2 | 2311.79 | 2663.99 | 3949.14 | 5025.04 | -94248.95 | -90441.58 | 2692.21 | 0.96 | 3.11E-06 | 0.27 | | |

| Fluxes Ficks Law NH4 | | | | | | | | | | | | | |
|---|---|---|---|---|---|---|---|---|---|---|---|---|---|
| Locations | | Concentrations of porewaters (NH4 - µmol/m3) | | | | Flux calculations | | | | | | | |
| Depth (m): | | 0.005 | -0.005 | -0.015 | -0.025 | Gradients of trendline Δc/Δz (µmol/m3 m) | Gradients Δc/Δz from max/min (µmol/m3 m) | SD (gradients trendline vs gradients max/min) | R2 of trendline | Flux NH4 (µmol/m2s) | Flux NH4 (µmol/m2d) | Average Flux NH4 (µmol/m2d) | SD of Flux |
| A | A1 | n.d. | 15826.09 | 55652.174 | 93913.04 | -3904347.83 | -3904347.83 | 0.00 | 1.00 | 2.40E-03 | 207.23 | 277.96 | 82.26 |
| | A2 | 7652.17 | 50608.70 | 146782.61 | 222608.70 | -7410434.78 | -7165217.39 | 173394.88 | 0.98 | 4.55E-03 | 393.32 | | |
| | A3 | 1391.30 | 112869.57 | 134086.96 | 140869.57 | -4396521.74 | -4649275.36 | 178723.80 | 0.76 | 2.70E-03 | 233.35 | | |
| B | B1 | 0 | 19400 | n.d. | 113200 | -3904285.71 | -3773333.33 | 92597.32 | 0.97 | 1.03E-03 | 89.01 | 64.75 | 18.48 |
| | B2 | 0 | n.d. | 25800 | 61400 | -1938571.43 | -2046666.67 | 76434.88 | 0.92 | 5.12E-04 | 44.20 | | |
| | B3 | 2400 | 13000 | 56400 | 77200 | -2678000.00 | -2493333.33 | 130579.05 | 0.95 | 7.07E-04 | 61.05 | | |
| C | C1 | 7800 | 13000 | 66200 | 95000 | -3148000 | -2906666.67 | 170648.44 | 0.93 | 6.31E-04 | 54.48 | 61.04 | 9.19 |
| | C2 | 5800 | 27200 | 98600 | 124600 | -4278000 | -3960000.00 | 224859.96 | 0.95 | 8.57E-04 | 74.03 | | |
| | C3 | 0 | 16800 | 63000 | 89800 | -3156000 | -2993333.33 | 115022.70 | 0.97 | 6.32E-04 | 54.62 | | |
| G | G1 | 0 | 25200 | 66400 | 103000 | -3502000 | -3433333.33 | 48554.67 | 0.99 | 4.08E-04 | 35.29 | 32.79 | 6.74 |
| | G2 | 0 | 21800 | 43400 | 70800 | -2340000 | -2360000.00 | 14142.14 | 1.00 | 2.73E-04 | 23.58 | | |
| | G3 | n.d. | 26600 | 79800 | 105000 | -3920000 | -3920000.00 | 0.00 | 0.96 | 4.57E-04 | 39.50 | | |
| H | H1 | 25400 | 88800 | 94200 | 139600 | -3480000 | -3806666.67 | 230988.22 | 0.92 | 2.64E-04 | 22.80 | 22.04 | 3.24 |
| | H2 | 23400 | 36200 | 118000 | 126200 | -3902000 | -3426666.67 | 336111.42 | 0.88 | 2.96E-04 | 25.57 | | |
| | H3 | 48000 | 39400 | 89400 | 121600 | -2708000 | -2453333.33 | 180076.53 | 0.84 | 2.05E-04 | 17.75 | | |
| K | K1 | 8800 | 150000 | 234200 | 237800 | -7712000 | -7633333.33 | 55625.73 | 0.86 | 5.74E-04 | 49.57 | 57.77 | 15.43 |
| | K2 | 11400 | 168800 | 296200 | 199000 | -6902000 | -6253333.33 | 458676.60 | 0.57 | 5.13E-04 | 44.36 | | |
| | K3 | 10400 | 122400 | 231200 | 385800 | -12350000 | -12513333.33 | 115494.11 | 0.99 | 9.19E-04 | 79.38 | | |
| L | L1 | 10400 | 130800 | 247200 | 270800 | -8976000 | -8680000.00 | 209303.61 | 0.94 | 5.35E-04 | 46.20 | 39.66 | 6.54 |
| | L2 | 7400 | 109600 | 159600 | 205200 | -6434000 | -6593333.33 | 112665.68 | 0.96 | 3.83E-04 | 33.12 | | |

## Calculated Diffusive Fluxes by Fick's Law: $PO_4^{3-}$ and $NO_3^-$

| Fluxes Ficks Law PO4 | | | | | | | | | | | | | |
|---|---|---|---|---|---|---|---|---|---|---|---|---|---|
| Locations | | Concentrations of porewaters (PO4 - µmol/m3) | | | | Flux calculations | | | | | | | |
| Depth (m) | | 0.005 | -0.005 | -0.015 | -0.025 | Gradients of trendline Δc/Δz (µmol/m3 m) | Gradients Δc/Δz from max/min (µmol/m3 m) | SD (gradients trendline vs gradients max/min) | R2 of trendline | Flux PO4 (µmol/m2s) | Flux PO4 (µmol/m2d) | Average Flux PO4 (µmol/m2d) | SD of Flux |
| A | A1 | 35121.95 | 18536.59 | 41951.22 | 17560.98 | 292682.93 | 585365.85 | 206958.08 | 0.10 | -5.17E-05 | -4.46 | -3.166 | 1.939 |
| | A2 | 19512.20 | n.d. | 42926.83 | 12682.93 | 27874.56 | 227642.28 | 141257.10 | 0.00 | -4.92E-06 | -0.43 | | |
| | A3 | 29268.29 | 16585.37 | 21463.41 | 17560.98 | 302439.02 | 390243.90 | 62087.42 | 0.46 | -5.34E-05 | -4.61 | | |
| B | B1 | 224.22 | 672.65 | n.d. | 2466.37 | -76873.80 | -74738.42 | 1509.94 | 0.98 | 5.83E-06 | 0.50 | 0.273 | 0.237 |
| | B2 | 1569.51 | 1569.51 | n.d. | 1345.29 | 8007.69 | 7473.84 | 377.49 | 0.89 | -6.07E-07 | -0.05 | | |
| | B3 | 0.00 | 2242.15 | 2466.37 | 1793.72 | -56053.81 | -59790.73 | 2642.40 | 0.42 | 4.25E-06 | 0.37 | | |
| C | C1 | 2752.29 | 8715.60 | n.d. | 8944.95 | -178571.43 | -206422.02 | 19693.34 | 0.60 | 1.03E-05 | 0.89 | 0.744 | 0.144 |
| | C2 | 2752.29 | 2522.94 | 2522.94 | 6422.02 | -110091.74 | -122324.16 | 8649.62 | 0.55 | 6.33E-06 | 0.55 | | |
| | C3 | 458.72 | 5504.59 | 5733.94 | 5733.94 | -160550.46 | -175840.98 | 10812.03 | 0.63 | 9.24E-06 | 0.80 | | |
| G | G1 | 515.46 | 1288.66 | 1288.66 | 2061.86 | -46391.75 | -51546.39 | 3644.88 | 0.90 | 1.55E-06 | 0.13 | 0.117 | 0.065 |
| | G2 | 3350.52 | 2577.32 | 3608.25 | 3350.52 | -10309.28 | 0.00 | 7289.76 | 0.09 | 3.45E-07 | 0.03 | | |
| | G3 | n.d. | 1030.93 | 2061.86 | 2319.59 | -64432.99 | -64432.99 | 0.00 | 0.89 | 2.16E-06 | 0.19 | | |
| H | H1 | 1142.86 | 571.43 | 285.71 | 1428.57 | -5714.29 | -9523.81 | 2693.74 | 0.02 | 1.25E-07 | 0.01 | 0.039 | 0.426 |
| | H2 | 7428.57 | 571.43 | 3714.29 | 16571.43 | -305714.29 | -304761.90 | 673.44 | 0.32 | 6.66E-06 | 0.58 | | |
| | H3 | 7714.29 | 3428.57 | 0.00 | 571.43 | 248571.43 | 238095.24 | 7407.79 | 0.83 | -5.42E-06 | -0.47 | | |
| K | K1 | 0.00 | 11666.67 | 42222.22 | 134722.22 | -4347222.22 | -4490740.74 | 101482.92 | 0.85 | 9.29E-05 | 8.03 | 4.486 | 2.531 |
| | K2 | 1388.89 | 10833.33 | 30000.00 | 52222.22 | -1716666.67 | -1694444.44 | 15713.48 | 0.97 | 3.67E-05 | 3.17 | | |
| | K3 | 0.00 | 11666.67 | 10000.00 | 41388.89 | -1225000.00 | -1379629.63 | 109339.66 | 0.79 | 2.62E-05 | 2.26 | | |
| L | L1 | 0.00 | 0.00 | 21084.34 | 75000.00 | -2460843.37 | -2500000.00 | 27687.92 | 0.80 | 4.21E-05 | 3.64 | 3.004 | 0.635 |
| | L2 | 1807.23 | 0.00 | 7530.12 | 52710.84 | -1602409.64 | -1696787.15 | 66734.98 | 0.68 | 2.74E-05 | 2.37 | | |

| Fluxes Ficks Law NO3 | | | | | | | | | | | | | |
|---|---|---|---|---|---|---|---|---|---|---|---|---|---|
| Locations | | Concentration of porewaters (NO3 - µmol/m3) | | | | Flux Calculations | | | | | | | |
| Depth (m) | | 0.005 | -0.005 | -0.015 | -0.025 | Gradients of trendline Δc/Δz (µmol/m3 m) | Gradients Δc/Δz from max/min (µmol/m3 m) | SD (gradients trendline vs gradients max/min) | R2 of trendline | Flux NO3 (µmol/m2s) | Flux NO3 (µmol/m2d) | Average Flux NO3 (µmol/m2d) | SD of Flux |
| A | A1 | 6944.44 | 7407.41 | 1157.41 | 0.00 | 270833.33 | 231481.48 | 27825.96 | 0.83 | -1.63E-04 | -14.11 | -4.34 | 7.08 |
| | A2 | 462.96 | 1157.41 | 0.00 | 0.00 | 25462.96 | 15432.10 | 7092.89 | 0.36 | -1.54E-05 | -1.33 | | |
| | A3 | 0.00 | 2314.81 | 0.00 | 2314.81 | -46296.30 | -77160.49 | 21824.28 | 0.20 | 2.79E-05 | 2.41 | | |
| B | B1 | 0.00 | 15740.74 | n.d | 0.00 | 112433.86 | 0.00 | 79502.75 | 0.04 | -2.91E-05 | -2.52 | -5.28 | 4.30 |
| | B2 | 0.00 | 15046.30 | 0.00 | 2083.33 | 87962.96 | -69444.44 | 111303.85 | 0.02 | -2.28E-05 | -1.97 | | |
| | B3 | 16898.15 | 0.00 | 0.00 | 0.00 | 506944.44 | 563271.60 | 39829.32 | 0.60 | -1.31E-04 | -11.35 | | |
| C | C1 | 2216.75 | 8374.38 | 17733.99 | 12315.27 | -396551.72 | -336617.41 | 42379.96 | 0.61 | 7.80E-05 | 6.74 | 3.35 | 2.45 |
| | C2 | 0.00 | 19211.82 | 10344.83 | 7389.16 | -133004.93 | -246305.42 | 80115.55 | 0.05 | 2.62E-05 | 2.26 | | |
| | C3 | 4433.50 | 19211.82 | 21674.88 | 5665.02 | -61576.35 | -41050.90 | 14513.69 | 0.01 | 1.21E-05 | 1.05 | | |
| G | G1 | 9359.61 | 25862.07 | 7389.16 | 0.00 | 465517.24 | 311986.86 | 108562.37 | 0.30 | -5.33E-05 | -4.61 | -1.19 | 4.55 |
| | G2 | 0.00 | 54926.11 | 7142.86 | 1724.14 | 426108.37 | -57471.26 | 341942.44 | 0.04 | -4.88E-05 | -4.22 | | |
| | G3 | | 9359.61 | 12807.88 | 19950.74 | -529556.65 | -529556.65 | 0.00 | 0.96 | 6.06E-05 | 5.24 | | |
| H | H1 | 8867.00 | 14285.71 | 0.00 | 2463.05 | 334975.37 | 213464.70 | 85921.02 | 0.45 | -2.49E-05 | -2.16 | 0.98 | 2.98 |
| | H2 | 0.00 | 7142.86 | 16748.77 | 22660.10 | -775862.07 | -755336.62 | 14513.69 | 0.99 | 5.78E-05 | 4.99 | | |
| | H3 | 2955.67 | 16256.16 | 1724.14 | 8374.38 | -17241.38 | -180623.97 | 115528.94 | 0.00 | 1.28E-06 | 0.11 | | |
| K | K1 | 5665.02 | 32019.70 | 22660.10 | 2955.67 | 174876.85 | 90311.99 | 59796.39 | 0.03 | -1.28E-05 | -1.10 | -1.85 | 1.09 |
| | K2 | 24630.54 | 7881.77 | 0.00 | 9359.61 | 536945.81 | 509031.20 | 19738.61 | 0.45 | -3.92E-05 | -3.39 | | |
| | K3 | 7389.16 | 492.61 | 5911.33 | 0.00 | 167487.68 | 246305.42 | 55732.55 | 0.33 | -1.22E-05 | -1.06 | | |
| L | L1 | 5172.41 | 10837.44 | 0.00 | 5665.02 | 93596.06 | -16420.36 | 77793.36 | 0.07 | -5.47E-06 | -0.47 | -0.82 | 0.34 |
| | L2 | 9113.30 | 8374.38 | 6896.55 | 1970.44 | 229064.04 | 238095.24 | 6386.02 | 0.85 | -1.34E-05 | -1.16 | | |

## 7.2 Appendix B: All chemical measurements

**Porewater measurements: DIC**

| Porewater measurements DIC (mM) - mmol/L | | | | | | | | | | | | | | | | | | | |
|---|---|---|---|---|---|---|---|---|---|---|---|---|---|---|---|---|---|---|---|
| **Locality** | **Depth (cm)** | **-0.5** | **0.5** | **1.5** | **2.5** | **3.5** | **4.5** | **5.5** | **6.5** | **7.5** | **8.5** | **9.5** | **11.5** | **13.5** | 15.5 | 17.5 | 19.5 | 24.5 | 29.5 |
| A(High) | A1 | 2.15 | 2.28 | 2.13 | 2.82 | 2.54 | 2.99 | 2.92 | 3.25 | 4.14 | 3.97 | 4.12 | | | | | | | |
| | A2 | 1.93 | 2.35 | 2.61 | 3.39 | 3.83 | 3.55 | 4.79 | 5.32 | 5.60 | | 6.19 | 6.84 | 7.33 | | | | | |
| | A3 | 2.11 | 2.34 | 2.80 | 3.12 | 3.08 | 3.16 | 3.56 | 3.77 | 4.88 | 4.03 | 4.76 | 4.54 | | | | | | |
| | Average | 2.06 | 2.32 | 2.51 | 3.11 | 3.15 | 3.23 | 3.76 | 4.11 | 4.87 | 4.00 | 5.02 | 5.69 | 7.33 | | | | | |
| | SD | 0.10 | 0.03 | 0.28 | 0.23 | 0.53 | 0.24 | 0.77 | 0.88 | 0.60 | 0.03 | 0.87 | 1.15 | 0.00 | | | | | |
| B(Low) | Depth (cm) | -0.5 | 0.5 | 1.5 | 2.5 | 3.5 | 4.5 | 5.5 | 6.5 | 7.5 | 8.5 | 9.5 | | | | | | | |
| | B1 | 1.95 | 1.93 | | 2.28 | 2.46 | 2.47 | 2.78 | 3.27 | 3.33 | 3.34 | 3.40 | | | | | | | |
| | B2 | 1.89 | 1.88 | 1.99 | 2.06 | 2.07 | 2.11 | | 2.19 | 2.43 | | | | | | | | | |
| | B3 | 2.00 | 2.04 | 2.39 | 2.20 | 2.25 | 2.28 | 2.43 | 2.95 | 2.67 | 3.15 | | | | | | | | |
| | Average | 1.95 | 1.95 | 2.19 | 2.18 | 2.26 | 2.29 | 2.61 | 2.80 | 2.81 | 3.24 | 3.40 | | | | | | | |
| | SD | 0.04 | 0.07 | 0.20 | 0.09 | 0.16 | 0.15 | 0.18 | 0.45 | 0.38 | 0.09 | 0.00 | | | | | | | |
| C (High) | Depth (cm) | -0.5 | 0.5 | 1.5 | 2.5 | 3.5 | 4.5 | 5.5 | 6.5 | | | | | | | | | | |
| | C1 | 2.13 | 2.08 | 2.17 | 2.08 | 2.33 | 2.64 | 3.22 | 3.30 | | | | | | | | | | |
| | C2 | 2.01 | 2.13 | 2.32 | 2.21 | 2.57 | 2.86 | | | | | | | | | | | | |
| | C3 | 2.16 | 2.51 | 2.13 | 2.37 | 2.44 | 3.08 | 3.18 | | | | | | | | | | | |
| | Average | 2.10 | 2.24 | 2.21 | 2.22 | 2.45 | 2.86 | 3.20 | 3.30 | | | | | | | | | | |
| | SD | 0.06 | 0.19 | 0.08 | 0.12 | 0.10 | 0.18 | 0.02 | 0.00 | | | | | | | | | | |
| | Average difference C-B | 0.15 | 0.29 | 0.02 | 0.04 | 0.19 | 0.57 | 0.60 | 0.49 | | | | | | | | | | |
| G(Low) | Depth (cm) | -0.5 | 0.5 | 1.5 | 2.5 | 3.5 | 4.5 | 5.5 | 6.5 | 7.5 | 8.5 | 9.5 | | | | | | | |
| | G1 | 2.39 | 2.14 | 2.31 | 2.24 | 2.59 | 2.52 | 2.86 | 3.56 | 3.01 | 3.15 | 3.24 | | | | | | | |
| | G2 | 1.96 | 2.11 | 1.98 | 1.94 | 2.23 | 2.21 | 2.64 | | | | | | | | | | | |
| | G3 | | 1.84 | 2.07 | 2.14 | 2.47 | 2.63 | 3.24 | | | 3.29 | 3.52 | | | | | | | |
| | Average | 2.17 | 2.03 | 2.12 | 2.11 | 2.43 | 2.46 | 2.91 | 3.56 | 3.01 | 3.22 | 3.38 | | | | | | | |
| | SD | 0.21 | 0.14 | 0.14 | 0.12 | 0.15 | 0.18 | 0.25 | 0.00 | 0.00 | 0.07 | 0.14 | | | | | | | |
| H(High) | Depth (cm) | -0.5 | 0.5 | 1.5 | 2.5 | 3.5 | 4.5 | 5.5 | 6.5 | 7.5 | 8.5 | 9.5 | 11.5 | 13.5 | 15.5 | | | | |
| | H1 | 2.56 | 2.46 | 3.05 | 3.07 | 3.60 | 4.49 | 4.41 | 4.79 | 4.70 | 4.59 | 4.82 | | | | | | | |
| | H2 | 2.29 | 2.32 | 2.42 | 2.67 | 3.05 | 3.56 | 3.78 | 4.04 | 4.24 | 4.18 | 3.95 | 3.77 | 3.83 | 3.70 | | | | |
| | H3 | 2.26 | 2.33 | 2.42 | 2.68 | 2.93 | 2.81 | 3.20 | 3.44 | 3.36 | 3.60 | 3.39 | | | | | | | |
| | Average | 2.37 | 2.37 | 2.63 | 2.81 | 3.20 | 3.62 | 3.80 | 4.09 | 4.10 | 4.12 | 4.05 | 3.77 | 3.83 | 3.70 | | | | |
| | SD | 0.13 | 0.07 | 0.30 | 0.18 | 0.29 | 0.69 | 0.49 | 0.55 | 0.55 | 0.41 | 0.59 | 0.00 | 0.00 | | | | | |
| | Average difference H-G | 0.20 | 0.34 | 0.51 | 0.70 | 0.77 | 1.16 | 0.88 | 0.53 | 1.09 | 0.90 | 0.67 | | | | | | | |
| K(High) | Depth (cm) | -0.5 | 0.5 | 1.5 | 2.5 | 3.5 | 4.5 | 5.5 | 6.5 | 7.5 | 8.5 | 9.5 | 11.5 | 13.5 | 15.5 | 17.5 | 19.5 | 24.5 | 29.5 |
| | K1 | 2.19 | 3.00 | 3.34 | 5.54 | 7.86 | 9.38 | | 12.07 | 12.74 | 14.73 | 16.77 | | | | | | | |
| | K2 | 2.21 | 3.20 | 4.41 | 5.74 | 7.22 | 9.29 | 11.28 | 12.16 | | 12.90 | 15.33 | 15.77 | 15.36 | 15.76 | 18.18 | | 19.86 | 22.11 |
| | K3 | 2.40 | 3.24 | 3.90 | 5.73 | 7.39 | 8.53 | 9.82 | 13.12 | 13.11 | 14.38 | 19.13 | 17.23 | 17.20 | 20.80 | 20.79 | 21.59 | 22.89 | |
| | Average | 2.27 | 3.15 | 3.88 | 5.67 | 7.49 | 9.07 | 10.55 | 12.45 | 12.92 | 14.00 | 17.08 | 16.50 | 16.28 | 18.28 | 19.49 | 21.59 | 21.38 | 22.11 |
| | SD | 0.09 | 0.10 | 0.44 | 0.09 | 0.27 | 0.38 | 0.73 | 0.47 | 0.19 | 0.80 | 1.57 | 0.73 | 0.92 | | | | | |
| L(Low) | Depth(cm) | -0.5 | 0.5 | 1.5 | 2.5 | 3.5 | 4.5 | 5.5 | 6.5 | 7.5 | 8.5 | 9.5 | 11.5 | 13.5 | 15.5 | 17.5 | 19.5 | 24.5 | |
| | L1 | 2.26 | 2.68 | 3.73 | 5.13 | 6.59 | 8.75 | 10.24 | 12.74 | 14.60 | 15.01 | 16.92 | 18.22 | 19.74 | 20.49 | 21.15 | 22.45 | 23.48 | |
| | L2 | 2.31 | 2.66 | 3.95 | 5.03 | 7.23 | 8.52 | 12.98 | 15.81 | 15.55 | 16.39 | 17.13 | 21.16 | 18.61 | 21.50 | 22.14 | 21.64 | | |
| | Average | 2.29 | 2.67 | 3.84 | 5.08 | 6.91 | 8.63 | 11.61 | 14.28 | 15.08 | 15.70 | 17.03 | 19.69 | 19.17 | 20.99 | 21.64 | 22.04 | 23.48 | |
| | SD | 0.02 | 0.01 | 0.11 | 0.05 | 0.32 | 0.12 | 1.37 | 1.53 | 0.48 | 0.69 | 0.10 | 1.47 | 0.57 | 0.50 | 0.49 | 0.41 | 0.00 | |
| | Average difference K-L | -0.02 | 0.48 | 0.05 | 0.59 | 0.58 | 0.44 | -1.06 | -1.83 | -2.16 | -1.70 | 0.05 | -3.18 | -2.89 | -2.71 | -2.15 | -0.45 | -2.10 | |

## Porewater measurements: $\delta^{13}C_{DIC}$

| Porewater measurements δ13C (‰) | | | | | | | | | | | | | | | | | | |
|---|---|---|---|---|---|---|---|---|---|---|---|---|---|---|---|---|---|---|
| **Locality** | **Depth (cm)** | **-0.5** | **0.5** | **1.5** | **2.5** | **3.5** | **4.5** | **5.5** | **6.5** | **7.5** | **8.5** | **9.5** | **11.5** | **13.5** | **15.5** | **17.5** | **19.5** | **24.5** | **29.5** |
| A(High) | A1 | -3.32 | -4.58 | -5.02 | -6.78 | -6.28 | -7.52 | -7.52 | -8.17 | -9.29 | -8.97 | -9.59 | | | | | | | |
| | A2 | -2.23 | -5.85 | -8.22 | -10.62 | -11.93 | -13.11 | -13.52 | -13.73 | -14.67 | n.d. | -15.11 | -14.95 | -15.39 | | | | | |
| | A3 | -3.26 | -7.65 | -7.59 | -8.10 | -8.32 | -9.77 | -10.46 | -10.05 | -13.17 | -10.77 | -11.35 | -12.21 | | | | | | |
| | Average | -2.94 | -6.03 | -6.94 | -8.50 | -8.84 | -10.13 | -10.50 | -10.65 | -12.37 | -9.87 | -12.02 | -13.58 | -15.39 | | | | | |
| | SD | 0.50 | 1.26 | 1.39 | 1.60 | 2.34 | 2.29 | 2.45 | 2.31 | 2.27 | 0.90 | 2.31 | 1.37 | 0.00 | | | | | |
| B(Low) | Depth (cm) | -0.5 | 0.5 | 1.5 | 2.5 | 3.5 | 4.5 | 5.5 | 6.5 | 7.5 | 8.5 | 9.5 | | | | | | | |
| | B1 | -1.62 | -4.10 | n.d. | -7.73 | -6.37 | -6.86 | -7.45 | -8.53 | -8.64 | -8.89 | -9.12 | | | | | | | |
| | B2 | -1.66 | -3.47 | -4.80 | -4.99 | -5.32 | -5.46 | | -5.70 | -6.00 | | | | | | | | | |
| | B3 | -1.68 | -4.09 | -5.35 | -5.57 | -7.35 | -6.72 | -7.64 | -7.81 | -8.08 | -8.70 | | | | | | | | |
| | Average | -1.65 | -3.89 | -5.08 | -6.10 | -6.35 | -6.35 | -7.54 | -7.35 | -7.57 | -8.79 | -9.12 | | | | | | | |
| | SD | 0.02 | 0.29 | 0.27 | 1.18 | 0.83 | 0.63 | 0.10 | 1.20 | 1.14 | 0.09 | 0.00 | | | | | | | |
| C(High) | Depth (cm) | -0.5 | 0.5 | 1.5 | 2.5 | 3.5 | 4.5 | 5.5 | 6.5 | | | | | | | | | | |
| | C1 | -1.76 | -3.50 | -4.64 | -5.33 | -6.40 | -7.52 | -8.42 | -8.87 | | | | | | | | | | |
| | C2 | -1.54 | -3.72 | -7.19 | -5.38 | -6.03 | -7.92 | | | | | | | | | | | | |
| | C3 | -1.51 | -4.91 | -3.68 | -4.09 | -3.98 | -5.83 | -4.92 | | | | | | | | | | | |
| | Average | -1.60 | -4.04 | -5.17 | -4.94 | -5.47 | -7.09 | -6.67 | -8.87 | | | | | | | | | | |
| | SD | 0.11 | 0.62 | 1.48 | 0.60 | 1.06 | 0.91 | 1.75 | 0.00 | | | | | | | | | | |
| | Average difference C-B | 0.05 | -0.15 | -0.09 | 1.16 | 0.87 | -0.74 | 0.88 | -1.53 | | | | | | | | | | |
| G(Low) | Depth (cm) | -0.5 | 0.5 | 1.5 | 2.5 | 3.5 | 4.5 | 5.5 | 6.5 | 7.5 | 8.5 | 9.5 | | | | | | | |
| | G1 | -2.25 | -4.28 | -5.31 | -6.06 | -6.87 | -8.11 | -7.26 | -7.22 | -8.40 | -8.52 | -8.40 | | | | | | | |
| | G2 | -1.62 | -3.93 | -4.25 | -5.04 | -6.03 | -6.76 | -7.80 | | | | | | | | | | | |
| | G3 | n.d. | -3.84 | -5.32 | -5.49 | -6.67 | -7.89 | -8.72 | | | -9.48 | -9.10 | | | | | | | |
| | Average | -1.93 | -4.02 | -4.96 | -5.53 | -6.53 | -7.59 | -7.93 | -7.22 | -8.40 | -9.00 | -8.75 | | | | | | | |
| | SD | 0.31 | 0.19 | 0.50 | 0.42 | 0.36 | 0.59 | 0.60 | 0.00 | 0.00 | 0.48 | 0.35 | | | | | | | |
| H(High) | Depth (cm) | -0.5 | 0.5 | 1.5 | 2.5 | 3.5 | 4.5 | 5.5 | 6.5 | 7.5 | 8.5 | 9.5 | 11.5 | 13.5 | 15.5 | | | | |
| | H1 | -3.20 | -4.45 | -6.00 | -6.91 | -8.62 | -9.82 | -10.58 | -10.81 | -11.48 | -11.47 | -11.53 | | | | | | | |
| | H2 | -1.84 | -3.52 | -5.18 | -6.41 | -7.45 | -8.99 | -8.83 | -9.56 | -10.57 | -11.13 | -10.65 | -7.98 | -10.90 | -11.48 | | | | |
| | H3 | -2.24 | -3.90 | -4.59 | -6.60 | -7.85 | -7.90 | -8.36 | -8.84 | -9.63 | -9.94 | -9.82 | | | | | | | |
| | Average | -2.42 | -3.96 | -5.26 | -6.64 | -7.97 | -8.90 | -9.26 | -9.74 | -10.56 | -10.85 | -10.67 | -7.98 | -10.90 | -11.48 | | | | |
| | SD | 0.57 | 0.38 | 0.58 | 0.21 | 0.49 | 0.78 | 0.95 | 0.81 | 0.76 | 0.66 | 0.70 | | | | | | | |
| | Average Difference H-G | -0.49 | 0.06 | -0.30 | -1.11 | -1.45 | -1.32 | -1.33 | -2.52 | -2.16 | -1.85 | -1.91 | -7.98 | -10.90 | -11.48 | | | | |
| K(High) | Depth (cm) | -0.5 | 0.5 | 1.5 | 2.5 | 3.5 | 4.5 | 5.5 | 6.5 | 7.5 | 8.5 | 9.5 | 11.5 | 13.5 | 15.5 | 17.5 | 19.5 | 24.5 | 29.50 |
| | K1 | -2.95 | -8.72 | -9.68 | -15.70 | -18.05 | -19.62 | n.d. | -20.04 | -20.58 | -20.39 | -19.00 | | | | | | | |
| | K2 | -3.80 | -8.89 | -13.24 | -16.12 | -17.27 | -19.78 | -20.36 | -20.55 | | -19.87 | -21.26 | -20.55 | -18.63 | -16.39 | -13.95 | | -7.27 | -5.77 |
| | K3 | -3.49 | -7.77 | -11.61 | -15.45 | -18.01 | -20.19 | -21.19 | -17.21 | -19.02 | -21.48 | -12.64 | -17.93 | -21.76 | -19.82 | -17.16 | -14.81 | -10.98 | |
| | Average | -3.41 | -8.46 | -11.51 | -15.76 | -17.77 | -19.86 | -20.78 | -19.27 | -19.80 | -20.58 | -17.64 | -19.24 | -20.19 | -18.11 | -15.56 | -14.81 | -9.13 | -5.77 |
| | SD | 0.35 | 0.49 | 1.45 | 0.28 | 0.36 | 0.24 | 0.42 | 1.47 | 0.78 | 0.67 | 3.65 | 1.31 | 1.56 | 1.71 | 1.60 | 0.00 | 1.86 | 0.00 |
| L(Low) | Depth(cm) | -0.5 | 0.5 | 1.5 | 2.5 | 3.5 | 4.5 | 5.5 | 6.5 | 7.5 | 8.5 | 9.5 | 11.5 | 13.5 | 15.5 | 17.5 | 19.5 | 24.5 | |
| | L1 | -3.62 | -7.26 | -10.56 | -15.54 | -19.04 | -20.29 | -21.01 | -20.47 | -22.45 | -22.74 | -22.40 | -20.62 | -17.44 | -14.78 | -11.50 | -9.39 | -4.44 | |
| | L2 | -3.93 | -8.47 | -12.77 | -15.79 | -15.16 | -18.52 | -12.87 | -18.40 | -19.83 | -21.02 | -22.80 | -16.52 | -16.94 | -12.92 | -10.37 | -8.91 | | |
| | Average | -3.77 | -7.86 | -11.67 | -15.66 | -17.10 | -19.40 | -16.94 | -19.43 | -21.14 | -21.88 | -22.60 | -18.57 | -17.19 | -13.85 | -10.93 | -9.15 | -4.44 | |
| | SD | 0.15 | 0.60 | 1.11 | 0.12 | 1.94 | 0.89 | 4.07 | 1.03 | 1.31 | 0.86 | 0.20 | 2.05 | 0.25 | 0.93 | 0.56 | 0.24 | 0.00 | |
| | Average difference K-L | 0.36 | -0.59 | 0.16 | -0.10 | -0.67 | -0.46 | -3.84 | 0.17 | 1.34 | 1.30 | 4.97 | -0.67 | -3.00 | -4.26 | -4.62 | -5.66 | -4.68 | |

## Porewater measurements: $NH_4^+$

| Porewater Measurements NH4 (µM) - µmol/L | | | | | | | | | | | | | | | | | | |
|---|---|---|---|---|---|---|---|---|---|---|---|---|---|---|---|---|---|---|
| **Locality** | **Depth (cm):** | **-0.5** | **0.5** | **1.5** | **2.5** | **3.5** | **4.5** | **5.5** | **6.5** | **7.5** | **8.5** | **9.5** | **11.5** | **13.5** | **15.5** | **17.5** | **19.5** | **24.5** | **29.5** |
| A | A1 | n.d | 15.83 | 55.65 | 93.91 | 115.13 | 149.04 | 253.91 | 445.22 | n.d | 273.04 | 276.52 | | | | | | | |
| | A2 | 7.65 | 50.61 | 146.78 | 222.61 | 294.78 | 311.48 | 450.43 | 511.30 | 587.83 | n.d | 702.61 | 720.00 | 766.96 | | | | | |
| | A3 | 1.39 | 112.87 | 134.09 | 140.87 | 152.52 | 185.91 | 273.04 | 191.30 | 393.04 | 187.83 | 267.83 | 377.39 | | | | | | |
| | Average | 4.52 | 59.77 | 112.17 | 152.46 | 187.48 | 215.48 | 325.80 | 382.61 | 490.43 | 230.43 | 415.65 | 548.70 | 766.96 | | | | | |
| | SD | 3.13 | 40.14 | 40.30 | 53.18 | 77.40 | 69.53 | 88.48 | 137.94 | 97.39 | 42.61 | 202.94 | 171.30 | 0.00 | | | | | |
| B (Low) | Depth (cm) | -0.5 | 0.5 | 1.5 | 2.5 | 3.5 | 4.5 | 5.5 | 6.5 | 7.5 | 8.5 | 9.5 | | | | | | | |
| | B1 | 0.00 | 19.40 | n.d. | 113.20 | 88.00 | 136.00 | 111.20 | 196.00 | 146.00 | 166.00 | 218.00 | | | | | | | |
| | B2 | 0.00 | n.d. | 25.80 | 61.40 | 57.40 | 58.20 | n.d. | 18.00 | n.d. | n.d. | 60.00 | | | | | | | |
| | B3 | 2.40 | 13.00 | 56.40 | 77.20 | 25.00 | 62.01 | 76.00 | 110.00 | 78.00 | 84.00 | 110.00 | | | | | | | |
| | Average | 0.80 | 16.20 | 41.10 | 83.93 | 56.80 | 85.40 | 93.60 | 108.00 | 112.00 | 125.00 | 129.33 | | | | | | | |
| | SD | 1.13 | 3.20 | 15.30 | 21.68 | 25.72 | 35.81 | 17.60 | 72.68 | 34.00 | 41.00 | 65.94 | | | | | | | |
| C (High) | Depth (cm) | -0.5 | 0.5 | 1.5 | 2.5 | 3.5 | 4.5 | 5.5 | | | | | | | | | | | |
| | C1 | 7.80 | 13.00 | 66.20 | 95.00 | 128.40 | 167.00 | 196.80 | | | | | | | | | | | |
| | C2 | 5.80 | 27.20 | 98.60 | 124.60 | 153.00 | 165.60 | | | | | | ` | | | | | | |
| | C3 | 0.00 | 16.80 | 63.00 | 89.80 | 107.80 | 134.20 | 114.60 | | | | | | | | | | | |
| | Average | 4.53 | 19.00 | 75.93 | 103.13 | 129.73 | 155.60 | 155.70 | | | | | | | | | | | |
| | SD | 3.31 | 6.00 | 16.08 | 15.33 | 18.48 | 15.14 | 41.10 | | | | | | | | | | | |
| | Average Difference C-B | 3.73 | 2.80 | 34.83 | 19.20 | 72.93 | 70.20 | 62.10 | | | | | | | | | | | |
| G (Low) | Depth (cm) | -0.5 | 0.5 | 1.5 | 2.5 | 3.5 | 4.5 | 5.5 | 6.5 | 7.5 | 8.5 | 9.5 | | | | | | | |
| | G1 | 0.00 | 25.20 | 66.40 | 103.00 | 110.60 | 131.20 | 44.00 | 110.00 | 116.00 | n.d. | 152.00 | | | | | | | |
| | G2 | 0.00 | 21.80 | 43.40 | 70.80 | 85.00 | 98.20 | 114.60 | | | | | | | | | | | |
| | G3 | n.d. | 26.60 | 79.80 | 105.00 | 138.80 | 157.20 | 141.20 | 164.00 | 168.00 | 334.00 | 258.00 | | | | | | | |
| | Average | 0.00 | 24.53 | 63.20 | 92.93 | 111.47 | 128.87 | 99.93 | 137.00 | 142.00 | 334.00 | 205.00 | | | | | | | |
| | SD | 0.00 | 2.02 | 15.03 | 15.67 | 21.97 | 24.14 | 41.01 | 27.00 | 26.00 | 0.00 | 53.00 | | | | | | | |
| H (High) | Depth (cm) | -0.5 | 0.5 | 1.5 | 2.5 | 3.5 | 4.5 | 5.5 | 6.5 | 7.5 | 8.5 | 9.5 | 11.5 | 13.5 | 15.5 | | | | |
| | H1 | 25.40 | 88.80 | 94.20 | 139.60 | 175.60 | 223.00 | 194.00 | 276.00 | n.d | 320.00 | 286.00 | | | | | | | |
| | H2 | 23.40 | 36.20 | 118.00 | 126.20 | 151.40 | 135.60 | n.d. | 228.00 | 204.00 | 368.00 | 212.00 | n.d. | 254.00 | 210.00 | | | | |
| | H3 | 48.00 | 39.40 | 89.40 | 121.60 | 188.00 | 128.80 | 238.00 | 392.00 | 514.00 | 234.00 | 350.00 | | | | | | | |
| | Average | 32.27 | 54.80 | 100.53 | 129.13 | 171.67 | 162.47 | 216.00 | 298.67 | 359.00 | 307.33 | 282.67 | n.d. | 254.00 | 210.00 | | | | |
| | SD | 11.16 | 24.08 | 12.51 | 7.64 | 15.20 | 42.89 | 22.00 | 68.84 | 155.00 | 55.43 | 56.39 | | | 0.00 | | | | |
| | Average Difference H-G | 32.27 | 30.27 | 37.33 | 36.20 | 60.20 | 33.60 | 116.07 | 161.67 | 217.00 | -26.67 | 77.67 | | | | | | | |
| K (High) | Depth (cm) | -0.5 | 0.5 | 1.5 | 2.5 | 3.5 | 4.5 | 5.5 | 6.5 | 7.5 | 8.5 | 9.5 | 11.5 | 13.5 | 15.5 | 17.5 | 19.5 | 24.5 | 29.5 |
| | K1 | 8.80 | 150.00 | 234.20 | 237.80 | 162.60 | 159.20 | | 1248.00 | 1330.00 | 1456.00 | 2062.00 | | | | | | | |
| | K2 | 11.40 | 168.80 | 296.20 | 199.00 | 327.80 | 321.00 | 938.00 | 1316.00 | 1350.00 | 1254.00 | 1352.00 | 1712.00 | 1394.00 | 2228.00 | 1658.00 | | 2838.00 | 2584.00 |
| | K3 | 10.40 | 122.40 | 231.20 | 385.80 | 349.80 | 338.80 | | 986.00 | 1030.00 | 1406.00 | 1296.00 | | 1736.00 | 1520.00 | 1438.00 | 2086.00 | 2460.00 | |
| | Average | 10.20 | 147.07 | 253.87 | 274.20 | 280.07 | 273.00 | 938.00 | 1183.33 | 1236.67 | 1372.00 | 1570.00 | 1712.00 | 1565.00 | 1874.00 | 1548.00 | 2086.00 | 2649.00 | 2584.00 |
| | SD | 1.07 | 19.06 | 29.96 | 80.49 | 83.55 | 80.80 | 0.00 | 142.27 | 146.36 | 85.90 | 348.65 | 0.00 | 171.00 | 354.00 | 110.00 | 0.00 | 189.00 | 0.00 |
| L (Low) | Depth(cm) | -0.5 | 0.5 | 1.5 | 2.5 | 3.5 | 4.5 | 5.5 | 6.5 | 7.5 | 8.5 | 9.5 | 11.5 | 13.5 | 15.5 | 17.5 | 19.5 | 24.5 | |
| | L1 | 10.40 | 130.80 | 247.20 | 270.80 | 233.60 | 222.80 | 966.00 | 1274.00 | 1350.00 | 1080.00 | 1196.00 | 1390.00 | 1802.00 | 2768.00 | 0.00 | 2568.00 | 1584.00 | |
| | L2 | 7.40 | 109.60 | 159.60 | 205.20 | 168.20 | 230.80 | 832.00 | 978.00 | 1038.00 | 1014.00 | 1322.00 | 1548.00 | 1508.00 | 2066.00 | 2228.00 | 2132.00 | | |
| | Average | 8.90 | 120.20 | 203.40 | 238.00 | 200.90 | 226.80 | 899.00 | 1126.00 | 1194.00 | 1047.00 | 1259.00 | 1469.00 | 1655.00 | 2417.00 | 1114.00 | 2350.00 | 1584.00 | |
| | SD | 1.50 | 10.60 | 43.80 | 32.80 | 32.70 | 4.00 | 67.00 | 148.00 | 156.00 | 33.00 | 63.00 | 79.00 | 147.00 | 351.00 | 1114.00 | 218.00 | 0.00 | |
| | Average Difference K-L | 1.3 | 26.866667 | 50.466667 | 36.2 | 79.166667 | 46.2 | 39 | 57.333333 | 42.666667 | 325 | 311 | 243 | -90 | -543 | 434 | -264 | 1065 | |

## Porewater measurements: $PO_4^{3-}$

| Porewater Measurements PO4 (µM) - µmol/L | | | | | | | | | | | | | | | | | | | |
|---|---|---|---|---|---|---|---|---|---|---|---|---|---|---|---|---|---|---|---|
| **Locality** | **Depth (cm)** | **-0.5** | **0.5** | **1.5** | **2.5** | **3.5** | **4.5** | **5.5** | **6.5** | **7.5** | **8.5** | **9.5** | **11.5** | **13.5** | **15.5** | **17.5** | **19.5** | **24.5** | **29.5** |
| A | A1 | 35.12 | 18.54 | 41.95 | 17.56 | 18.54 | 15.61 | 6.83 | 27.32 | n.d. | 18.54 | 7.80 | | | | | | | |
| | A2 | 19.51 | 0.00 | 42.93 | 12.68 | 9.76 | 1.95 | 109.27 | 37.07 | 9.76 | n.d. | 11.71 | 58.54 | 24.39 | | | | | |
| | A3 | 29.27 | 16.59 | 21.46 | 17.56 | 58.54 | 22.44 | 26.34 | 36.10 | 42.93 | 70.24 | 44.88 | 56.59 | | | | | | |
| | Average | 27.97 | 11.71 | 35.45 | 15.93 | 28.94 | 13.33 | 47.48 | 33.50 | 26.34 | 44.39 | 21.46 | 57.56 | 24.39 | | | | | |
| | SD | 6.44 | 8.32 | 9.90 | 2.30 | 21.23 | 8.52 | 44.41 | 4.39 | 16.59 | 25.85 | 16.63 | 0.98 | 0.00 | | | | | |
| B (Low) | Depth (cm) | -0.5 | 0.5 | 1.5 | 2.5 | 3.5 | 4.5 | 5.5 | 6.5 | 7.5 | 8.5 | 9.5 | | | | | | | |
| | B1 | 0.22 | 0.67 | n.d. | 2.47 | 0.45 | n.d. | 9.64 | 10.54 | 11.88 | 13.23 | 14.80 | | | | | | | |
| | B2 | 1.57 | 1.57 | 2.24 | 1.35 | 11.43 | 3.81 | 1.35 | 2.47 | 3.81 | n.d. | 1.57 | | | | | | | |
| | B3 | 0.00 | 2.24 | 2.47 | 1.79 | | 2.69 | 4.48 | 9.19 | 13.00 | 18.39 | 20.63 | | | | | | | |
| | Average | 0.60 | 1.49 | 2.35 | 1.87 | 5.94 | 3.25 | 5.16 | 7.40 | 9.57 | 15.81 | 12.33 | | | | | | | |
| | SD | 0.69 | 0.64 | 0.11 | 0.46 | 5.49 | 0.56 | 3.42 | 3.53 | 4.09 | 2.58 | 7.97 | | | | | | | |
| C (High) | Depth (cm) | -0.5 | 0.5 | 1.5 | 2.5 | 3.5 | 4.5 | 5.5 | | | | | | | | | | | |
| | C1 | 2.75 | 8.72 | n.d. | 8.94 | 8.72 | 10.32 | 12.61 | | | | | | | | | | | |
| | C2 | 2.75 | 2.52 | 2.52 | 6.42 | 3.90 | 10.55 | | | | | | | | | | | | |
| | C3 | 0.46 | 5.50 | 5.73 | 5.73 | 4.59 | 5.73 | 8.49 | | | | | | | | | | | |
| | Average | 1.99 | 5.58 | 4.13 | 7.03 | 5.73 | 8.87 | 10.55 | | | | | | | | | | | |
| | SD | 1.08 | 2.53 | 1.61 | 1.38 | 2.13 | 2.22 | 2.06 | | | | | | | | | | | |
| | Average Difference C-B | 1.39 | 4.09 | 1.77 | 5.17 | -0.21 | 5.62 | 5.39 | | | | | | | | | | | |
| G (Low) | Depth (cm) | -0.5 | 0.5 | 1.5 | 2.5 | 3.5 | 4.5 | 5.5 | 6.5 | 7.5 | 8.5 | 9.5 | | | | | | | |
| | G1 | 0.52 | 1.29 | 1.29 | 2.06 | 6.44 | 12.11 | 20.88 | 22.16 | 23.20 | | 17.27 | | | | | | | |
| | G2 | 3.35 | 2.58 | 3.61 | 3.35 | 7.73 | 2.06 | 20.62 | | | | | | | | | | | |
| | G3 | | 1.03 | 2.06 | 2.32 | 6.96 | 18.81 | 20.36 | 21.91 | 22.94 | 21.65 | 25.00 | | | | | | | |
| | Average | 1.93 | 1.63 | 2.32 | 2.58 | 7.04 | 11.00 | 20.62 | 22.04 | 23.07 | 21.65 | 21.13 | | | | | | | |
| | SD | 1.42 | 0.68 | 0.96 | 0.56 | 0.53 | 6.88 | 0.21 | 0.13 | 0.13 | 0.00 | 3.87 | | | | | | | |
| H (High) | Depth (cm) | -0.5 | 0.5 | 1.5 | 2.5 | 3.5 | 4.5 | 5.5 | 6.5 | 7.5 | 8.5 | 9.5 | 11.5 | 13.5 | 15.5 | | | | |
| | H1 | 1.14 | 0.57 | 0.29 | 1.43 | 1.14 | 0.00 | 0.00 | 0.00 | 0.00 | 0.00 | 0.00 | | | | | | | |
| | H2 | 7.43 | 0.57 | 3.71 | 16.57 | 0.00 | 5.14 | | 0.00 | 0.00 | 0.00 | 9.14 | 0.00 | | 3.71 | | | | |
| | H3 | 7.71 | 3.43 | 0.00 | 0.57 | 2.86 | 3.14 | 2.86 | 0.00 | 2.00 | 4.00 | | | | | | | | |
| | Average | 5.43 | 1.52 | 1.33 | 6.19 | 1.33 | 2.76 | 1.43 | 0.00 | 0.67 | 1.33 | 4.57 | 0.00 | | 3.71 | | | | |
| | SD | 3.03 | 1.35 | 1.69 | 7.35 | 1.17 | 2.12 | 1.43 | 0.00 | 0.94 | 1.89 | 4.57 | 0.00 | | 0.00 | | | | |
| | Average Difference H-G | 3.496 | -0.108 | -0.986 | 3.613 | -5.711 | -8.235 | -19.190 | -22.036 | -22.400 | -20.316 | -16.563 | 0.000 | | 3.714 | | | | |
| K (High) | Depth (cm) | -0.5 | 0.5 | 1.5 | 2.5 | 3.5 | 4.5 | 5.5 | 6.5 | 7.5 | 8.5 | 9.5 | 11.5 | 13.5 | 15.5 | 17.5 | 19.5 | 24.5 | 29.5 |
| | K1 | 0.00 | 11.67 | 42.22 | 134.72 | 88.06 | 75.00 | n.d. | 73.33 | 74.72 | 90.83 | 105.83 | | | | | | | |
| | K2 | 1.39 | 10.83 | 30.00 | 52.22 | 94.72 | 89.17 | 51.11 | 62.22 | 48.89 | 48.89 | 59.72 | 57.78 | 54.17 | 72.22 | 79.72 | | 35.28 | 36.39 |
| | K3 | 0.00 | 11.67 | 10.00 | 41.39 | 55.83 | 51.11 | n.d. | 60.28 | 66.39 | 102.78 | 77.78 | n.d. | 81.67 | 45.28 | 40.83 | 61.11 | 37.22 | |
| | Average | 0.46 | 11.39 | 27.41 | 76.11 | 79.54 | 71.76 | 51.11 | 65.28 | 63.33 | 80.83 | 81.11 | 57.78 | 67.92 | 58.75 | 60.28 | 61.11 | 36.25 | 36.39 |
| | SD | 0.65 | 0.39 | 13.28 | 41.68 | 16.98 | 15.70 | 0.00 | 5.75 | 10.77 | 23.11 | 18.97 | 0.00 | 13.75 | 13.47 | 19.44 | 0.00 | 0.97 | 0.00 |
| L (Low) | Depth(cm) | -0.5 | 0.5 | 1.5 | 2.5 | 3.5 | 4.5 | 5.5 | 6.5 | 7.5 | 8.5 | 9.5 | 11.5 | 13.5 | 15.5 | 17.5 | 19.5 | 24.5 | |
| | L1 | 0.00 | 0.00 | 21.08 | 75.00 | 45.48 | 67.47 | 75.00 | 84.94 | 53.92 | 47.29 | 65.66 | 134.94 | 16.27 | 28.61 | 53.01 | 56.02 | 61.75 | |
| | L2 | 1.81 | 0.00 | 7.53 | 52.71 | 70.48 | 72.89 | 71.99 | 58.43 | 49.40 | 33.73 | 73.19 | 45.48 | 58.13 | 88.25 | 58.43 | 62.35 | n.d. | |
| | Average | 0.90 | 0.00 | 14.31 | 63.86 | 57.98 | 70.18 | 73.49 | 71.69 | 51.66 | 40.51 | 69.43 | 90.21 | 37.20 | 58.43 | 55.72 | 59.19 | 61.75 | |
| | SD | 0.90 | 0.00 | 6.78 | 11.14 | 12.50 | 2.71 | 1.51 | 13.25 | 2.26 | 6.78 | 3.77 | 44.73 | 20.93 | 29.82 | 2.71 | 3.16 | 0.00 | |
| | Average difference K-L | -0.44 | 11.39 | 13.10 | 12.26 | 21.56 | 1.58 | -22.38 | -6.41 | 11.68 | 40.32 | 11.68 | -32.43 | 30.72 | 0.32 | 4.55 | 1.92 | -25.50 | |

## Porewater measurements: $NO_3^-$

| Porewater measurements NO3 (µM) - µmol/L | | | | | | | | | | | | | |
|---|---|---|---|---|---|---|---|---|---|---|---|---|---|
| **Locality** | **Depth (cm)** | **-0.5** | **0.5** | **1.5** | **2.5** | **3.5** | **4.5** | **5.5** | **6.5** | **7.5** | **8.5** | **9.5** | **11.5** |
| A | A1 | 6.94 | 7.41 | 1.16 | 0.00 | 0.00 | 0.00 | 0.00 | 0.00 | 0.00 | 0.00 | 0.93 | |
| | A2 | 0.46 | 1.16 | 0.00 | 0.00 | 0.00 | 0.00 | 3.70 | 0.00 | 0.00 | | 0.00 | 0.00 |
| | A3 | 0.00 | 2.31 | 0.00 | 2.31 | 1.16 | 0.00 | 0.00 | 11.11 | 60.42 | 35.65 | 0.00 | 0.00 |
| | Average | 2.47 | 3.63 | 0.39 | 0.77 | 0.39 | 0.00 | 1.23 | 3.70 | 20.14 | 17.82 | 0.31 | 0.00 |
| | SD | 3.17 | 2.71 | 0.55 | 1.09 | 0.55 | 0.00 | 1.75 | 5.24 | 28.48 | 17.82 | 0.44 | 0.00 |
| B(Low) | Depth (cm) | -0.5 | 0.5 | 1.5 | 2.5 | 3.5 | 4.5 | 5.5 | 6.5 | 7.5 | 8.5 | 9.5 | |
| | B1 | 0.00 | 15.74 | | 0.00 | 0.00 | 0.00 | 5.56 | 0.46 | 1.62 | 0.00 | 3.70 | |
| | B2 | 0.00 | 15.05 | 0.00 | 2.08 | 4.63 | 0.00 | 0.00 | 4.86 | 14.35 | | 0.00 | |
| | B3 | 16.90 | 0.00 | 0.00 | 0.00 | | 0.00 | 0.93 | 5.09 | 0.00 | | 0.00 | |
| | Average | 5.63 | 10.26 | 0.00 | 0.69 | 2.31 | 0.00 | 2.16 | 3.47 | 5.32 | 0.00 | 1.23 | |
| | SD | 7.97 | 7.26 | 0.00 | 0.98 | 2.31 | 0.00 | 2.43 | 2.13 | 6.42 | 0.00 | 1.75 | |
| C(High) | Depth (cm) | -0.5 | 0.5 | 1.5 | 2.5 | 3.5 | 4.5 | 5.5 | | | | | |
| | C1 | 2.22 | 8.37 | 17.73 | 12.32 | 19.70 | 11.58 | 0.74 | | | | | |
| | C2 | 0.00 | 19.21 | 10.34 | 7.39 | 5.17 | 3.69 | | | | | | |
| | C3 | 4.43 | 19.21 | 21.67 | 5.67 | 9.61 | 0.49 | 8.13 | | | | | |
| | Average | 2.22 | 15.60 | 16.58 | 8.46 | 11.49 | 5.25 | 4.43 | | | | | |
| | SD | 1.81 | 5.11 | 4.70 | 2.82 | 6.08 | 4.66 | 3.69 | | | | | |
| | Average difference C-B | -3.42 | 5.34 | 16.58 | 7.76 | 9.18 | 5.25 | 2.27 | | | | | |
| G(Low) | Depth (cm) | -0.5 | 0.5 | 1.5 | 2.5 | 3.5 | 4.5 | 5.5 | | | | | |
| | G1 | 9.36 | 25.86 | 7.39 | 0.00 | 9.11 | 0.00 | | | | | | |
| | G2 | 0.00 | 54.93 | 7.14 | 1.72 | 0.00 | 0.00 | | | | | | |
| | G3 | | 9.36 | 12.81 | 19.95 | 0.00 | 9.11 | 0.00 | | | | | |
| | Average | 4.68 | 30.05 | 9.11 | 7.22 | 3.04 | 3.04 | 0.00 | | | | | |
| | SD | 4.68 | 18.84 | 2.61 | 9.03 | 4.30 | 4.30 | 0.00 | | | | | |
| H(High) | Depth (cm) | -0.5 | 0.5 | 1.5 | 2.5 | 3.5 | 4.5 | | | | | | |
| | H1 | 8.87 | 14.29 | 0.00 | 2.46 | 0.00 | 27.83 | | | | | | |
| | H2 | 0.00 | 7.14 | 16.75 | 22.66 | 0.00 | 10.59 | | | | | | |
| | H3 | 2.96 | 16.26 | 1.72 | 8.37 | 1.48 | 0.00 | | | | | | |
| | Average | 3.94 | 12.56 | 6.16 | 11.17 | 0.49 | 12.81 | | | | | | |
| | SD | 3.69 | 3.92 | 7.52 | 8.48 | 0.70 | 11.47 | | | | | | |
| | Average Difference H-G | -0.74 | -17.49 | -2.96 | 3.94 | -2.55 | 9.77 | | | | | | |
| K(High) | Depth (cm) | -0.5 | 0.5 | 1.5 | 2.5 | 3.5 | 4.5 | | | | | | |
| | K1 | 5.67 | 32.02 | 22.66 | 2.96 | 18.23 | 0.00 | | | | | | |
| | K2 | 24.63 | 7.88 | 0.00 | 9.36 | 0.00 | 0.00 | | | | | | |
| | K3 | 7.39 | 0.49 | 5.91 | 0.00 | 7.64 | 7.14 | | | | | | |
| | Average | 12.56 | 13.46 | 9.52 | 4.11 | 8.62 | 2.38 | | | | | | |
| | SD | 8.56 | 13.46 | 9.60 | 3.91 | 7.47 | 3.37 | | | | | | |
| L(Low) | Depth(cm) | -0.5 | 0.5 | 1.5 | 2.5 | 3.5 | 4.5 | | | | | | |
| | L1 | 5.17 | 10.84 | 0.00 | 5.67 | 16.50 | 5.67 | | | | | | |
| | L2 | 9.11 | 8.37 | 6.90 | 1.97 | 0.00 | 0.00 | | | | | | |
| | Average | 7.14 | 9.61 | 3.45 | 3.82 | 8.25 | 2.83 | | | | | | |
| | SD | 1.97 | 1.23 | 3.45 | 1.85 | 8.25 | 2.83 | | | | | | |
| | Average difference K-L | 5.42 | 3.86 | 6.08 | 0.29 | 0.37 | -0.45 | | | | | | |

## Sediment measurements: $\delta^{13}C_{total}$, $\delta^{15}N_{total}$, TC and TN
## Locality B and C

| B2 | | | | | B1 | | | | | δ15Ntotaltotal vs Air, ‰ | | | | δ13Ctotal vs VPDB ‰ | | | TN% | | | TC% | | |
|---|---|---|---|---|---|---|---|---|---|---|---|---|---|---|---|---|---|---|---|---|---|---|
| Depth (cm) | δ15Ntotaltotal vs Air ‰ | δ13Ctotal vs VPDB ‰ | TN% | TC% | Depth (cm) | δ15Ntotal vs Air ‰ | δ13C vs VPDB ‰ | TN% | TC% | Depth (cm) | Average B (L) | SD | SD (%) | Average B (L) | SD | SD (%) | Average B(L) | SD | SD (%) | Average B (L) | SD | SD (%) |
| 0.50 | 3.73 | -23.92 | 0.16 | 1.28 | 0.50 | 3.20 | -23.78 | 0.13 | 1.06 | 0.50 | 3.47 | 0.26 | 7.63 | -23.85 | 0.07 | -0.29 | 0.14 | 0.01 | 8.83 | 1.17 | 0.11 | 9.55 |
| 1.50 | 2.84 | -23.89 | 0.13 | 0.99 | 1.50 | 2.92 | -24.01 | 0.13 | 1.06 | 1.50 | 2.88 | 0.04 | 1.33 | -23.95 | 0.06 | -0.25 | 0.13 | 0.00 | 0.76 | 1.02 | 0.03 | 3.29 |
| 2.50 | 2.65 | n.d. | 0.12 | 1.05 | 2.50 | 3.67 | -24.14 | 0.16 | 1.39 | 2.50 | 3.16 | 0.51 | 16.06 | -24.14 | 0.00 | 0.00 | 0.14 | 0.02 | 12.33 | 1.22 | 0.17 | 13.68 |
| 3.50 | 2.53 | -22.83 | 0.13 | -0.13 | 3.50 | 3.42 | -23.99 | 0.16 | 1.35 | 3.50 | 2.98 | 0.44 | 14.92 | -23.41 | 0.58 | -2.49 | 0.15 | 0.01 | 7.06 | 0.61 | 0.74 | 121.66 |
| 4.50 | 3.73 | -23.06 | 0.22 | 1.77 | 4.50 | 3.32 | -23.81 | 0.14 | 1.25 | 4.50 | 3.52 | 0.21 | 5.93 | -23.44 | 0.37 | -1.60 | 0.18 | 0.04 | 22.17 | 1.51 | 0.26 | 17.25 |
| 5.50 | 2.36 | -22.71 | 0.10 | -0.12 | 5.50 | 2.58 | -23.60 | 0.13 | 1.16 | 5.50 | 2.47 | 0.11 | 4.56 | -23.15 | 0.44 | -1.91 | 0.11 | 0.02 | 15.07 | 0.52 | 0.64 | 122.85 |
| 6.50 | 1.64 | -22.84 | 0.11 | -0.04 | 6.50 | 1.99 | -23.45 | 0.14 | 1.19 | 6.50 | 1.82 | 0.17 | 9.60 | -23.15 | 0.31 | -1.33 | 0.12 | 0.01 | 10.83 | 0.58 | 0.61 | 106.92 |
| | | | | | 7.50 | 1.91 | -23.24 | 0.15 | 1.23 | 7.50 | 1.91 | 0.00 | 0.00 | -23.24 | 0.00 | 0.00 | 0.15 | 0.00 | 0.00 | 1.23 | 0.00 | 0.00 |
| | | | | | 8.50 | 1.64 | -23.25 | 0.14 | 1.25 | 8.50 | 1.64 | 0.00 | 0.00 | -23.25 | 0.00 | 0.00 | 0.14 | 0.00 | 0.00 | 1.25 | 0.00 | 0.00 |
| | | | | | 9.50 | 2.26 | -23.28 | 0.14 | 1.14 | 9.50 | 2.26 | 0.00 | 0.00 | -23.28 | 0.00 | 0.00 | 0.14 | 0.00 | 0.00 | 1.14 | 0.00 | 0.00 |

| C1 | | | | | C2 | | | | | δ15Ntotal vs Air, ‰ | | | | δ13Ctotal vs VPDB ‰ | | | TN% | | | TC% | | |
|---|---|---|---|---|---|---|---|---|---|---|---|---|---|---|---|---|---|---|---|---|---|---|
| Depth (cm) | δ15Ntotal vs Air ‰ | δ13Ctotal vs VPDB ‰ | TN% | TC% | Depth (cm) | δ15Ntotal vs Air ‰ | δ13Ctotal vs VPDB ‰ | TN% | TC% | Depth (cm) | Average C (H) | SD | SD (%) | Average C (H) | SD | SD (%) | Average C (H) | SD | SD (%) | Average C (H) | SD | SD (%) |
| 0.50 | 2.74 | -24.11 | 0.20 | 1.55 | 0.50 | 2.06 | -24.40 | 0.17 | 1.40 | 0.50 | 2.40 | 0.34 | 14.28 | -24.26 | 0.14 | -0.58 | 0.19 | 0.01 | 6.48 | 1.48 | 0.08 | 5.15 |
| 1.50 | 3.13 | -24.14 | 0.16 | 1.31 | 1.50 | 3.10 | -24.20 | 0.19 | 1.53 | 1.50 | 3.12 | 0.01 | 0.41 | -24.17 | 0.03 | -0.11 | 0.18 | 0.02 | 8.95 | 1.42 | 0.11 | 7.70 |
| 2.50 | 2.29 | -23.92 | 0.14 | 1.11 | 2.50 | 3.32 | -23.97 | 0.17 | 1.46 | 2.50 | 2.81 | 0.52 | 18.40 | -23.94 | 0.03 | -0.12 | 0.15 | 0.02 | 11.96 | 1.29 | 0.18 | 13.60 |
| 3.50 | 2.96 | -23.43 | 0.11 | 0.89 | 3.50 | 2.62 | -23.63 | 0.15 | 1.20 | 3.50 | 2.79 | 0.17 | 6.07 | -23.53 | 0.10 | -0.41 | 0.13 | 0.02 | 12.60 | 1.04 | 0.15 | 14.57 |
| 4.50 | 4.07 | -22.80 | 0.18 | 1.53 | 4.50 | 1.65 | -23.50 | 0.14 | 1.15 | 4.50 | 2.86 | 1.21 | 42.41 | -23.15 | 0.35 | -1.51 | 0.16 | 0.02 | 12.81 | 1.34 | 0.19 | 14.08 |
| 5.50 | 3.27 | -22.95 | 0.18 | 1.60 | 5.50 | 2.20 | -23.45 | 0.11 | 0.85 | 5.50 | 2.73 | 0.53 | 19.52 | -23.20 | 0.25 | -1.08 | 0.15 | 0.03 | 23.61 | 1.23 | 0.37 | 30.50 |
| 6.50 | 3.48 | -21.54 | 0.16 | -0.13 | 6.50 | 2.58 | -23.37 | 0.11 | 0.79 | 6.50 | 3.03 | 0.45 | 14.72 | -22.46 | 0.92 | -4.09 | 0.13 | 0.03 | 19.62 | 0.33 | 0.46 | 137.66 |
| 7.50 | 1.77 | -23.53 | 0.12 | 1.08 | 7.50 | 2.59 | -21.19 | 0.09 | 0.75 | 7.50 | 2.18 | 0.41 | 18.78 | -22.36 | 1.17 | -5.24 | 0.10 | 0.01 | 13.71 | 0.92 | 0.17 | 18.12 |
| 8.50 | 2.47 | -23.26 | 0.12 | 0.92 | 8.50 | 3.00 | -17.30 | 0.08 | 0.69 | 8.50 | 2.73 | 0.27 | 9.80 | -20.28 | 2.98 | -14.68 | 0.10 | 0.02 | 20.36 | 0.80 | 0.11 | 13.95 |

## Sediment measurements: $\delta^{13}C_{total}$, $\delta^{15}N_{total}$, TC and TN
## Locality H and G

| H1 | | | | | H2 | | | | | δ15Ntotal vs Air ‰ | | | | δ13Ctotal vs VPDB ‰ | | | TN% | | | TC% | | |
|---|---|---|---|---|---|---|---|---|---|---|---|---|---|---|---|---|---|---|---|---|---|---|
| Depth (cm) | δ15Ntotal vs Air ‰ | δ13Ctotal vs VPDB ‰ | TN% | TC% | Depth (cm) | δ15Ntotal vs Air ‰ | δ13Ctotal vs VPDB ‰ | TN% | TC% | Depth (cm) | Average H (H) | SD | SD (%) | Average H (H) | SD | SD (%) | Average H (H) | SD | SD (%) | Average H (H) | SD | SD (%) |
| 0.50 | 3.55 | -24.18 | 0.26 | 1.88 | 0.50 | 3.24 | -24.08 | 0.29 | 2.14 | 0.50 | 3.39 | 0.15 | 4.44 | -24.13 | 0.05 | -0.21 | 0.27 | 0.01 | 4.63 | 2.01 | 0.13 | 6.60 |
| 1.50 | 3.06 | -24.16 | 0.25 | 2.05 | 1.50 | 3.04 | -23.97 | 0.31 | 2.41 | 1.50 | 3.05 | 0.01 | 0.35 | -24.06 | 0.09 | -0.38 | 0.28 | 0.03 | 9.79 | 2.23 | 0.18 | 7.88 |
| 2.50 | 3.41 | -23.84 | 0.22 | 1.75 | 2.50 | 3.52 | -23.66 | 0.44 | 3.28 | 2.50 | 3.46 | 0.05 | 1.50 | -23.75 | 0.09 | -0.38 | 0.33 | 0.11 | 34.51 | 2.51 | 0.76 | 30.42 |
| 3.50 | 3.35 | -23.82 | 0.27 | 2.16 | 3.50 | 3.34 | -23.78 | 0.27 | 2.09 | 3.50 | 3.34 | 0.01 | 0.16 | -23.80 | 0.02 | -0.08 | 0.27 | 0.00 | 1.15 | 2.12 | 0.04 | 1.68 |
| 4.50 | 2.64 | -24.00 | 0.20 | 1.59 | 4.50 | 3.09 | -23.69 | 0.23 | 1.88 | 4.50 | 2.86 | 0.22 | 7.80 | -23.85 | 0.16 | -0.66 | 0.22 | 0.02 | 8.75 | 1.74 | 0.15 | 8.64 |
| 5.50 | 2.75 | -23.94 | 0.16 | 1.30 | 5.50 | 2.70 | -23.75 | 0.20 | 1.58 | 5.50 | 2.72 | 0.03 | 1.00 | -23.85 | 0.10 | -0.42 | 0.18 | 0.02 | 10.47 | 1.44 | 0.14 | 9.88 |
| 6.50 | 3.28 | -23.58 | 0.16 | 1.27 | 6.50 | 2.05 | -22.80 | 0.11 | 0.78 | 6.50 | 2.66 | 0.61 | 23.09 | -23.19 | 0.39 | -1.68 | 0.13 | 0.03 | 19.39 | 1.03 | 0.25 | 23.93 |
| 7.50 | 1.92 | -22.84 | 0.13 | 1.11 | 7.50 | 3.10 | -19.49 | 0.09 | 0.68 | 7.50 | 2.51 | 0.59 | 23.48 | -21.16 | 1.68 | -7.92 | 0.11 | 0.02 | 19.90 | 0.89 | 0.21 | 23.84 |
| 8.50 | 1.80 | -21.39 | 0.10 | 0.81 | 8.50 | 4.06 | -19.52 | 0.09 | 0.64 | 8.50 | 2.93 | 1.13 | 38.51 | -20.45 | 0.93 | -4.57 | 0.09 | 0.01 | 6.47 | 0.73 | 0.08 | 11.26 |
| 9.50 | 2.34 | -17.15 | 0.08 | 0.68 | 9.50 | 2.84 | -16.21 | 0.08 | 0.78 | 9.50 | 2.59 | 0.25 | 9.64 | -16.68 | 0.47 | -2.82 | 0.08 | 0.00 | 3.14 | 0.73 | 0.05 | 6.75 |
| 10.50 | 2.05 | -16.94 | 0.07 | 0.59 | 10.50 | 2.92 | -17.49 | 0.09 | 0.81 | 10.50 | 2.49 | 0.43 | 17.33 | -17.22 | 0.27 | -1.58 | 0.08 | 0.01 | 9.56 | 0.70 | 0.11 | 15.26 |
| | | | | | 11.50 | 3.20 | -14.64 | 0.08 | 0.92 | 11.50 | 3.20 | 0.00 | 0.00 | -14.64 | 0.00 | 0.00 | 0.08 | 0.00 | 0.00 | 0.92 | 0.00 | 0.00 |
| | | | | | 12.50 | 3.69 | -12.78 | 0.08 | 0.93 | 12.50 | 3.69 | 0.00 | 0.00 | -12.78 | 0.00 | 0.00 | 0.08 | 0.00 | 0.00 | 0.93 | 0.00 | 0.00 |
| | | | | | 13.50 | 3.19 | -11.79 | 0.08 | 1.01 | 13.50 | 3.19 | 0.00 | 0.00 | -11.79 | 0.00 | 0.00 | 0.08 | 0.00 | 0.00 | 1.01 | 0.00 | 0.00 |
| | | | | | 14.50 | 3.61 | -10.60 | 0.08 | 1.24 | 14.50 | 3.61 | 0.00 | 0.00 | -10.60 | 0.00 | 0.00 | 0.08 | 0.00 | 0.00 | 1.24 | 0.00 | 0.00 |
| | | | | | 15.50 | 3.34 | -8.66 | 0.08 | 1.43 | 15.50 | 3.34 | 0.00 | 0.00 | -8.66 | 0.00 | 0.00 | 0.08 | 0.00 | 0.00 | 1.43 | 0.00 | 0.00 |

| G2 | | | | | G3 | | | | | δ15Ntotal vs Air ‰ | | | | δ13Ctotal vs VPDB ‰ | | | TN% | | | TC% | | |
|---|---|---|---|---|---|---|---|---|---|---|---|---|---|---|---|---|---|---|---|---|---|---|
| Depth (cm) | δ15Ntotal vs Air ‰ | δ13Ctotal vs VPDB ‰ | TN% | TC% | Depth (cm) | δ15Ntotal vs Air ‰ | δ13Ctotal vs VPDB ‰ | TN% | TC% | Depth (cm) | Average G (L) | SD | SD (%) | Average G (L) | SD | SD (%) | Average G (L) | SD | SD (%) | Average G (L) | SD | SD (%) |
| 0.50 | 2.11 | -24.34 | 0.18 | 1.31 | 0.50 | 3.10 | -24.54 | 0.24 | 1.77 | 0.50 | 2.60 | 0.50 | 19.13 | -24.44 | 0.10 | -0.42 | 0.21 | 0.03 | 13.84 | 1.54 | 0.23 | 14.87 |
| 1.50 | 2.06 | -24.27 | 0.16 | 1.26 | 1.50 | 2.69 | -24.42 | 0.18 | 1.38 | 1.50 | 2.37 | 0.32 | 13.39 | -24.34 | 0.07 | -0.29 | 0.17 | 0.01 | 5.71 | 1.32 | 0.06 | 4.57 |
| 2.50 | 2.25 | -23.94 | 0.13 | 1.03 | 2.50 | 3.21 | -24.05 | 0.13 | 0.87 | 2.50 | 2.73 | 0.48 | 17.73 | -23.99 | 0.05 | -0.23 | 0.13 | 0.00 | 1.44 | 0.95 | 0.08 | 8.30 |
| 3.50 | 2.07 | -23.60 | 0.12 | 0.95 | 3.50 | 1.54 | -23.89 | 0.10 | 0.78 | 3.50 | 1.81 | 0.27 | 14.81 | -23.75 | 0.14 | -0.61 | 0.11 | 0.01 | 7.76 | 0.87 | 0.08 | 9.66 |
| 4.50 | 1.58 | -23.47 | 0.11 | 0.82 | 4.50 | 2.65 | -23.81 | 0.12 | 0.94 | 4.50 | 2.12 | 0.54 | 25.45 | -23.64 | 0.17 | -0.73 | 0.11 | 0.00 | 2.56 | 0.88 | 0.06 | 7.08 |
| 5.50 | 1.79 | -23.47 | 0.10 | 0.73 | 5.50 | 1.89 | -23.75 | 0.12 | 0.99 | 5.50 | 1.84 | 0.05 | 2.63 | -23.61 | 0.14 | -0.59 | 0.11 | 0.01 | 9.88 | 0.86 | 0.13 | 15.46 |
| 6.50 | 2.41 | -23.38 | 0.09 | 0.53 | | | | | | 6.50 | 2.41 | 0.00 | 0.00 | -23.38 | 0.00 | 0.00 | 0.09 | 0.00 | 0.00 | 0.53 | 0.00 | 0.00 |
| 7.50 | 2.27 | -21.13 | 0.09 | 0.60 | | | | | | 7.50 | 2.27 | 0.00 | 0.00 | -21.13 | 0.00 | 0.00 | 0.09 | 0.00 | 0.00 | 0.60 | 0.00 | 0.00 |

## Sediment measurements: $\delta^{13}C_{total}$, $\delta^{15}N_{total}$, TC and TN
## Locality K, L and A

| K2 (H) | | | | |
|---|---|---|---|---|
| Depth (cm) | δ15Ntotal vs Air ‰ | δ13Ctotal vs VPDB ‰ | TN% | TC% |
| 0.50 | 2.67 | -24.21 | 0.90 | 6.60 |
| 1.50 | 2.94 | -24.30 | 0.81 | 6.04 |
| 2.50 | 3.20 | -24.33 | 0.75 | 5.56 |
| 3.50 | 3.32 | -24.15 | 0.76 | 5.60 |
| 4.50 | 3.76 | -24.34 | 0.81 | 5.79 |
| 5.50 | 3.51 | -24.32 | 0.83 | 5.94 |
| 6.50 | 3.54 | -24.15 | 0.89 | 6.32 |
| 7.50 | 3.68 | -24.22 | 0.67 | 4.89 |
| 8.50 | 3.84 | -24.00 | 0.62 | 4.62 |
| 9.50 | 3.85 | -24.04 | 0.61 | 4.49 |
| 10.50 | 3.58 | -23.89 | 0.54 | 4.23 |
| 11.50 | 3.68 | -23.79 | 0.55 | 4.28 |
| 12.50 | 3.62 | -23.77 | 0.56 | 4.45 |
| 13.50 | 3.84 | -23.73 | 0.55 | 4.29 |
| 14.50 | 3.81 | -23.69 | 0.53 | 4.21 |
| 15.50 | 3.46 | -23.63 | 0.51 | 4.10 |
| 16.50 | 3.77 | -23.47 | 0.52 | 4.10 |
| 17.50 | 3.40 | -23.37 | 0.53 | 4.19 |
| 18.50 | 3.86 | -23.54 | 0.49 | 3.92 |
| 19.50 | 2.92 | -23.40 | 0.49 | 3.94 |
| 20.50 | 3.58 | -23.48 | 0.51 | 4.08 |
| 21.50 | 3.10 | -23.18 | 0.46 | 3.85 |
| 22.50 | 3.02 | -23.05 | 0.42 | 3.70 |
| 23.50 | 3.10 | -22.52 | 0.44 | 3.92 |
| 24.50 | 2.81 | -23.17 | 0.38 | 3.29 |
| 25.50 | 3.04 | -23.08 | 0.39 | 3.37 |
| 26.50 | 2.52 | -23.18 | 0.41 | 3.51 |
| 27.50 | 2.43 | -23.16 | 0.46 | 3.80 |
| 28.50 | 1.88 | -23.09 | 0.41 | 3.41 |

| L1 (L) | | | | |
|---|---|---|---|---|
| Depth (cm) | δ15Ntotal vs Air ‰ | δ13Ctotal vs VPDB ‰ | TN% | TC% |
| 0.50 | 2.87 | -24.30 | 0.76 | 5.68 |
| 1.50 | 2.93 | -24.35 | 0.53 | 4.02 |
| 2.50 | 3.43 | -24.10 | 0.69 | 5.12 |
| 3.50 | 3.36 | -24.16 | 0.70 | 5.22 |
| 4.50 | 3.61 | -24.13 | 0.68 | 5.04 |
| 5.50 | 3.08 | -24.23 | 0.63 | 4.93 |
| 6.50 | 3.36 | -24.20 | 0.61 | 4.89 |
| 7.50 | 3.45 | -24.11 | 0.64 | 4.91 |
| 8.50 | 3.47 | -24.12 | 0.60 | 4.84 |
| 9.50 | 3.34 | -24.07 | 0.59 | 4.79 |
| 10.50 | 3.42 | -24.24 | 0.56 | 4.57 |
| 11.50 | 3.74 | -23.80 | 0.60 | 4.81 |
| 12.50 | 3.07 | -24.04 | 0.47 | 3.91 |
| 13.50 | 3.24 | -24.31 | 0.45 | 3.74 |
| 14.50 | 3.41 | -24.43 | 0.50 | 4.10 |
| 15.50 | 2.75 | -24.36 | 0.47 | 3.96 |
| 16.50 | 3.16 | -24.17 | 0.49 | 3.99 |
| 17.50 | 3.29 | -23.80 | 0.46 | 3.83 |
| 18.50 | 3.40 | -23.45 | 0.49 | 3.92 |
| 19.50 | 3.33 | -22.83 | 0.38 | 3.18 |
| 20.50 | 3.23 | -23.26 | 0.41 | 3.18 |
| 21.50 | 3.83 | -23.46 | 0.36 | 2.88 |
| 22.50 | 3.86 | -23.31 | 0.36 | 2.93 |
| 23.50 | 3.27 | -23.52 | 0.60 | 4.93 |
| 24.50 | 3.88 | -23.68 | 0.46 | 3.97 |
| 25.50 | 3.62 | -23.86 | 0.34 | 2.98 |
| 26.50 | 3.07 | -23.79 | 0.40 | 3.49 |
| 27.50 | 3.87 | -23.61 | | |

| A1 (H) | | | | |
|---|---|---|---|---|
| Depth (cm) | δ15Ntotal vs Air ‰ | δ13Ctotal vs VPDB ‰ | TN% | TC% |
| 0.50 | 2.68 | -24.02 | 0.28 | 0.02 |
| 1.50 | 2.70 | -23.71 | 0.25 | |
| 2.50 | 5.13 | -24.17 | 0.29 | 2.15 |
| 3.50 | 2.76 | -23.85 | 0.22 | 1.96 |
| 4.50 | 3.34 | -23.91 | 0.27 | 2.12 |
| 5.50 | 3.49 | -23.88 | 0.20 | 1.73 |
| 6.50 | 1.77 | -23.68 | 0.20 | 1.66 |
| 7.50 | 2.94 | -24.00 | 0.13 | 1.03 |
| 8.50 | 0.89 | -24.02 | 0.12 | 0.96 |
| 9.50 | 2.07 | -24.09 | 0.16 | 1.25 |
| 10.50 | 3.74 | -23.42 | 0.23 | 1.88 |
| 12.50 | n.d | n.d | n.d. | n.d. |
| 13.50 | 3.93 | -23.42 | 0.26 | 1.88 |

## Sediment measurements: $\delta^{13}C_{TOC}$, TOC, TN and $C_{TOC}$/N ratios
## Locality B,C, G and H

| B1 | | | B2 | | | δ13C TOC vs VPDB ‰ | | | TOC% | | TN% | | | C/N |
|---|---|---|---|---|---|---|---|---|---|---|---|---|---|---|
| Depth (cm) | δ13C TOC vs VPDB ‰ | TOC% | Depth (cm) | δ13C TOC vs VPDB ‰ | TOC% | Depth (cm) | Average B (L) | SD | Average B (L) | SD | Average B (L) | SD | SD (%) | Average B (L) |
| 0.5 | -24.73 | 0.92 | 0.5 | -25.58 | 1.05 | 0.5 | -25.16 | 0.43 | 0.98 | 0.07 | 0.14 | 0.01 | 8.83 | 6.86 |
| 1.5 | -25.40 | 1.36 | 1.5 | -25.70 | 1.00 | 1.5 | -25.55 | 0.15 | 1.18 | 0.18 | 0.13 | 0.00 | 0.76 | 9.33 |
| 2.5 | -25.41 | 1.26 | 2.5 | -24.79 | 0.97 | 2.5 | -25.10 | 0.31 | 1.12 | 0.15 | 0.14 | 0.02 | 12.33 | 7.84 |
| 3.5 | -25.44 | 1.14 | 3.5 | -24.97 | 0.95 | 3.5 | -25.20 | 0.23 | 1.04 | 0.10 | 0.15 | 0.01 | 7.06 | 7.18 |
| 4.5 | -25.11 | 1.18 | 4.5 | -25.30 | 1.69 | 4.5 | -25.21 | 0.10 | 1.43 | 0.26 | 0.18 | 0.04 | 22.17 | 8.10 |
| 5.5 | -25.09 | 1.07 | 5.5 | -25.15 | 0.69 | 5.5 | -25.12 | 0.03 | 0.88 | 0.19 | 0.11 | 0.02 | 15.07 | 7.73 |
| 6.5 | -24.77 | 1.12 | 6.5 | -25.27 | 0.76 | 6.5 | -25.02 | 0.25 | 0.94 | 0.18 | 0.12 | 0.01 | 10.83 | 7.67 |
| 7.5 | -24.51 | 1.01 | | | | 7.5 | -24.51 | 0.00 | 1.01 | 0.00 | 0.15 | 0.00 | 0.00 | 6.91 |
| 8.5 | -24.38 | 1.24 | | | | 8.5 | -24.38 | 0.00 | 1.24 | 0.00 | 0.14 | 0.00 | 0.00 | 8.65 |
| 9.5 | -24.40 | 1.00 | | | | 9.5 | -24.40 | 0.00 | 1.00 | 0.00 | 0.14 | 0.00 | 0.00 | 7.09 |

| C1 | | | C2 | | | δ13C TOC vs VPDB ‰ | | | TOC% | | TN% | | | C/N |
|---|---|---|---|---|---|---|---|---|---|---|---|---|---|---|
| Depth (cm) | δ13C TOC vs VPDB ‰ | TOC% | Depth (cm) | δ13C TOC vs VPDB ‰ | TOC% | Depth (cm) | Average C (H) | SD | Average C (H) | SD | Average C (H) | SD | SD (%) | Average C (H) |
| 0.5 | -25.34 | 1.37 | 0.5 | -25.54 | 1.18 | 0.5 | -25.44 | 0.10 | 1.28 | 0.10 | 0.19 | 0.01 | 6.48 | 6.90 |
| 1.5 | -25.50 | 1.05 | 1.5 | -25.63 | 1.23 | 1.5 | -25.56 | 0.07 | 1.14 | 0.09 | 0.18 | 0.02 | 8.95 | 6.45 |
| 2.5 | -25.40 | 0.88 | 2.5 | -25.13 | 1.33 | 2.5 | -25.26 | 0.13 | 1.11 | 0.22 | 0.15 | 0.02 | 11.96 | 7.18 |
| 3.5 | -25.19 | 0.89 | 3.5 | -24.76 | 1.17 | 3.5 | -24.97 | 0.22 | 1.03 | 0.14 | 0.13 | 0.02 | 12.60 | 7.87 |
| 4.5 | -25.10 | 0.98 | 4.5 | -24.61 | 1.22 | 4.5 | -24.85 | 0.25 | 1.10 | 0.12 | 0.16 | 0.02 | 12.81 | 7.01 |
| 5.5 | -24.96 | 1.32 | 5.5 | -24.90 | 0.95 | 5.5 | -24.93 | 0.03 | 1.13 | 0.18 | 0.15 | 0.03 | 23.61 | 7.78 |
| 6.5 | -24.83 | 1.14 | 6.5 | -24.74 | 0.83 | 6.5 | -24.79 | 0.04 | 0.98 | 0.16 | 0.13 | 0.03 | 19.62 | 7.52 |
| 7.5 | -24.85 | 0.91 | 7.5 | -25.42 | 0.68 | 7.5 | -25.13 | 0.29 | 0.80 | 0.12 | 0.10 | 0.01 | 13.71 | 7.64 |
| 8.5 | -24.75 | 0.78 | 8.5 | -26.04 | 0.16 | 8.5 | -25.40 | 0.65 | 0.47 | 0.31 | 0.10 | 0.02 | 20.36 | 4.88 |

| G2 | | | G3 | | | δ13C TOC vs VPDB ‰ | | | TOC% | | TN% | | | C/N |
|---|---|---|---|---|---|---|---|---|---|---|---|---|---|---|
| Depth (cm) | δ13C TOC vs VPDB ‰ | TOC% | Depth (cm) | δ13C TOC vs VPDB ‰ | TOC% | Depth (cm) | Average G (L) | SD | Average G (L) | SD | Average G | SD | SD (%) | Average G (L) |
| 0.5 | -25.29 | 0.92 | 0.5 | -24.96 | 1.86 | 0.5 | -25.13 | 0.16 | 1.39 | 0.47 | 0.21 | 0.03 | 13.84 | 6.68 |
| 1.5 | -25.28 | 1.44 | 1.5 | -25.41 | 1.36 | 1.5 | -25.34 | 0.06 | 1.40 | 0.04 | 0.17 | 0.01 | 5.71 | 8.30 |
| 2.5 | -25.01 | 0.85 | 2.5 | -25.30 | 0.79 | 2.5 | -25.16 | 0.15 | 0.82 | 0.03 | 0.13 | 0.00 | 1.44 | 6.43 |
| 3.5 | -24.57 | 0.87 | 3.5 | -25.09 | 0.72 | 3.5 | -24.83 | 0.26 | 0.79 | 0.07 | 0.11 | 0.01 | 7.76 | 7.25 |
| 4.5 | -24.47 | 0.71 | 4.5 | -24.84 | 0.96 | 4.5 | -24.65 | 0.19 | 0.83 | 0.13 | 0.11 | 0.00 | 2.56 | 7.29 |
| 5.5 | -24.51 | 0.67 | 5.5 | -24.56 | 0.98 | 5.5 | -24.53 | 0.02 | 0.82 | 0.15 | 0.11 | 0.01 | 9.88 | 7.24 |
| 6.5 | -24.59 | 0.57 | | | | 6.5 | -24.59 | 0.00 | 0.57 | 0.00 | 0.09 | 0.00 | 0.00 | 6.75 |
| 7.5 | -24.21 | 0.55 | | | | 7.5 | -24.21 | 0.00 | 0.55 | 0.00 | 0.09 | 0.00 | 0.00 | 6.45 |

| H1 | | | H2 | | | δ13C TOC vs VPDB ‰ | | | TOC% | | TN% | | | C/N |
|---|---|---|---|---|---|---|---|---|---|---|---|---|---|---|
| Depth (cm) | δ13C TOC vs VPDB ‰ | TOC% | Depth (cm) | δ13C TOC vs VPDB ‰ | TOC% | Depth (cm) | Average H (H) | SD | Average H (H) | SD | Average H (H) | SD | SD (%) | Average H (H) |
| 0.5 | -25.67 | 2.09 | 0.5 | -25.39 | 1.86 | 0.5 | -25.53 | 0.14 | 1.98 | 0.11 | 0.27 | 0.01 | 4.63 | 7.24 |
| 1.5 | -25.32 | 2.24 | 1.5 | -25.40 | 1.79 | 1.5 | -25.36 | 0.04 | 2.01 | 0.23 | 0.28 | 0.03 | 9.79 | 7.15 |
| 2.5 | -24.35 | 4.35 | 2.5 | -24.97 | 2.72 | 2.5 | -24.66 | 0.31 | 3.53 | 0.81 | 0.33 | 0.11 | 34.51 | 10.72 |
| 3.5 | n.d. | n.d. | 3.5 | -25.22 | 1.83 | 3.5 | -25.22 | 0.00 | 1.83 | 0.00 | 0.27 | 0.00 | 1.15 | 6.75 |
| 4.5 | n.d. | n.d. | 4.5 | -25.18 | 1.61 | 4.5 | -25.18 | 0.00 | 1.61 | 0.00 | 0.22 | 0.02 | 8.75 | 7.48 |
| 5.5 | -25.11 | 1.31 | 5.5 | -25.05 | 1.48 | 5.5 | -25.08 | 0.03 | 1.40 | 0.08 | 0.18 | 0.02 | 10.47 | 7.73 |
| 6.5 | -24.99 | 1.01 | 6.5 | -25.09 | 0.71 | 6.5 | -25.04 | 0.05 | 0.86 | 0.15 | 0.13 | 0.03 | 19.39 | 6.51 |
| 7.5 | -25.10 | 0.89 | 7.5 | -26.46 | 0.55 | 7.5 | -25.78 | 0.68 | 0.72 | 0.17 | 0.11 | 0.02 | 19.90 | 6.60 |
| 8.5 | -24.97 | 0.80 | 8.5 | -27.07 | 0.51 | 8.5 | -26.02 | 1.05 | 0.65 | 0.14 | 0.09 | 0.01 | 6.47 | 6.99 |
| 9.5 | -25.82 | 0.46 | 9.5 | -27.00 | 0.52 | 9.5 | -26.41 | 0.59 | 0.49 | 0.03 | 0.08 | 0.00 | 3.14 | 5.99 |
| 10.5 | -24.83 | 0.49 | 10.5 | -25.60 | 0.61 | 10.5 | -25.22 | 0.39 | 0.55 | 0.06 | 0.08 | 0.01 | 9.56 | 6.90 |
| | | | 11.5 | -25.97 | 0.53 | 11.5 | -25.97 | 0.00 | 0.53 | 0.00 | 0.08 | 0.00 | 0.00 | 6.34 |
| | | | 12.5 | -26.35 | 0.54 | 12.5 | -26.35 | 0.00 | 0.54 | 0.00 | 0.08 | 0.00 | 0.00 | 6.95 |
| | | | 13.5 | -26.21 | 0.51 | 13.5 | -26.21 | 0.00 | 0.51 | 0.00 | 0.08 | 0.00 | 0.00 | 6.52 |
| | | | 14.5 | -26.67 | 0.45 | 14.5 | -26.67 | 0.00 | 0.45 | 0.00 | 0.08 | 0.00 | 0.00 | 5.33 |
| | | | 15.5 | -26.71 | 0.60 | 15.5 | -26.71 | 0.00 | 0.60 | 0.00 | 0.08 | 0.00 | 0.00 | 7.58 |

## Sediment measurements: $\delta^{13}C_{TOC}$, TOC, TN and $C_{TOC}$/N ratios
## Locality K, L and A

| K2 (H) | | | | |
|---|---|---|---|---|
| Depth (cm) | δ13C TOC vs VPDB ‰ | TOC% | TN% | C/N |
| 0.5 | -25.97 | 5.63 | 0.90 | 6.26 |
| 1.5 | -25.28 | 5.20 | 0.81 | 6.43 |
| 2.5 | -25.97 | 4.03 | 0.75 | 5.39 |
| 3.5 | -25.76 | 4.78 | 0.76 | 6.26 |
| 4.5 | -22.81 | 4.78 | 0.81 | 5.94 |
| 5.5 | -25.85 | 5.24 | 0.83 | 6.29 |
| 6.5 | -25.57 | 4.99 | 0.89 | 5.58 |
| 7.5 | -25.63 | 4.16 | 0.67 | 6.18 |
| 8.5 | -25.66 | 3.39 | 0.62 | 5.46 |
| 9.5 | -25.63 | 3.94 | 0.61 | 6.47 |
| 10.5 | -24.55 | 3.82 | 0.54 | 7.04 |
| 11.5 | -25.00 | 3.30 | 0.55 | 5.95 |
| 12.5 | -25.15 | 4.07 | 0.56 | 7.22 |
| 13.5 | -25.27 | 3.92 | 0.55 | 7.10 |
| 14.5 | -25.47 | 3.66 | 0.53 | 6.85 |
| 15.5 | -25.72 | 3.29 | 0.51 | 6.41 |
| 16.5 | -25.66 | 3.86 | 0.52 | 7.38 |
| 17.5 | -25.24 | 3.26 | 0.53 | 6.20 |
| 18.5 | -25.48 | 2.71 | 0.49 | 5.49 |
| 19.5 | -26.56 | 2.82 | 0.49 | 5.80 |
| 20.5 | -25.52 | 3.82 | 0.51 | 7.49 |
| 21.5 | -25.15 | 3.51 | 0.46 | 7.69 |
| 22.5 | -24.86 | 3.36 | 0.42 | 7.93 |
| 23.5 | -24.99 | 3.29 | 0.44 | 7.51 |
| 24.5 | -25.32 | 2.94 | 0.38 | 7.83 |
| 25.5 | -25.20 | 2.90 | 0.39 | 7.37 |
| 26.5 | -25.07 | 2.97 | 0.41 | 7.17 |
| 27.5 | -24.91 | 3.34 | 0.46 | 7.21 |
| 28.5 | -24.67 | 2.93 | 0.41 | 7.20 |

| L1 (L) | | | | |
|---|---|---|---|---|
| Depth (cm) | δ13C TOC vs VPDB ‰ | TOC% | TN% | C/N |
| 0.5 | -26.39 | 4.86 | 0.76 | 6.39 |
| 1.5 | -26.01 | 4.65 | 0.53 | 8.83 |
| 2.5 | -25.91 | 4.38 | 0.69 | 6.34 |
| 3.5 | -25.06 | 5.02 | 0.70 | 7.20 |
| 4.5 | -25.86 | 4.22 | 0.68 | 6.22 |
| 5.5 | -25.83 | 4.04 | 0.63 | 6.46 |
| 6.5 | -25.83 | 4.02 | 0.61 | 6.56 |
| 7.5 | -24.99 | 3.62 | 0.64 | 5.67 |
| 8.5 | -26.22 | 4.03 | 0.60 | 6.67 |
| 9.5 | -25.55 | 1.83 | 0.59 | 3.08 |
| 10.5 | -25.35 | 5.24 | 0.56 | 9.33 |
| 11.5 | -24.61 | 4.04 | 0.60 | 6.70 |
| 12.5 | -25.69 | 3.60 | 0.47 | 7.66 |
| 13.5 | -25.58 | 3.28 | 0.45 | 7.23 |
| 14.5 | -25.51 | 3.42 | 0.50 | 6.91 |
| 15.5 | -25.62 | 3.46 | 0.47 | 7.33 |
| 16.5 | -25.87 | 3.49 | 0.49 | 7.13 |
| 17.5 | -25.79 | 3.35 | 0.46 | 7.23 |
| 18.5 | -25.21 | 2.90 | 0.49 | 5.98 |
| 19.5 | -25.80 | 2.81 | 0.38 | 7.34 |
| 20.5 | -25.88 | 2.69 | 0.41 | 6.63 |
| 21.5 | -25.94 | 2.65 | 0.36 | 7.40 |
| 22.5 | -25.40 | 3.03 | 0.36 | 8.47 |
| 23.5 | -24.99 | 0.86 | 0.60 | 1.44 |
| 24.5 | -24.78 | 3.79 | 0.46 | 8.18 |
| 25.5 | -24.94 | 2.65 | 0.34 | 7.77 |
| 26.5 | -24.88 | 3.74 | 0.40 | 9.29 |
| 27.5 | -24.73 | 3.19 | | |

| A1 (H) | | | | |
|---|---|---|---|---|
| Depth (cm) | δ13C TOC vs VPDB ‰ | TOC% | TN% | C/N |
| 0.5 | -25.94 | 1.82 | 0.28 | 6.41 |
| 1.5 | -25.52 | 1.62 | 0.25 | 6.39 |
| 2.5 | -25.67 | 1.85 | 0.29 | 6.32 |
| 3.5 | -25.43 | 1.74 | 0.22 | 7.99 |
| 4.5 | -24.52 | 3.23 | 0.27 | 12.09 |
| 5.5 | -25.44 | 1.70 | 0.20 | 8.40 |
| 6.5 | -24.92 | 1.81 | 0.20 | 8.96 |
| 7.5 | -25.30 | 0.89 | 0.13 | 7.03 |
| 8.5 | -25.45 | 0.90 | 0.12 | 7.27 |
| 9.5 | -25.37 | 1.14 | 0.16 | 7.24 |
| 10.5 | -24.79 | 1.24 | 0.23 | 5.50 |
| 11.5 | -24.51 | 1.66 | n.d. | n.d. |
| 12.5 | -24.89 | 1.88 | n.d. | n.d. |
| 13.5 | -24.96 | 1.64 | 0.26 | 6.36 |

## Sediment measurements: Chlorophyll concentrations

| Chlorophyll - average chl (µg/cm³) | | | | | | | | | | | | | | | | | | | | | | | | | | | | | | | | |
|---|---|---|---|---|---|---|---|---|---|---|---|---|---|---|---|---|---|---|---|---|---|---|---|---|---|---|---|---|---|---|---|---|
| **Locality** | **Depth (cm):** | **0.5** | **1.5** | **2.5** | **3.5** | **4.5** | **5.5** | **6.5** | **7.5** | **8.5** | **9.5** | **10.5** | **11.5** | **12.5** | **13.5** | **14.5** | **15.5** | **16.5** | **17.5** | **18.5** | **19.5** | **20.5** | **21.5** | **22.5** | **23.5** | **24.5** | **25.5** | **26.5** | **27.5** | **28.5** | **29.5** | **30.5** |
| A(High) | A1 | 9.47 | 7.41 | 4.84 | 4.99 | 5.67 | 5.35 | 4.55 | 3.07 | 2.31 | 2.46 | 2.42 | 3.47 | 3.25 | 3.83 | | | | | | | | | | | | | | | | | |
| | A2 | 13.81 | 6.25 | 4.37 | 3.72 | 4.12 | 4.41 | 3.18 | 2.60 | 1.88 | 1.81 | 2.35 | | | | | | | | | | | | | | | | | | | | |
| | A3 | 11.57 | 7.73 | 5.24 | 4.66 | 3.90 | 4.41 | 3.69 | 2.10 | 2.13 | 2.35 | 2.24 | | | | | | | | | | | | | | | | | | | | |
| | Average A (H) | 11.61 | 7.13 | 4.82 | 4.46 | 4.57 | 4.72 | 3.81 | 2.59 | 2.11 | 2.20 | 2.34 | 3.47 | 3.25 | 3.83 | | | | | | | | | | | | | | | | | |
| | SD | 1.77 | 0.64 | 0.35 | 0.54 | 0.79 | 0.44 | 0.57 | 0.40 | 0.18 | 0.28 | 0.07 | 0.00 | 0.00 | 0.00 | | | | | | | | | | | | | | | | | |
| B(Low) | Depth (cm) | 0.50 | 1.50 | 2.50 | 3.50 | 4.50 | 5.50 | 6.50 | 7.50 | 8.50 | 9.50 | | | | | | | | | | | | | | | | | | | | | |
| | B1 | 5.57 | 5.10 | 4.30 | 3.87 | 2.60 | 2.49 | 2.49 | 1.99 | 2.13 | 2.13 | | | | | | | | | | | | | | | | | | | | | |
| | B2 | 4.19 | 3.83 | 3.25 | 3.04 | 2.71 | 1.73 | 1.70 | | | | | | | | | | | | | | | | | | | | | | | | |
| | B3 | 6.00 | 5.28 | 4.41 | 4.12 | 3.83 | 3.00 | 2.57 | | | | | | | | | | | | | | | | | | | | | | | | |
| | Average B (L) | 5.25 | 4.73 | 3.99 | 3.67 | 3.05 | 2.41 | 2.25 | 1.99 | 2.13 | 2.13 | | | | | | | | | | | | | | | | | | | | | |
| | SD | 0.77 | 0.64 | 0.52 | 0.46 | 0.56 | 0.52 | 0.39 | 0.00 | 0.00 | 0.00 | | | | | | | | | | | | | | | | | | | | | |
| C(High) | Depth (cm) | 0.5 | 1.5 | 2.5 | 3.5 | 4.5 | 5.5 | 6.5 | 7.5 | 8.5 | | | | | | | | | | | | | | | | | | | | | | |
| | C1 | 10.37 | 9.94 | 4.70 | 3.80 | 4.45 | 4.37 | 5.10 | 2.75 | 2.17 | | | | | | | | | | | | | | | | | | | | | | |
| | C2 | 11.93 | 6.25 | 3.51 | 2.82 | 2.24 | 1.70 | 1.01 | 0.00 | 0.00 | | | | | | | | | | | | | | | | | | | | | | |
| | C3 | 7.34 | 3.80 | 2.78 | 2.06 | 2.31 | 2.78 | | | | | | | | | | | | | | | | | | | | | | | | | |
| | Average C (H) | 9.88 | 6.66 | 3.66 | 2.89 | 3.00 | 2.95 | 3.05 | 1.37 | 1.08 | | | | | | | | | | | | | | | | | | | | | | |
| | SD | 1.91 | 2.53 | 0.79 | 0.71 | 1.02 | 1.10 | 2.04 | 1.37 | 1.08 | | | | | | | | | | | | | | | | | | | | | | |
| G(Low) | Depth (cm) | 0.5 | 1.5 | 2.5 | 3.5 | 4.5 | 5.5 | 6.5 | 7.5 | | | | | | | | | | | | | | | | | | | | | | | |
| | G1 | 8.31 | 6.69 | 4.73 | 2.89 | 2.86 | | | | | | | | | | | | | | | | | | | | | | | | | | |
| | G2 | 7.30 | 4.92 | 3.87 | 2.39 | 1.95 | 1.88 | 1.70 | 1.48 | | | | | | | | | | | | | | | | | | | | | | | |
| | G3 | 8.46 | 6.87 | 4.81 | 3.33 | 3.61 | 2.64 | | | | | | | | | | | | | | | | | | | | | | | | | |
| | Average G (L) | 8.02 | 6.16 | 4.47 | 2.87 | 2.81 | 2.26 | 1.70 | 1.48 | | | | | | | | | | | | | | | | | | | | | | | |
| | SD | 0.51 | 0.88 | 0.43 | 0.38 | 0.68 | 0.38 | 0.00 | 0.00 | | | | | | | | | | | | | | | | | | | | | | | |
| H(High) | Depth (cm) | 0.5 | 1.5 | 2.5 | 3.5 | 4.5 | 5.5 | 6.5 | 7.5 | 8.5 | 9.5 | 10.5 | 11.5 | 12.5 | 13.5 | 14.5 | 15.5 | 16.5 | | | | | | | | | | | | | | |
| | H1 | 13.41 | 5.96 | 5.24 | 7.27 | 4.48 | 2.60 | 2.17 | 1.95 | 1.01 | 0.77 | 0.83 | | | | | | | | | | | | | | | | | | | | |
| | H2 | 9.87 | 5.02 | 3.51 | 2.75 | 4.41 | 3.22 | 0.61 | 0.11 | 0.00 | 0.40 | 0.07 | 0.00 | 0.00 | 0.00 | 0.00 | 0.00 | | | | | | | | | | | | | | | |
| | H3 | 11.93 | 4.81 | 4.01 | 4.92 | 4.23 | 4.34 | 5.75 | 8.82 | 5.53 | 3.29 | 1.16 | 0.04 | 0.00 | 0.00 | 0.00 | 0.00 | 0.00 | | | | | | | | | | | | | | |
| | Average H (H) | 11.73 | 5.27 | 4.25 | 4.98 | 4.37 | 3.39 | 2.84 | 3.63 | 2.18 | 1.49 | 0.69 | 0.02 | 0.00 | 0.00 | 0.00 | 0.00 | | | | | | | | | | | | | | | |
| | SD | 1.45 | 0.50 | 0.73 | 1.84 | 0.11 | 0.72 | 2.15 | 3.75 | 2.40 | 1.28 | 0.45 | 0.02 | 0.00 | 0.00 | 0.00 | 0.00 | | | | | | | | | | | | | | | |
| K(High) | Depth (cm) | 0.5 | 1.5 | 2.5 | 3.5 | 4.5 | 5.5 | 6.5 | 7.5 | 8.5 | 9.5 | 10.5 | 11.5 | 12.5 | 13.5 | 14.5 | 15.5 | 16.5 | 17.5 | 18.5 | 19.5 | 20.5 | 21.5 | 22.5 | 23.5 | 24.5 | 25.5 | 26.5 | 27.5 | 28.5 | 29.5 | |
| | K1 | 7.85 | 5.60 | 4.73 | 5.24 | 5.20 | 4.55 | 4.23 | 4.55 | 4.59 | 4.37 | 4.88 | 4.41 | 4.77 | 6.14 | 4.73 | 3.76 | 3.90 | 2.31 | 4.05 | 4.34 | 4.12 | 4.05 | 2.10 | 2.13 | 2.64 | 3.11 | 1.63 | 2.78 | | | |
| | K2 | 9.25 | 2.17 | 1.45 | 2.82 | 4.08 | 2.10 | 1.73 | 1.55 | 1.99 | 2.35 | 2.78 | 4.84 | 3.11 | 4.01 | 1.59 | 2.39 | 2.24 | 2.60 | 2.39 | 2.67 | 3.54 | 2.31 | 1.63 | 1.70 | 1.95 | 2.06 | 1.37 | 1.99 | 1.73 | | |
| | K3 | 8.60 | 8.67 | 4.01 | 4.01 | 3.87 | 3.80 | 3.61 | 3.83 | 2.82 | 3.90 | 2.86 | 3.11 | 2.96 | 3.54 | 2.60 | 5.42 | 4.52 | 5.42 | 5.64 | 9.11 | 1.49 | 8.13 | 3.80 | 3.90 | 2.42 | 2.49 | 1.99 | 2.35 | 2.20 | 1.81 | |
| | Average K (H) | 8.57 | 5.48 | 3.40 | 4.02 | 4.39 | 3.48 | 3.19 | 3.31 | 3.13 | 3.54 | 3.51 | 4.12 | 3.61 | 4.57 | 2.98 | 3.86 | 3.55 | 3.45 | 4.02 | 5.37 | 3.05 | 4.83 | 2.51 | 2.58 | 2.34 | 2.55 | 1.66 | 2.37 | 1.97 | 1.81 | |
| | SD | 0.57 | 2.66 | 1.41 | 0.99 | 0.59 | 1.03 | 1.06 | 1.28 | 1.09 | 0.86 | 0.97 | 0.74 | 0.82 | 1.13 | 1.31 | 1.24 | 0.96 | 1.40 | 1.33 | 2.73 | 1.13 | 2.44 | 0.93 | 0.95 | 0.29 | 0.43 | 0.25 | 0.33 | 0.23 | 0.00 | |
| L(Low) | Depth (cm) | 0.5 | 1.5 | 2.5 | 3.5 | 4.5 | 5.5 | 6.5 | 7.5 | 8.5 | 9.5 | 10.5 | 11.5 | 12.5 | 13.5 | 14.5 | 15.5 | 16.5 | 17.5 | 18.5 | 19.5 | 20.5 | 21.5 | 22.5 | 23.5 | 24.5 | 25.5 | 26.5 | 27.5 | 28.5 | 29.5 | 30.5 |
| | L1 | 2.28 | 2.75 | 2.13 | 1.95 | 1.81 | 1.23 | 1.70 | 1.55 | 1.73 | 2.78 | 2.57 | 2.39 | 1.63 | 1.45 | 1.77 | 1.92 | 1.99 | 3.04 | 9.98 | 6.18 | 4.16 | 3.40 | 3.43 | 2.71 | 2.20 | 2.71 | 2.60 | | | | |
| | L2 | 5.96 | 5.31 | 4.99 | 3.98 | 3.58 | 4.05 | 2.49 | 4.01 | 3.00 | 3.29 | 3.04 | 2.67 | 4.19 | 4.63 | 6.07 | 5.46 | 3.51 | 3.94 | 4.16 | 4.41 | 6.04 | 3.36 | 2.06 | 2.86 | 3.07 | 2.82 | 2.82 | 2.10 | 1.81 | 1.88 | 1.73 |
| | L3 | 4.81 | 3.69 | 3.33 | 2.86 | 3.11 | 3.98 | 3.11 | 1.88 | 2.78 | 2.39 | 2.35 | 5.24 | 5.89 | 2.49 | 2.39 | 2.57 | 3.54 | 2.78 | 2.71 | 2.96 | 3.47 | 2.96 | 2.71 | 3.11 | 3.07 | 2.24 | 1.99 | 2.10 | | | |
| | Average L (L) | 4.35 | 3.92 | 3.48 | 2.93 | 2.83 | 3.08 | 2.43 | 2.48 | 2.51 | 2.82 | 2.65 | 3.43 | 3.90 | 2.86 | 3.41 | 3.31 | 3.01 | 3.25 | 5.61 | 4.52 | 4.55 | 3.24 | 2.73 | 2.89 | 2.78 | 2.59 | 2.47 | 2.10 | 1.81 | 1.88 | 1.73 |
| | SD | 1.54 | 1.06 | 1.17 | 0.83 | 0.75 | 1.31 | 0.58 | 1.09 | 0.55 | 0.37 | 0.29 | 1.29 | 1.75 | 1.32 | 1.90 | 1.54 | 0.72 | 0.50 | 3.14 | 1.32 | 1.08 | 0.20 | 0.56 | 0.16 | 0.41 | 0.25 | 0.35 | 0.00 | 0.00 | 0.00 | 0.00 |